

Tracer-Test Planning Using the Efficient Hydrologic Tracer-Test Design (EHTD) Program



Cover Photo

Uranine (Acid Yellow 73) release into the underground river in Sainte Anne Cave, Belgium
(photo courtesy of Philippe Meus).

EPA/600/R-03/034
April 2003

**Tracer-Test Planning Using the
Efficient Hydrologic Tracer-Test
Design (EHTD) Program**

National Center for Environmental Assessment–Washington Office
Office of Research and Development
U.S. Environmental Protection Agency
Washington, DC 20460

DISCLAIMER

This document has been reviewed in accordance with U.S. Environmental Protection Agency policy and approved for publication. Mention of trade names or commercial products does not constitute endorsement or recommendation for use.

Preferred citation:

U.S. Environmental Protection Agency (EPA). (2003) Tracer-Test Planning Using the Efficient Hydrologic Tracer-Test Design (EHTD) Program. National Center for Environmental Assessment, Washington, DC; EPA/600/R-03/034. Available from: National Technical Information Service, VA; PB2003-103271, and <<http://www.epa.gov/ncea>>.

Contents

LIST OF TABLES	vii
LIST OF FIGURES	viii
PREFACE	ix
ORGANIZATION OF THIS DOCUMENT	x
AUTHOR and REVIEWERS	xi
ABSTRACT	xiv

I BACKGROUND 1

1. INTRODUCTION	2
1.1. QUICK START PROGRAM USAGE	4
1.1.1. Simple Program Usage	4
1.1.2. Example Test Files	5
2. REVIEW OF PREVIOUS TRACER TEST DESIGN METHODS	6
2.1. TRACER MASS ESTIMATION AND SAMPLING FREQUENCIES	7
2.1.1. Tracer Mass Estimation by Conjecture	7
2.1.1.1. <i>Recent Arguments Opposing Rigorous Tracer Mass Estimation.</i>	10
2.1.2. Tracer Mass Estimation by Mathematical Equation	11
2.1.2.1. <i>Review of Tracer-Mass Estimation Equations.</i>	11
2.1.2.2. <i>Review of Sampling Frequencies.</i>	22
2.2. EFFICIENT HYDROLOGIC TRACER-TEST DESIGN (EHTD)	23
2.2.1. Basic Design of EHTD	23
2.2.2. Range of Capabilites of EHTD	25
2.3. TRACER-TEST DESIGN RESULTS USING PREVIOUS METHODS	25
2.3.1. Examination of Tracer-Mass Estimation Equations	26
2.3.1.1. <i>Porous Media.</i>	26
2.3.1.2. <i>Karstic Media.</i>	29
2.4. EHTD ANALYSIS OF THE TWO TRACER TESTS	29
2.4.1. EHTD Results	31
2.4.1.1. <i>EHTD Porous-Media Analysis Results.</i>	36
2.4.1.2. <i>EHTD Karstic-Media Analysis Results.</i>	36
2.4.2. Mass Required as Related to Sorption by Detectors	36
2.5. TRAVEL TIMES AND SAMPLING FREQUENCIES	37
2.5.1. Travel Times	37
2.5.2. Sampling times	37
2.5.2.1. <i>Porous Media Sampling Times.</i>	38

2.5.2.2. <i>Karstic Media Sampling Times.</i>	38
2.6. NOTATIONS FOR SECTION 2.	38

II MODEL THEORY AND METHOD DEVELOPMENT 41

3. TRACER-TEST DESIGN METHODOLOGY	42
3.1. SOLUTE-TRANSPORT MODELING	42
3.2. TRACER MASS ESTIMATION	43
3.2.1. Model Solutions	44
3.2.1.1. <i>Impulse Release for BVP.</i>	44
3.2.1.2. <i>Pulse Release for BVP.</i>	45
3.2.1.3. <i>Uniform Initial Concentration (IVP).</i>	46
3.2.1.4. <i>Exponential Production (PVP).</i>	46
3.2.2. Tracer Retardation and Tracer Decay	47
3.3. SOLUTE TRANSPORT	47
3.4. HYDRAULIC AND GEOMETRIC PARAMETERS	48
3.4.1. Measured Parameters	48
3.4.2. Functional Relationships	48
3.4.3. Travel Time Estimates	50
3.5. CONTINUOUS STIRRED TANK REACTOR (CSTR)	51
3.5.1. Travel Times and Velocity	52
3.5.2. Tracer Dispersion Estimates	52
3.5.2.1. <i>Estimating Dispersion by the Method of Moments.</i>	52
3.5.2.2. <i>Estimating Dispersion by the Chatwin Method.</i>	53
3.6. TRACER SAMPLE COLLECTION DESIGN	54
3.6.1. Sample Collection	54
3.6.1.1. <i>Sampling Frequency.</i>	54
3.6.1.2. <i>Initial Sample Collection.</i>	55
3.7. METHODOLOGY EVALUATION	55
3.7.1. Simulation	57

III BASIC PROGRAM USAGE 64

4. USING EHTD TO DESIGN A TRACER TEST	65
4.1. EHTD PROGRAM USAGE AND EXAMPLE DATA FILES	65
4.1.1. Loading EHTD and Example Data Files	65
4.2. EHTD EXECUTION	66
4.3. USER-REQUESTED LATIN HYPERCUBE SAMPLING (LHS) ROUTINE	70
4.4. USER-SUGGESTED SOLUTE MASS	72
4.5. SCREEN OUTPUT	74
4.5.1. Screen Output of Error Messages	75
4.5.1.1. <i>Warning Messages.</i>	75

4.5.1.2.	<i>Error Messages.</i>	75
4.5.2.	Screen Output of Optimization Results	77
4.6.	COMPUTER GRAPHICS	78
4.6.1.	Features of the Interactive Graphics Loop	78
4.6.1.1.	<u>F</u> ile.	81
4.6.1.2.	<u>E</u> dit.	81
4.6.1.3.	<u>V</u> iew.	81
4.6.1.4.	<u>S</u> tate.	81
4.6.1.5.	<u>W</u> indow.	82
4.6.1.6.	<u>H</u> elp.	82
4.7.	EHTD SOURCE	82
5.	EHTD USE OF INPUT FILES	83
5.1.	DESCRIPTION OF INPUT FILES	83
5.1.1.	Line-by-Line Description of Input Files	89
6.	EHTD OUTPUT FILES	97
6.1.	DESCRIPTION OF OUTPUT FILES	97
6.1.1.	EHTD-Produced Data Output Files	105
6.1.1.1.	<i>Data Output File Header Material.</i>	105
6.1.1.2.	<i>Input Data Units.</i>	105
6.1.1.3.	<i>Initial Data Input Reprise.</i>	105
6.1.1.4.	<i>Sampling Station Name.</i>	105
6.1.1.5.	<i>Table 1.1. Input Factors.</i>	115
6.1.1.6.	<i>Output Data Units.</i>	115
6.1.1.7.	<i>Table 2.1.1. Initial Hydraulic Factors.</i>	115
6.1.1.8.	<i>Table 2.1.2. Final Hydraulic Factors.</i>	115
6.1.1.9.	<i>Table 3.1. Final Tracer Mass Estimate.</i>	115
6.1.1.10.	<i>Table 4.1. Estimated Sampling Frequency.</i>	116
6.1.1.11.	<i>Calculated Tracer-Mass.</i>	116
6.1.1.12.	<i>Error Codes.</i>	116
6.1.1.13.	<i>Recommended Tracer-Mass.</i>	116
6.1.1.14.	<i>Date and Time of Processing.</i>	116
6.2.	THE QUALITY OF EHTD-PREDICTED RESULTS	117
6.3.	EFFECT OF INITIAL CONCENTRATION AND EXPONENTIAL PRO- DUCTION	118
6.3.1.	Effect of an Initial Concentration	118
6.3.2.	Effect of Exponential Production	118
6.3.3.	Breakthrough Curve Shape	118
6.3.4.	Average and Peak Concentration Estimates	125

7. TRACER TEST DESIGN EXAMINATION DATA SETS	128
7.1. FLOWING STREAMS	128
7.1.1. Small Creek	129
7.1.2. Large River	129
7.1.3. Solution Conduit	129
7.1.4. Meltwater Channel	130
7.2. POROUS MEDIA	130
7.2.1. Natural-Gradient Tracer Test	130
7.2.2. Forced-Gradient Tracer Test	131
7.2.3. Injection-Withdrawal Tracer Test	131
7.2.4. Recirculation	132
7.3. TRACER-TEST DESIGN RESULTS	132
7.3.1. Flowing Streams Results	133
7.3.1.1. <i>Uvas Creek Tracer Test.</i>	133
7.3.1.2. <i>Missouri River Tracer Test.</i>	137
7.3.1.3. <i>Dyers Spring Tracer Test.</i>	138
7.3.1.4. <i>Variegated Glacier Tracer Test.</i>	140
7.3.2. Porous Media Results	141
7.3.2.1. <i>Test Site Wilerwald Tracer Test.</i>	145
7.3.2.2. <i>Kirchdorf-Unteropfingen Tracer Test.</i>	146
7.3.2.3. <i>Mobile Site Tracer Test.</i>	148
7.3.2.4. <i>Chalk River Site Tracer Test.</i>	149
 IV ADDITIONAL APPLICATION OF EHTD	 151
8. APPLICATION OF EHTD TO SUPPORT RISK ASSESSMENTS	152
8.1. EXPOSURE ASSESSMENT OVERVIEW	152
8.2. FORECASTING POLLUTION FOR RISK ASSESSMENTS	154
8.2.1. Dimensionless Dye-Recovery Curve	154
8.2.2. EHTD for Forecasting pollution Effects	154
8.2.2.1. <i>Using EHTD Directly to Forecast Pollution.</i>	155
8.2.2.2. <i>Using the LHS-Routine in EHTD to Forecast Pollution.</i>	156
 9. SUMMARY AND CONCLUSIONS	 159
 NOTATIONS	 162
 REFERENCES	 166

List of Tables

1	Average dye manufacturers' purities for selected powder dyes.	9
2	Percent pure dye content for selected fluorescent dyes.	10
3	Some equations for estimating tracer injection mass.	12
4	Aquifer and tracer-dependent coefficients $T_{C_1} - T_{C_4}$	15
5	Aquifer and tracer-dependent coefficient T_{C_5}	17
6	Tracer dependent coefficient T_{C_6}	17
7	Prevailing test conditions coefficient T_{C_7}	18
8	Tracer-dye mass per 1000 m of traced distance.	20
9	General sampling schedule for a karst terrane.	24
10	Specific sampling schedule for a karst terrane.	24
11	Tracer test design parameters.	27
12	Tracer-mass estimates.	28
13	EHTD tracer test design parameters.	30
14	EHTD tracer test analysis results.	32
15	Tracer-dye mass per 1000 m of traced distance.	35
16	Tracer test design parameters.	57
17	Predicted tracer mass and tracer concentration.	59
18	Recommended sampling times for selected tracer reaction conditions.	61
19	Table illustrating the form of the EHTD-created plot file.	69
20	Variable parameter types used in the LHS routine.	72
21	Screen display of a typical EHTD warning message.	75
22	Screen display of a typical EHTD warning message.	76
23	Typical screen display of optimization results.	77
24	Pull-down menu items available in EHTD.	80
25	Description of the input file components listed in Figures 10 and 11.	86
26	Example test data sets.	128
27	Required flowing stream tracer test design specifics.	133
28	EHTD-predicted BTCs versus measured BTCs for the flowing stream tracer tests.	134
29	EHTD-predicted results versus measured results for the flowing stream tracer tests.	135
30	Required porous media tracer test design specifics.	142
31	EHTD-Predicted BTCs versus measured BTCs for the porous media tracer tests.	143
32	EHTD-predicted results versus measured results for the porous media tracer tests.	144

List of Figures

1	EHTD results for an impulse release for the porous media test parameters.	33
2	EHTD results for an impulse release for the karstic test parameters.	33
3	EHTD results for a pulse release for the porous media test parameters.	34
4	EHTD results for a pulse release for the karstic test parameters.	35
5	Preliminary BTC from a hypothetical CSTR	58
6	Predicted BTC for Prospect Hill Spring for retardation effects	59
7	Predicted BTC for Prospect Hill Spring for tracer decay effects	60
8	Initial EHTD screen title	67
9	Equations used to calculate univariate statistics for an input file	73
10	Generic example of an flowing stream input file format	84
11	Generic example of an porous media input file format	85
12	Typical example input file	98
13	Standard-form example BTC	99
14	Data file used to produce Figure 13	100
15	Standard-form example output file	106
16	Comparison of EHTD-predicted BTC to measured BTC	117
17	Example input file with an initial concentration and exponential production constants	119
18	Data file used to produce Figure 19	120
19	Effect of including an initial concentration and exponential production	125
20	Comparison of the effect of including an initial concentration and exponential production	126
21	Modified EHTD-produced portion of Table 3.1	127
22	Example EHTD-produced Table 5.1	127
23	Comparison of measured data for the Uvas Creek site tracer test	136
24	Comparison of measured data for the Missouri River tracer test	138
25	Comparison of measured data for the Dyers Spring tracer test	139
26	Comparison of measured data for the Variegated Glacier tracer test	140
27	Comparison of measured data for the Test Site Wilerwald tracer test	145
28	Comparison of measured data for the Kirchdorf-Unteropfingen site tracer test	147
29	Comparison of measured data for the Mobile site tracer test	148
30	Comparison of measured data for the Chalk River site tracer test	150
31	Uncertainties associated with exposure assessments	153
32	Seven BTC's developed by the U.S. Geological Survey	155
33	Standardized curve- and EHTD-predicted BTC for Dyers Spring	157
34	LHS-generated input file of means using the Dyers Spring parameters.	158

PREFACE

The National Center for Environmental Assessment has prepared this document for the benefit of the U.S. Environmental Protection Agency regional offices, states, and the general public because of the need to develop a fast and easy method for designing tracer tests in hydrologic systems. Application of the methodology described in this document can provide individuals with the information necessary for designing reliable and safe tracer tests while eliminating much of the guesswork typical of first time tracer testing in a new environment.

The purpose of this document is to serve as a technical guide to various groups who must address potential or existing contamination problems in hydrologic systems. Tracing studies are always appropriate and probably necessary, but initial design work is usually relegated to guesses as to the amount of tracer to release and when to collect samples. This document and associated computer programs alleviate some of these problems.

The Efficient Hydrologic Tracer-test Design (EHTD) program uses a few basic field measurements combined in functional relationships that are coupled with the concept of a continuous stirred tank reactor and solute-transport theory to develop the basic design of a tracer test. Initial solute-transport parameters are produced by EHTD, which although imprecise because they are only predictive, still provide adequate information for effective tracer-test design.

EHTD produces a detailed assessment of expected tracer-test results before a tracer test is ever initiated. It also produces a likely tracer-breakthrough curve for each sampling station. Preliminary testing of EHTD has shown it to be reliable in most instances. It is believed that as EHTD is used, improvements in its design will grow as suggestions are made.

ORGANIZATION OF THIS DOCUMENT

This document serves as a “user’s manual” for the computer program EHTD. It is arranged in four parts:

- Part I Background
- Part II Model Theory and Method Background
- Part III Basic Program Usage
- Part IV Additional Application of EHTD

Part I introduces the program and provides the necessary for the new user to begin running the program immediately. This is then followed by an in-depth review and discussion of previous attempts at tracer test design.

Part II consists on a single section that is a comprehensive discussion of the relationship between solute-transport theory and tracer test design as applied by EHTD. This section will most likely be of interest to the more academic-type of scientists and engineers. More practically-oriented individuals will likely want to skip reading this section.

Part III discusses the basic usage of EHTD. Section 4 explains how to run EHTD including usage of the pull-down menus for manipulating screen display. Section 5 covers the creation/modification of the input file read by EHTD. Section 6 is a detailed examination of the output files produced by EHTD. Lastly, Section 7 validates EHTD functioning by comparing the EHTD predictions for eight selected examples with actual tracer-test results.

Part IV also consists of just a single section that explains how EHTD can be used to forecast the potential effects of inadvertent or deliberate pollutant releases. In addition, it briefly illustrates the development of an input file of mean values for parameters created by a Latin Hypercube Routine.

AUTHOR AND REVIEWERS

The National Center for Environmental Assessment within the U.S. Environmental Protection Agency's Office of Research and Development was responsible for preparing of this document and provided overall direction and coordination during the production effort.

AUTHOR

Malcolm S. Field, Ph.D.
National Center for Environmental Assessment
Office of Research and Development
U.S. Environmental Protection Agency
Washington, D.C.

REVIEWERS

Feike J. Leij, Ph.D.
U.S. Salinity Laboratory
450 West Big Springs Road
Riverside, Ca.

Laboratoire d'Etude des Transferts en
Hydrologie et Environnement (LTHE)
1023 rue de la Piscine
BP 53, Domaine Universitaire
F-38041 Grenoble, Cedex 9, France

Philippe Meus, Ph.D.
Ministère de la Région wallonne
Direction générale des Ressources naturelles
et de l'Environnement
Division de l'Eau
Direction des Eaux souterraines
avenue Prince de Liège 15
B-5100 Jambes (Namur)
Belgique

European Water Tracing Services
rue de la Chapelle 43
B-4550 Nandrin
Belgique

Arthur N. Palmer, Ph.D.
Earth Sciences Department
209 Science Building 1
State University of New York
Oneonta, N.Y.

Michaël Verrault, M.Sc.A
Centre d'études sur les ressources minérales
Université du Québec à Chicoutimi
Chicoutimi, Québec
Canada

Les Laboratoires SL
1309, blv St-Paul
Chicoutimi, Québec
Canada

ABSTRACT

Hydrological tracer testing is the most reliable diagnostic technique available for establishing flow trajectories and hydrologic connections and for determining basic hydraulic and geometric parameters necessary for establishing operative solute-transport processes. Tracer-test design can be difficult because of a lack of prior knowledge of the basic hydraulic and geometric parameters desired and the appropriate tracer mass to release. A new efficient hydrologic tracer-test design (EHTD) methodology has been developed that combines basic measured field parameters (e.g., discharge, distance, cross-sectional area) in functional relationships that describe solute-transport processes related to flow velocity and time of travel. The new method applies these initial estimates for time of travel and velocity to a hypothetical continuously stirred tank reactor as an analog for the hydrologic flow system to develop initial estimates for tracer concentration and axial dispersion, based on a preset average tracer concentration. Root determination of the one-dimensional advection-dispersion equation (ADE) using the preset average tracer concentration then provides a theoretical basis for an estimate of necessary tracer mass.

Application of the predicted tracer mass with the hydraulic and geometric parameters in the ADE allows for an approximation of initial sample-collection time and subsequent sample-collection frequency where a maximum of 65 samples were determined to be necessary for describing the predicted tracer-breakthrough curve (BTC). Inclusion of tracer retardation and decay cause a net increase in tracer-mass estimates so that the preset average tracer concentration will be maintained, with a consequent steepening of the BTC, but retardation also causes BTC spreading and a delay in tracer arrival.

Determining the necessary tracer mass, the initial sample-collection time, and the subsequent sample-collection frequency for a proposed tracer test are the three most difficult aspects to estimate prior to conducting the test. To facilitate tracer-mass estimation, 33 mass-estimation equations have been developed over the past century. The 33 equations are reviewed here; 32 of them were evaluated using previously published tracer-test design examination parameters. Comparison of the results produced a wide range of estimated tracer mass, but no means is available by which one equation may be reasonably selected over the others. Each equation produces a simple approximation for tracer mass. Most of the equations are based primarily on estimates or measurements of discharge, transport distance, and suspected transport times.

Although the basic field parameters commonly employed are appropriate for estimating

tracer mass, the 33 equations are problematic in that they were all probably based on the original developer's experience in a particular field area and not necessarily on measured hydraulic parameters or solute-transport theory. Suggested sampling frequencies are typically based primarily on probable transport distance, but with little regard to expected travel times. This too is problematic in that tracer sampling remains a haphazard process that tends to result in false negatives or data aliasing.

Simulations from the recently developed EHTD methodology were compared with those obtained from 32 of the 33 published tracer-mass estimation equations and suggested sampling frequencies. EHTD applies functional relationships developed from hydrologic measurements in a solute-transport model to develop a preliminary BTC that has been shown to reasonably predict actual tracer-test results.

Effective tracer-test design requires that the likely results be predicted in advance of test initiation to ensure tracer-testing success. EHTD-predicted BTCs for various hydrological conditions were compared with measured BTCs obtained from actual tracer tests. The hydrologic conditions for the tracer tests ranged from flowing streams to porous-media systems. The tracer tests evaluated included flowing streams tracer tests conducted in small and large surface-water streams, a karst solution conduit, and a glacial-meltwater stream and porous-media systems conducted as natural-gradient, forced-gradient, injection-withdrawal, and recirculation tracer tests.

Comparisons of the actual tracer tests and the predicted results showed that tracer breakthrough, hydraulic characteristics, and sample-collection frequency may be forecasted sufficiently well in most instances to facilitate good tracer-test design. However, comparisons were generally improved by including tracer decay and/or retardation in the simulations. Inclusion of tracer decay in the simulations also tended to require an increase in set average tracer concentration to facilitate matching peak concentrations in the measured BTCs. Both nonreactive tracer and reactive tracer predictions produced recommended sample-collection frequencies that would adequately define the actual BTCs, but estimated tracer-mass estimates were less precise.

EHTD may also be used to facilitate drinking-water protection strategies. EHTD provides water managers with the ability to conduct release-scenario simulations by overriding the set average concentration. The simulations can be used to predict toxic substance arrival times (time to leading edge, time to peak, persistence), axial dispersion, dilution, and arrival concentrations. By combining the EHTD-simulation results with risk assessment analyses for acute exposures, water managers can develop a set of alternatives as part of an

overall strategy for protecting human health. This set of alternatives could range from no action (i.e., no significant concern) to disconnecting the water-supply system, announcing a no-contact warning, and arranging for the supply of an alternative water source.

Part I

BACKGROUND



Flow of diluted uranine (Acid Yellow 73) through Sainte Anne Cave, Belgium. The tracer release is depicted on the cover of this document (photo courtesy of Philippe Meus).

1. INTRODUCTION

Tracer tests are regularly applied in many hydrologic systems to determine various hydraulic and geometric parameters. However, the success of a tracer test depends on the release of sufficient—but not excessive—tracer material into the flow regime for reliable tracer detection based on appropriate initial sample collection time and sampling frequency. Determination of the optimal quantity of tracer material to release into a flow system to maximize the probability of achieving positive results while maintaining safe concentrations in the environment and minimizing public concern has been of considerable interest for a long time.

To maintain safe tracer concentrations and to minimize public concerns regarding colored water, Field et al. (1995) suggested that fluorescent dye concentrations at downstream receptors be maintained at or below $1\text{--}2\text{ mg L}^{-1}$. They arrived at these concentrations by conducting an in-depth evaluation of available toxicological information on 12 fluorescent dyes and one dye intermediate using a U.S. Environmental Protection Agency (EPA) approved assessment method for cases where actual data were lacking. Field et al. urged the use of only that quantity of tracer dye actually needed to ensure positive results. The use of significantly more than is needed might adversely affect the environment and human health, although the degree of adversity was not quantified. In addition, excessive amounts of tracer could compromise tracer test interpretations. However, determining the adequate and safe amounts of tracer substance, dye or otherwise, to use in a tracing study can be difficult (Käb, 1998, p. 327).

An optimal tracer mass that meets both hydrologic and environmental criteria is dependent on a number of relatively indeterminate factors, such as the volume of water that dilutes the tracer, hydrological conditions during high-flow and low-flow periods, residence time, number and direction of discharge points, transport distance(s), sorption, decay, and degree and type of pollution. Therefore, the quantity of tracer needed for release at any particular site and time may be significantly different from that needed at another site or at the same site at another time.

For example, a preliminary tracer test at a Superfund site in Tennessee using 0.7 g of Rhodamine WT resulted in a conventional, positively skewed tracer-breakthrough curve (BTC) and nearly 100% mass recovery (Field and Pinsky, 2000). A subsequent tracer test at the same site 48 hours later using 71 g of Rhodamine WT produced a very abrupt BTC with a very long tail and only 28% mass recovery. A large storm that preceded the second

tracer test was deemed responsible for the differing results (Field and Pinsky, 2000).

To alleviate some of the difficulties associated with estimating the mass of tracer to be released, numerous empirical equations have been developed by various individuals (Field, 2002a). In nearly every instance these equations appear to have been devised without regard to solute transport theory and, at times, without regard to site hydrology. Rather, they appear to have been developed solely as a result of the developer’s experience from one or more tracer tests. Also, in many instances various—and sometimes unexplained—multipliers are incorporated into the equations to account for potentially inadequate tracer mass estimates (Field, 2002a).

Initial sample collection times and sampling frequencies are also generally unknown quantities because solute fluxes are typically unknown. However, application of functional relationships developed from measured parameters can be used to estimate solute transport parameters. The determination of solute transport parameters translates into appropriate sampling frequencies.

The purpose of this paper is to answer three basic questions common at the start of any hydrologic tracer test: (1) How much tracer mass should be released? (2) When should sampling start? and (3) At what frequency should samples be collected? In this paper an efficient hydrologic tracer test design (EHTD) methodology for estimating tracer mass based on solute transport theory is developed. Use of the methodology developed here leads to a better understanding of the probable transport processes operating in the system prior to conducting the tracer test. Improved understanding of the transport processes then leads to better estimates of tracer mass to be released. In addition, initial sample collection times and sample collection frequencies are calculated using solute transport theory.

Although this tracer-design methodology is expected to be reliable in most instances, it does not address the common occurrences of multimodal BTCs and long-tailed BTCs because such BTCs require much more complex analyses with numerous unknown parameters (Małoszewski et al., 1992a; Toride et al., 1993). Density-induced sinking effects that may occur in natural gradient porous-media tracer tests (Oostrom et al., 1992; Barth et al., 2001) are also not addressed. The methodology introduced here is tracer independent, whereas density-induced sinking is a tracer-dependent process and requires a separate analysis to determine how much, if any, tracer sinking may occur.

1.1. QUICK START PROGRAM USAGE

Begin by copying all EHTD files (i.e., Ehtd.exe., Grfont.dat, Rgb.txt, and *.in) to the hard drive of a computer. (See Section 4.1.1. on page 65 for a detailed discussion on the copying of EHTD files to a hard drive.) Once stored on the hard drive, EHTD is ready to be run. (NOTE: EHTD functions best with a display = 1024×768 pixels; adequately with a display = 800×600 pixels; and not so well for further reduced display settings.)

1.1.1. Simple Program Usage

To run EHTD, please perform the following:

1. Execute the EHTD.exe file by *Left Double-Clicking* on it using a mouse.
2. Follow on screen instructions:
 - (a) Press <ENTER> to run the default input file (i.e., EHTD.in),
 - (b) Press <ENTER> to create the default output name (i.e., EHTD.out),
 - (c) Press <ENTER> to skip producing a PostScript plot file.
3. Use the pull-down menus to manipulate the plot. For example:

FILE: To save a BITMAP file of the screen plot or print.

VIEW: To change the screen display to view the entire plot all at once.

WINDOW: Move from GRAPHIC2 (plot screen) back to GRAPHIC1
(text display screen) for additional computation.

In the GRAPHIC1 (text display screen) screen press <ENTER> for completion of EHTD (i.e., writing of all output data to the output file). If this step is not completed then some computational results (e.g., final tracer mass estimate) will not be written to the output file.

Note: It is essential that the program be ended by moving from the GRAPHIC2 screen to the GRAPHIC1 screen using the WINDOW pull-down menu and that <ENTER> be pressed so that final computational results may be recorded in the output file and that all requested plot files get created. Also, a date/time stamp is written to the bottom of the file.

4. Open the output file and/or the plot file created using a standard Windows viewer (e.g., Notepad) to see the results.

1.1.2. Example Test Files

The following example data files are provided on the CD-ROM that accompanies this document so that the user may examine the functioning of EHTD under differing environmental conditions:

Clarke1.in	Single spring discharge site for a complexly folded karst terrane (Field, 2000)
Clarke2.in ¹	Multiple spring discharge sites for a complexly folded karst terrane (Field, 2000)
Mull.in	Karst window to spring tracer test (Mull et al., 1988a, pp. 61–66)
Lost.in	Lost River Cave System (Field and Pinsky, 2000)
G1.in	Tenn. example from a quarry (Davies, <i>pers. comm.</i>)
G2.in	Tenn. example from a quarry (repeat tracer test of above)
Miss1.in	Surface water tracer test example (Yotsukura et al., 1970, pp. G3–G6)
Miss2.in	Surface water tracer test example (repeat tracer test of above)
Step.in	Created example for continuous release
Borden.in	Borden tracer test (Mackay et al., 1986)
Ehtd.in	Injection-withdrawal test example (default) (Molz et al., 1986a, pp. 52–60, 71)
Chalk.in	Recirculation test example (Huyakorn et al., 1986)

¹EHTD sums total estimated tracer mass to be released at the end of the program.

2. REVIEW OF PREVIOUS TRACER TEST DESIGN METHODS

Quantitative hydrologic tracer testing is the most reliable method for establishing solute transport trajectories and for defining solute transport parameters. Determining the necessary tracer mass to release, when to start collecting samples, and at what frequency all subsequent samples should be collected can be very difficult to estimate, especially in karstic terranes. In most tracing studies in karstic terranes, design efforts are focused on predicting where tracer will arrive and where best to release tracer. The tracer mass released is typically a guess based on the experience of the practitioner. Although attempting to predict where the tracer will arrive and where best to release the tracer are important and valuable aspects of conducting a tracer test, guessing the appropriate tracer mass to release is a fallacious practice that almost ensures that too much or too little tracer will be released.

To facilitate the determination of necessary tracer mass for a successful tracer test, at least 33 tracer mass estimation equations have been developed over the last century. Although a considerable improvement over the typical method of guessing an appropriate tracer mass to release, these equations are also problematic. With the exception of two equations, they were all developed on the false assumption that a simple algebraic expression that appears to function adequately for a selected hydrologic setting will then adequately function in all hydrologic settings. In addition, these equations fail to properly account for the important effects of axial dispersion and solute transport theory (Field, 2002a).

Tracer test sample collection frequency in karstic terranes is typically a haphazard procedure based on expected transport distance and supposed travel time. The haphazardness of sample collection is further exacerbated when qualitative tracing tests are conducted. In general, a preliminary sample collection frequency is determined before the tracing test is initiated but is subject to revision during the tracer test as time passes with or without tracer recovery.

In this paper, the 33 tracer mass estimation equations are briefly reviewed; 32 were evaluated using previously published tracer test design-examination parameters. For this review, unless otherwise indicated, the published tracer mass estimation equations were all probably intended to estimate the mass of tracer on an “as-sold basis,” which often necessarily includes a large quantity of diluent. In addition, conventional sample collection frequency determinations are briefly reviewed. The results of the review and examination of the 33 mass estimation equations and the typical sampling frequencies are compared with the recently developed EHTD method that has been shown to be theoretically sound and

more reliable than previous methods.

2.1. TRACER MASS ESTIMATION AND SAMPLING FREQUENCIES

Hydrologic tracing requires that an appropriate mass of tracer be released such that detectable concentrations of the tracer may be recovered at the sampling stations. Commonly, an estimate of the mass of tracer to release consists of nothing more than a guess that is sometimes based on the general experience of particular individuals (Alexander and Quinlan, 1992, p. 19; Aley, 1999, p. 14) or on prior experience at the location to be traced (e.g., Meigs and Beauheim, 2001). Other times, the guess is whatever sounds good at the time. In rare instances, a tracer mass estimation equation may be used to determine the appropriate tracer mass to release. Although general tracing experience is beneficial and specific site experience is better still for determining the quantities of tracer to release, neither approach may be regarded as scientifically rigorous. Worse, the former suggests that only select individuals are adequately qualified to assess tracer needs, and the latter suggests the possibility of numerous tracer release efforts at a site before success may be obtained.

2.1.1. Tracer Mass Estimation by Conjecture

There are four reasons beyond practical experience that may explain why a guess is used to estimate the necessary tracer mass to release. The first is the over-reliance on qualitative tracing in karstic terranes using common fluorescent dyes. Qualitative tracing is the use of packets of activated carbon (commonly known as “detectors” or “bugs” in North America and “fluocapteurs” in France) to sorb the fluorescent dye as it exits the underground. This method is believed to facilitate karst tracing in that these detectors can be distributed throughout the area where tracer dye is expected to exit the subsurface and may be collected when convenient.

Although qualitative tracing is commonly applied in Great Britain and the United States, the method is scientifically untenable because false-positive results (Gunn and Lowe, 2000; Lutz and Parriaux, 1988) and false-negative results (Smart et al., 1986) are common. Sorption onto detectors allows for reduced tracer dye concentrations because activated carbon reportedly increases tracer dye concentrations 400 times the concentration in water (Aley, 1999, p. 21), although published research suggests that dye concentration by activated carbon is probably 3 to 4 times the concentration in water but may be as high as 1000 times the concentration (Käb, 1998, pp. 100–103).

Unfortunately, activated carbon also enhances background concentrations (fluorescent

dyes and other similarly appearing compounds), which may be advantageous for visual determination of dye but which adversely affects the signal-to-noise ratio of modern analytical instruments (Worthington, *pers. comm.*). Excess sorption of background concentrations requires that the estimated tracer dye concentration to be released exceed background concentrations at the sampling stations by 10 times to ensure detection (Crawford, *pers. comm.*), an undesirable practice from both an aesthetic and an ecological perspective (Smart and Karunaratne, 2001).

Excessive and extensive background sorption also causes ambiguous results, erroneously suggesting tracer recovery at most or all of the sampling stations (McCann and Krothe, 1992) because the method does not lend itself to establishing that the sorbed and “identified” compound is in fact the fluorescent dye of interest. Even more basic, it may be regarded as nonsense on its face. By requiring an injection concentration that results in a downstream concentration >10 times background, it is assumed that a multitude of background samples (typically three) have been collected and that the maximum concentration or some statistical value (e.g., mean, median, etc.) for which a 10-fold increase is intended was used as a measure. Second, it is very difficult to translate an upstream concentration at a ground-water injection point into a downstream concentration. Third, the method for this calculation requires appropriate field measurements and numerical analysis, which are typically avoided.

More recent research suggests that fluorescent dye sorption by detectors may not be as straightforward as once thought. Research at the University of Minnesota (Davies, *pers. comm.*) suggests that the occurrence of false negatives and false positives may occur far more frequently than has previously been recognized, primarily because of the vagaries of fluorescent dye sorption/desorption by the detectors. For example, sodium fluorescein (uranine [45350 C.I. Acid Yellow 73]) was found to be readily sorbed by activated carbon, but it was also desorbed almost immediately. Rhodamine WT (C.I. Acid Red 388), however, was not readily sorbed and was difficult to elute. The rapid sorption-desorption of short-wavelength dyes and the slow sorption and difficult elution of long-wavelength dyes compromise the use of activated carbon for detection (Smart and Simpson, 2001).

Other peculiarities related to sorption by activated carbon and sample handling (Smart and Friederich, 1982; Smart and Zabo, 1997) also prevent replication of the results, a basic requirement of any scientific endeavor. The difficulties are further exacerbated by the fluorescence spectra shift caused by the high pH of the elutants (Käb, 1998, p. 102). In addition, specific tracer types may result in varying sorptive behaviors (Sutton et al., 2001).

Table 1. Average dye manufacturers' purities for selected powder dyes.

Colour Index Generic Name	Common Name	Colour Index Constitution No.	Average Purity ^a Range, %
Acid Red 9	eriglaucine	42090	73–75
Acid Red 52	Sulpho Rhodamine B	45100	85–90
Acid Red 87	eosin	45380	65–70
Acid Red 388	Rhodamine WT	...	82–85
Acid Yellow 73	Na-fluorescein	45350	75
Basic Violet 10	Rhodamine B	45170	90
Fluorescent Brightener 351	Tinopal CBS-X	...	60
Solvent Green 7	pyranine	59040	80

^a Values are for the “crude” form of the dyes only.

The second reason the tracer mass to be released is guessed at stems from the lack of knowledge regarding the volume and degree of spreading necessary for estimating the extent of tracer dilution. Sorptive characteristics of the transport medium and tracer are also typically unknown. Although surface-water volume and degree of spreading can be reasonably estimated, aquifer volume and degree of spreading remain virtual unknowns until a quantitative tracer test is conducted and numerically evaluated. Understanding tracer losses due to tracer sorption generally requires extensive testing and analysis using a selected tracer and specific materials and the results are not readily transferable.

A third reason why necessary tracer masses are guessed at may relate to the relative purities of the various fluorescent dyes supplied by different manufacturers. Table 1 lists the average dye manufacturers' purities of some common fluorescent dyes used for hydrological tracing and Table 2 lists the average percent pure dye content of the dyes supplied by one distributor. This range of fluorescent dye purities complicates the determination of dye mass to release.

The fourth and final reason that the tracer mass to release is guessed is because of the relative obscurity, confusing nature, and inconsistency surrounding the use of existing tracer mass estimation equations. In general, these equations have been found to be less exact than is commonly desired (Käß, 1998, p. 323).

Table 2. Percent pure dye content for selected fluorescent dyes.

Tracer Dye (Common Name)	Powder Dye ^a Content, % ^b	Liquid Dye ^a Content, % ^b
eriolglaucine ^c	74.0	37.0
Sulpho Rhodamine B	90-92.0	18.0
eosin	86.0	26.0
Rhodamine WT ^d	85.0	17.0
Na-fluorescein	60.0	30.0
Rhodamine B ^e	90.0	45.0
Tinopal CBS-X	60.0	...
pyranine	80.0	...

^a Values listed are within $\pm 5.0\%$.

^b $\% = \frac{C_0 A_{b,d}}{C_0 A_{b,s}} \times 100$.

^c Erioglaucine is also sold with a Food, Drug and Cosmetic (FD&C) purity equal to 92.0%.

^d Rhodamine WT is not commercially available in powder form and rarely exceeds 18% purity in liquid form.

^e Rhodamine B as a liquid is mixed with glacial acetic acid.

Note: The values listed are specific to one manufacturer — crude dye stocks can and will vary significantly with manufacturer.

2.1.1.1. Recent Arguments Opposing Rigorous Tracer Mass Estimation. It has recently been argued that a rigorous approach to estimating tracer mass is unnecessary. It has further been argued that promoting such an endeavor may lead to uninformed regulators’ deciding the mass of tracer necessary for the proposed experiment. However, neither of these arguments is justifiable.

The argument suggesting that a rigorous tracer-mass estimation is an unnecessary effort is promoted by those individuals who have traditionally relied on the method of conjecture as a means for estimating tracer mass. Conjecture abrogates the need for taking time-consuming field measurements and it suggests an air of all-knowing by the conjecturer. It may just be adequate for these individuals because they are uninterested in conducting a quantitative tracer test. A qualitative trace that only roughly approximates tracer trajectories and velocities is all that is desired, so a good estimate of tracer mass to release is not considered because of the vagaries of tracer sorption by activated carbon.

The argument that inexperienced or “know-nothing” regulators will begin deciding appropriate tracer masses may be regarded as fallacious. It is a useful scare tactic often

employed to keep regulators away and to further the perception of the “all-knowing” expert. More significantly, however, it may be appropriate for regulators to estimate tracer masses if they are going to be taking the necessary field measurements that the tracer hydrologists are avoiding. If nothing else, it provides the regulator with a useful check on the conjecturer.

2.1.2. Tracer Mass Estimation by Mathematical Equation

Many equations for calculating the amount of tracer material to release into a flow system have been published. Thirty-three empirically determined equations are considered here (Table 3) (see Section 2.6., page 38 for a description of the parameters used in Table 3). It will be noted that some of the equations listed in Table 3 do not appear in original form, as they have been modified for consistency of units and to yield mass in grams. An examination of these equations reveals little about each except that most rely to some extent on volumetric flow rate (discharge). Presumably, the reliance on discharge by the originators of the equations was intended to address probable dilution effects. The 33 equations were developed empirically, so maintaining mass balance appears not to have been an important consideration. Although not apparent from Table 3, 5 of the 33 equations incorporate different systems of measurement in their original form.

Sources for the equations were not always specific about which type of tracer a particular equation was meant for in the design or about whether it even matters, but most were probably designed for the fluorescent dye Na-fluorescein. Also, it is not always clear whether an equation was intended for visual tracer detection, instrument detection in water samples, or sample collectors designed to enhance tracer concentrations (e.g., carbon sorption of fluorescent dyes via detectors).

Some equations require a “fudge factoring” constant that takes into consideration the relative detectability of the tracer to be used, the residence time within the aquifer, the type of sampling done, the method of sample collection, and/or the method of analysis. Specifics such as tracer type, methods of sampling and analysis, and fudge factor multipliers should generally be regarded as inappropriate when calculating necessary tracer mass unless a clear scientific basis for such can be established (e.g., solution-conduit sinuosity ≤ 1.5).

2.1.2.1. Review of Tracer-Mass Estimation Equations. Worthington (*pers. comm.*) examined more than 3000 tracer tests and was able to fit a straight line through a double-logarithmic plot in two separate instances. In the first instance a double-logarithmic plot of *Mass* injected versus *Time* \times *Discharge* \times *Concentration* showed a clear relationship

Table 3. Some equations for estimating tracer injection mass.

Number	Equation ^a	Secondary ^b Reference	Primary Reference
(1a)	$M = 0.56 \left(\frac{Q C_p t_p}{1000} \right)^{0.91}$...	(Worthington, <i>pers. comm.</i>) ^c
(1b)	$M = 0.56 \left(\frac{L Q C_p}{1000 v_p} \right)^{0.91}$...	(Worthington, <i>pers. comm.</i>) ^c
(2)	$M = 17 \left(\frac{Q C_p L}{3.60 \times 10^6} \right)^{0.93}$...	(Worthington, <i>pers. comm.</i>) ^c
(3)	$M = \frac{T_{C_1} L}{10}$	(Parriaux et al., 1988, p. 7)	(UNESCO, 1973-1983)
(4)	$M = T_{C_2} \left(\frac{Q L}{8.64 \times 10^4 v} \right) + \frac{V}{5.0 \times 10^4}$	(Parriaux et al., 1988, p. 7)	(UNESCO, 1973-1983)
(5a)	$M = \frac{T_{C_3} Q L}{3600}$	(Parriaux et al., 1988, p. 8) (Käß, 1998, p. 323)	(Bendel, 1948) (Dienert, 1913) ^d
(5b)	$M = \frac{T_{C_4} Q L}{3600}$	(Milanović, 1981, p. 276)	(Dienert, ?) ^e
(6)	$M = \frac{t_d C_p Q A_{d_1} S_f}{2000}$	(Parriaux et al., 1988, p. 8) (Gaspar, 1987, p. 49)	(Leibungut, 1974) (Leibungut, 1974) (Leibundgut and Wernli, 1982)
(7a)	$M = \frac{b W [2 L C_p + A_{d_2} (2 L - W)]}{3731}$	(Parriaux et al., 1988, p. 8) (Käß, 1998, p. 326)	(Leibundgut, 1981)
(7b)	$M = \frac{b L \theta [2 L C_p + A_{d_2} (2 L - W)]}{2 g}$	(Käß, 1998, p. 325)	(Leibundgut and Wernli, 1982)
(8)	$M = \frac{Q L}{3600}$	(Milanović, 1981, p. 276) (Gaspar, 1987, p. 49) (Bögli, 1980, p. 139)	(Martel, 1940) ^{c,e,f} (Martel, 1940) ^{c,e,f} (Thurner, 1967) ^e

continued on next page

Table 3. Some equations for estimating tracer injection mass (*continued*).

Number	Equation ^a	Secondary ^b Reference	Primary Reference
(9)	$M = \frac{T_{C_4} Q L}{q}$	(Milanović, 1981, p. 276) (Gaspar, 1987, p. 49)	(Guillard, ?) ^e (Guillard, ?) ^e
(10)	$M = T_{C_5} L$	(Käß, 1998, p. 325)	(Siline-Bektchourine, 1951)
(11)	$M = L T_{C_6} T_{C_7}$	(Schudel et al., 2002, p 21)	(Käß, 1998, p. 327)
(12)	$M = L \left[\left(1 + \frac{Q}{1.8 \times 10^4} \right) + \frac{Q}{3600} \right]$	(Milanović, 1981, p. 276) (Gaspar, 1987, p. 49)	(Stepinac, 1969) ^e (Stepinac, 1969) ^e
(13)	$M = \left(\frac{Q^2 L}{3600 q} \right)$	(Gaspar, 1987, p. 49)	(Heys, 1968)
(14)	$M = \frac{t_d Q P S_f}{8.64 \times 10^4}$...	(Gaspar, 1987, p. 50)
(15)	$M = \frac{T_{M_1} Q}{3600}$	(Sweeting, 1973, p. 228)	(Jenko, ?) ^e
(16)	$M = \frac{T_{M_2} q}{3600}$	(Sweeting, 1973, p. 228)	(Jenko, ?) ^e
(17)	$M = \frac{L Q}{40}$	(Davis et al., 1985, p. 101)	(Drew and Smith, 1969)
(18)	$M = \frac{C_p T_p Q L}{2500 v}$	(Aley and Fletcher, 1976, p. 7)	(Dunn, 1968)
(19)	$M = 5.0 Q$...	(Haas, 1959)
(20)	$M = 9.5 V L$...	(Haas, 1959)
(21)	$M = \frac{Q L}{366}$	(Aley and Fletcher, 1976, p. 30)	(Haas, 1959)
(22)	$M = 1478 \sqrt{\frac{Q L}{3.6 \times 10^6 v}}$...	(Aley and Fletcher, 1976, p. 9)
(23)	$M = \frac{Q C_p t_p T_p}{3398}$...	(Rantz, 1982, p. 237)

continued on next page

Table 3. Some equations for estimating tracer injection mass (*continued*).

Number	Equation ^a	Secondary ^b Reference	Primary Reference
(24)	$M = \frac{Q C_p \bar{t} T_p T_p}{747.23}$...	(Kilpatrick and Cobb, 1985, p. 8)
(25)	$M = \frac{Q C_p T_p t_2}{1000}$...	(Rathbun, 1979, p. 26) (Rantz, 1982, p. 236) (Kilpatrick and Cobb, 1985, p. 17),
(26)	$M = \frac{Q C_p \bar{t} T_p T_p}{498.15}$...	(Mull et al., 1988a, p. 37)
(27)	$M = \frac{C_p T_p T_p}{2.94} \left(\frac{Q \bar{t}}{149.53} \right)^{0.94}$...	(Kilpatrick and Wilson, 1989, p. 14)
(28)	$M = \frac{Q L}{20}$...	(Käß, 1998, p. 324)
(29)	$M = \frac{T_{M3} L I A_{pp}}{1000}$...	(Alexander and Quinlan, 1992, p. 19)
(30)	$M = S_m L$	(Käß, 1998, p. 324)	(Timeus, 1926) ^e
(31)	$M = \frac{S_m V}{100}$	(Käß, 1998, p. 324)	(Timeus, 1926) ^e
(32)	$M = \frac{V}{200}$...	(Kilpatrick, 1993, p. 14)
(33)	$M_p = Q t_p P_h$	(Käß, 1998, p. 327)	(Kinnunen, 1978)

^aSome equations slightly modified to allow consistency of units.

^bSecondary references do not always correctly reproduce the original equations.

^cSee also (Worthington and Smart, 2001).

^dDienert (1913) contains no equation for estimating tracer mass (Worthington, *pers. comm.*)

^ePrimary reference not always properly identified or readily available.

^fThe correct citation is (Martel, 1913) (Worthington, *pers. comm.*)

See the Notations list in Section 2.6., page 38.

defined by Equation (1) (Table 3). In the second instance a double-logarithmic plot of *Mass* injected versus *Length* \times *Discharge* \times *Concentration* also resulted in a clear relationship defined by Equation (2). Equations (1) and (2) provide a means for estimating the mass of dye to be injected such that positive tracer recoveries are likely.

Table 4. Aquifer and tracer-dependent coefficients $T_{C_1}-T_{C_4}$ ^a.

Aquifer	Tracer	T_{C_i}
<i>Tracer-Dependent Coefficient, T_{C_1}</i>		
clay	...	5 – 20
sand	...	2 – 10
fractured rock	...	2 – 20
karst	...	2 – 10
<i>Tracer-Dependent Coefficient, T_{C_2}</i>		
porous media	...	5.0×10^2
fractured rock	...	3.0×10^3
<i>Tracer-Dependent Coefficient, T_{C_3}</i>		
very permeable aquifers	Na-fluorescein	2.5×10^{-1}
slightly permeable aquifers	...	1.0×10^0
...	NaCl	2.5×10^2
<i>Tracer-Dependent Coefficient, T_{C_4}</i>		
...	Na-fluorescein	2.5×10^{-9}

^a Source: Adapted from Parriaux et al. (1988).

Equations (3)–(7a) were published by Parriaux et al. (1988) in a tracing guide that was intended to be practical but is obscure and difficult to obtain. Equation (7b) is a slightly more complicated form of Equation (7a). According to Parriaux et al. (1988), citing Zötl (1974), Equations (3)–(7a) were developed for Na-fluorescein, but they may be used for tracing with *Lycopodium* spores by using 1.5–2.0 times the weight of Na-fluorescein. Zötl further suggests that higher amounts can only be advantageous. Equations (3)–(5) also include an aquifer and/or tracer-dependent coefficient T_{C_i} (Table 4), which is intended to adjust the tracer mass to be injected. Equation (4) is valid for Na-fluorescein, but for

eosin (45380 C.I. Acid Red 87), five to 10 times more dye is required (Parriaux et al., 1988, p. 7). Quoting from Zötl (1974), Parriaux et al. (1988, p. 8) suggest that although Equation (5a) is appropriate for Na-fluorescein sorption onto detectors, two to three times more dye is required for water samples. Although not stated, Zötl was probably referring to visual detection of fluorescent dye in water when detectors are not being used. Equation (5b) appears similar to Equation (5a), but the full citation and primary reference are not provided in Milanović (1981, p. 276), and it includes a tracer-dependent coefficient T_{C_4} , which may be a misprint.

Equations (6) and (7) include a sorption coefficient A_{d_i} that is intended to increase tracer mass for which units are either not clearly provided [Equation (6)] or are inconsistent with common application [Equation (7)]. For Equation (6), Parriaux et al. (1988, p. 8) recommend $t_d = 3L/v$, suggesting that the tracer test duration is expected to be three times the mean residence time distribution \bar{t} . For Equation (7), $A_{d_2} = 1.0 \text{ mg m}^{-3}$ for Na-fluorescein and $A_{d_2} > 1.0 \text{ mg m}^{-3}$ for all other dyes depending on their respective sorption characteristics (Käb, 1998, p. 325).

Equation (7) includes an additional “safety factor” S_f that is not intended to protect human health or the environment from excessive tracer mass releases. Rather, S_f is intended to ensure adequate tracer-mass injection by acting as a fudge factor multiplier to increase the mass of tracer to be released. Equation (7b) is the equivalent of Equation (7a) adjusted for some tracer entrance angle other than 30° . The original form of Equation (7b) listed in Käb (1998, p. 325) includes what appears to be some time value multiplied by gravitational acceleration g , but these parameters are not identified and no units are provided. It is probable that Equation (7b) required multiplication by g^{-1} in suitable units (e.g., cm s^{-2} , m s^{-2}). For this review, Equation (7b) has been appropriately adjusted.

Equations (8)–(28) are generally similar to Equations (3)–(7). Equation (8) was intended for visual detection of Na-fluorescein. Equations (9), (10), and (11) each include an aquifer- and/or tracer-dependent coefficient T_{C_i} (Tables 4 – 7).

Table 5. Aquifer and tracer-dependent coefficient T_{C_5} ^a.

Tracer Dye	Clay Stone	Sandstone	Fractured Rock	Karst
Na-fluorescein	0.5 – 2.0	0.2 – 1.0	0.2 – 2.0	0.2 – 1.0
eosin	0.5 – 2.0	0.2 – 1.0	0.2 – 2.0	0.2 – 1.0
erthrosine	1.0 – 4.0	1.0 – 3.0	1.0 – 4.0	1.0 – 4.0
congo red	2.0 – 8.0	2.0 – 6.0	2.0 – 8.0	2.0 – 8.0
Methyl blue	2.0 – 8.0	2.0 – 6.0	2.0 – 8.0	2.0 – 8.0
Spirit blue	2.0 – 8.0	2.0 – 7.0	2.0 – 8.0	2.0 – 8.0
Ponceau red	1.0 – 4.0	1.0 – 3.0	1.0 – 4.0	1.0 – 4.0

^a Source: Adapted from (Käb, 1998, p. 325).

Table 6. Tracer dependent coefficient T_{C_6} ^a.

Tracer Material	T_{C_6}	T_{C_6} ^b
Na-fluorescein	1.0×10^0	1.0×10^0
eosin	5.5×10^0	$2.0 - 3.0 \times 10^0$
Sulpho Rhodamine G	2.0×10^0	2.0×10^0
Rhodamine B	1.5×10^1	...
Sulpho Rhodamine B	4.0×10^0	4.0×10^0
Rhodamine WT	2.0×10^1	...
Pyranine	5.5×10^0	5.0×10^0
Na-Naphthionate	1.5×10^1	1.5×10^1
Tinopal	3.0×10^0	2.5×10^2
Duasyne	...	4.0×10^0
NaCl	2.0×10^4	1.0×10^4
LiCl	1.0×10^3	1.0×10^3
KCl	1.0×10^4	...
KBr	...	$3.0 - 5.0 \times 10^3$
spores	1.5×10^0	...
surfactants	2.0×10^1	...
phages (particle count)	1.0×10^{13}	1.0×10^{12}
<i>Serratia marcescens</i>	1.0×10^{13}	...
microspheres	1.0×10^{12}	1.0×10^{12}
indium	1.0×10^{-1}	...

^a Source: Adapted from (Käb, 1998, p. 327).

^b Modifications to T_{C_6} from (Schudel et al., 2002, p 21).

Equation (11) as listed in Käb (1998, p. 327) requires two independent coefficients, T_{C_6}

Table 7. Prevailing test conditions coefficient T_{C_7} ^a.

Prevailing Condition	T_{C_7}	T_{C_7} ^b
Rapid flow in channels	0.1 – 0.9	...
Photosensitive decay	2.0 – 4.0	...
Surface-water flow $Q > 3.6 \times 10^6$	2.0 – 4.0	...
River-bank filtration $Q \leq 1.8 \times 10^4$	2.0 – 4.0	...
Ground-water flow $K < 0.36 \text{ m h}^{-1}$...	1.00 <i>b</i>
Ground-water flow $K < 3.6 \text{ m h}^{-1}$ [?]	2.0 – 4.0	...
Ground-water flow $0.36 < K < 3.6 \text{ m h}^{-1}$...	0.50 <i>b</i>
Ground-water flow $K > 3.6 \text{ m h}^{-1}$...	0.25 <i>b</i>
Fractured-rock studies	...	0.2 – 2.0
Fractured-rock studies with $\psi > 60^\circ$	2.0 – 4.0	2.0 – 4.0
Karstic aquifers in general	...	0.2 – 1.0
Karstic aquifers with inflow	...	$10 \left(\frac{Q}{3.6 \times 10^5} \right)^{0.93}$
Unsaturated zone 1–30 m thick	2.0 – 4.0	...
Low tracer-background levels	2.0 – 4.0	...
Turbid samples or samples with natural fluorescence	2.0 – 4.0	...
Unsaturated zone >30 m thick	5.0 – 10.0	...
Soil zone with cohesive soils	5.0 – 10.0	...
Studies near a ground-water divide	5.0 – 10.0	...
Multiple recovery stations likely	5.0 – 10.0	...

^a Source: Adapted from (Käb, 1998, p. 328).

^b Modifications to T_{C_7} from (Schudel et al., 2002, p 21).

and T_{C_7} (Tables 6 and 7), which requires considerable insight and/or experience on the part of the practitioner. Modifications to T_{C_6} and T_{C_7} were obtained from Schudel et al. (2002, p 21) as shown in Tables 6 and 7 but the requirements of insight and experience have not been alleviated.

Equation (12) is listed as being valid only when $Q \leq 5.0 \text{ m}^3 \text{ s}^{-1}$ and $L \geq 12 \text{ km}$. Equation (13) uses a ratio of swallet inflow to spring discharge Q/q , although the reasoning for this is not explained. Equation (13) is expected to overestimate tracer mass for predominantly vadose systems $> 1 \text{ km}$ (Gaspar, 1987, p. 49).

Equation (14) is intended for use with In-EDTA, and it also includes a loss coefficient $P = 1\text{--}3$ and a safety factor $S_f < 2$. The loss coefficient P represents the mass injected to the mass recovered, and it is justified on the reasoning that some mass of the tracer will be retained in the system (Gaspar, 1987, p. 50). The rationale for setting S_f at < 2 is not

explained.

Equations (15) and (16) rely on a set amount of dye to be injected per rate of spring discharge or swallet inflow, respectively. These two equations are probably intended for visual detection and, reportedly, reduced amounts of fluorescent dye could be released if detectors are used for dye sorption (Sweeting, 1973, p. 228).

Equation (17) is described in a very confusing manner in Davis et al. (1985, p. 101). The description appears as: “They [(Drew and Smith, 1969)] recommended using 60 grams of dye per kilometer of underground travel, per 0.15 cubic meters per second of discharge, at the largest likely rising.” A more clearly worded statement would have stated that 60 grams of dye is recommended for every kilometer of underground travel for 15% of discharge ($\text{m}^3 \text{s}^{-1}$) at the largest likely rising.

Equations (18), (21), and (22) were published by Aley and Fletcher (1976) in a tracing guide that was also intended to be a practical guide. Equation (18) is listed as being applicable for surface water and was intended for time-of-travel studies using Rhodamine WT. It includes an unidentified multiplier that may be a unit conversion factor, although this is not clear. The original form of Equation (18) is reported as a volume with units of milliliters (Aley and Fletcher, 1976, p. 7), but this requires that the unidentified multiplier be a unit conversion factor representing tracer density. The multiplier appears much too large to solely represent tracer density, so it is likely that it is a combined conversion factor representing density and a fudge factor. Equation (18) is a modification of the original equation by Aley and Fletcher (1976, p. 7) to obtain mass in grams, on the assumption that the original equation really was intended to yield a volume in milliliters.

Equations (19)–(21) represent a progression in development as technology improved (Haas, 1959) and are really only variants of Equation (8). Equation (19) was intended for visual detection and relates a specific amount of tracer dye mass to discharge and distance. Equation (20) was intended for ultraviolet light enhancement and relates tracer dye mass to system volume and distance. Equation (21) was intended for adsorption onto activated carbon and relates tracer dye mass to discharge and distance, but it may be expected to yield excessive amounts of tracer material (Aley and Fletcher, 1976, p. 9).

Equation (22) is intended for tracing ground-water flow using Na-fluorescein and is applicable to waters of $\text{pH} > 5.5$, transport via solution conduits, and dye sorption by detectors. Substituting Rhodamine WT for Na-fluorescein requires 2 to 10 times more tracer dye (Aley and Fletcher, 1976, p. 9). This equation supposedly results in reduced tracer quantities because it does not rely on proposed downstream C_p (Aley and Fletcher,

Table 8. Tracer-dye mass per 1000 m of traced distance.

Tracer Material	T_{M_3} , grams
Na-fluorescein	282
Rhodamine WT	280
Diphenyl Brilliant Flavine 7GFF	≥ 846
Tinopal 5BM GX	≥ 846
Tinopal BBH Pure	≥ 846
Phorwite AR	1694

1976, p. 7–9), although the unsuitability of such a reliance is not clear.

Equations (23)–(27) specifically relate to actual dye mass, they mix English and Metric units, and they require multiplication by unidentified unit conversion factors. Each of these four equations requires the use of the specific tracer dye factors of density and purity, but they were primarily intended for use with liquid Rhodamine WT. Equations (23)–(25) were intended for discharge measurements in surface-water streams, where Equations (23) and (24) represent an impulse release and Equation (25) a long-pulse release (e.g., $t_2 > \bar{t}$). Equation (25) appears very differently in the three primary references, but application of consistent units and simplification shows that the original forms of Equation (25) are identical.

Equation (26) is a slight modification of Equation (24) and is intended for solution conduits in that it includes the multiplier 1.5 to account for solution conduit sinuosity. Equation (27) was designed for time-of-travel studies in surface-water streams and will produce slightly different results from those obtained with Equation (23) (Kilpatrick and Wilson, 1989, p. 14) and Equation (24).

Equation (28) is identified in the United States as a “rule of thumb” formula for determining the appropriate mass of *Lycopodium* spores to release. It relates a percentage of discharge with a percentage of distance to obtain the mass needed (Käß, 1998, p. 325).

Equations (29)–(33) are somewhat different from most of the other equations. Equation (29) has also been generally considered as a rule of thumb in the United States for tracing flow in solution conduits. Unlike most of the previous 28 equations, Equation (29) does not rely on discharge to determine the appropriate tracer mass to be used. Rather, it relies on mass associated with a specific tracer dye type required for the expected travel distance (Table 8). It was originally intended for visual dye confirmation in elutant ($I = 1.0$), but the

use of analytical instruments has allowed a reduction in required tracer mass ($I = 0.01$ to $I = 0.1$). For tracing in the Appalachians, approximately five times as much dye is needed for success (Quinlan, *pers. comm.*).

Equations (30) and (31) are considered valid for tracing water flow in solution conduits using Na-fluorescein (Käb, 1998, p. 324). For Equation (30), $S_m = 1.0$ for $L > 100$ m up to some unspecified upper limit and $S_m = 2.0$ for $L > 1000$ m also up to some unspecified upper limit. Equation (31) suggests 1 to 2 grams of dye per 100 m³ of water to be traced.

Equations (32) and (33) are for conditions different from those of the previous 30 equations. Equation (32) was designed to estimate tracer mass for lakes and estuaries with a 1 µg L⁻¹ average concentration at the expected sampling locations. Equation (33) was designed for phage tracing and includes a phage factor. It appears to be little different from the other equations in that it also relies on discharge and peak arrival. However, it utilizes a phage factor and rather than having units of mass in grams it has units of N_p m³ where N_p represents the number of phage.

Flow discharge is clearly the main factor for the majority of the 33 equations listed, suggesting that tracer dilution estimates were an overriding concern during development. Expected transport distance or transport time are also generally common elements. All other factors included in the equations were intended to address either known complications (e.g., transport distance) or unknown complications (e.g., sorption) that are expected to influence final downstream concentrations.

It should be noted that many of the parameters listed in Table 3 require preliminary calculations. For example, $t_d = 3\bar{t}$ (Parriaux et al., 1988, p. 8) for tracer tests in solution conduits may be estimated from

$$t_d = \frac{3L}{v} = \frac{3LA}{Q}, \quad (34)$$

and t_d for forced-gradient tracer tests in porous media may be estimated from

$$t_d = \frac{3L}{v} = \frac{3L^2 \pi b n_e}{Q}. \quad (35)$$

Such essential calculations are not immediately obvious, however.

It is also necessary to point out that any equations that require tracer purity T_p in the calculations, for example, Equations (18) and (23)–(27), will be greatly affected by minor changes in the value of T_p . For these equations, fluorescent dye type can profoundly affect how much tracer will be recommended because of the varying concentrations of different dyes and their form, liquids or powders.

2.1.2.2. Review of Sampling Frequencies. The most uncertain aspect of any tracing study is the schedule for sample collection (Kilpatrick and Wilson, 1989, p. 16). Whereas much effort has gone into estimating tracer mass for a tracing study, very little appears to have been done in terms of determining sample collection frequency. Sampling frequencies are generally based on travel distances, which suggests a direct relationship between travel distance and expected time of arrival. This relationship is obviously correct, but it is ambiguous because transport velocity as a function of residence time is unknown. Transport velocities can achieve extreme ranges, rendering invalid sampling schedules based on transport distances that are devoid of residence time estimates.

Tracer test sampling frequencies are typically based on two approaches. In the first instance, for transport via solution conduits, tracer recovery from qualitative tracing tests (e.g., sorption of fluorescent dyes onto detectors) that are sampled every few hours, days, or weeks (Alexander and Quinlan, 1992, p. 21) (most commonly every 1 to 2 weeks) serves as a basis for determining appropriate sampling frequencies for quantitative-tracing tests. Sampling schedules based on qualitative tracing tests have been found to result in false positive results (Field, 2000, pp. 11–14) and false negative results (Smart et al., 1986) and cannot be relied upon for predicting sampling times.

In the second instance, sampling frequencies may be based on transport distances from tracer injection points to expected tracer recovery stations with due consideration to travel times. For surface-water streams, Kilpatrick and Wilson (1989, p. 16) suggest that

$$t_p = 2.78 \times 10^{-4} \frac{L}{v_p} \quad (36)$$

can be used to determine when to initiate sampling for detection of the tracer leading edge and 10% of the trailing edge. Leading edge is given by (Kilpatrick and Wilson, 1989, p. 18)

$$t_l = t_p - \frac{t_{d_{10}}}{3} \quad (37)$$

and 10% of the tracer trailing edge by (Kilpatrick and Wilson, 1989, p. 18)

$$t_{t_{10}} = t_p + \frac{2t_{d_{10}}}{3} \quad (38)$$

Although no criteria were specified, (Kilpatrick and Wilson, 1989, p. 18) suggest that the number of samples to be collected can be determined by dividing $t_{d_{10}}$ by 30, which will result in an appropriate sampling frequency necessary for describing the BTC.

A general sampling schedule is shown in Table 9, where sampling times are based on travel distance and daily lack of tracer recovery. A specific schedule is shown in Table 10,

where sampling times are based on travel distance and lack of timely recovery. In both these instances sampling frequency was initially determined as a factor of transport distance, but it is iteratively adjusted to longer times as tracer recovery is delayed.

A simpler but more realistic method uses average expected travel velocity that is based on current-meter measurements for surface streams. For a porous medium, Darcy's law may be used to gain a general sense of tracer time of arrival, provided required parameters (e.g., effective porosity) are available. For solution conduits, an expected average transport velocity equal to 0.02 m s^{-1} may be used as the basis for designing a sampling schedule (Worthington et al., 2000). This average transport velocity of 0.02 m s^{-1} was statistically determined by regression analyses of 2877 tracing tests between sinking streams and springs in carbonates in 37 countries (Worthington et al., 2000). It has been suggested that sampling frequency should not be based on average velocity because the leading edge will be missed (Kilpatrick and Wilson, 1989, p. 12), but this can be overcome by recognizing that the average velocity is a rough estimate and represents a rough average travel time. The suggested sampling frequency can be appropriately adjusted to ensure that initial sample collection begins prior to likely tracer breakthrough.

2.2. EFFICIENT HYDROLOGIC TRACER-TEST DESIGN (EHTD)

To better facilitate tracer testing in hydrologic systems, the EHTD methodology was developed (Field, 2002a). Unsuccessful quantitative tracer tests using several of the tracer mass estimation equations listed in Table 3 and recommended sample collection frequencies listed in Tables 9 and 10 and previous qualitative tracer test results led to the development of EHTD. Application of EHTD to the study site resulted in successful tracer tests and showed that good tracer test design can be developed prior to initiating a tracer test (Field, 2000, p. 26).

2.2.1. Basic Design of EHTD

EHTD is based on the theory that field-measured parameters (e.g., discharge, distance, cross-sectional area) can be combined in functional relationships that describe solute transport processes related to flow velocity and times of travel. EHTD applies these initial estimates for times of travel and velocity to a hypothetical continuous stirred tank reactor (CSTR) as an analog for the hydrologic flow system to develop initial estimates for tracer concentration and axial dispersion based on a preset average tracer concentration. Root determination of the one-dimensional advection-dispersion equation (ADE) using the preset

Table 9. General sampling schedule for a karst terrane^a.

Distance, km	Sampling Interval, hours					
	Day 1	Day 2	Day 3	Days 4–6	Day 6	Day 15
1	2	3	4–6	8–12	24	24
1–10	4	6	8	12	24	48
>10	12	12	12	12	24	48

^a Source: Adapted from (Milanović, 1981, p. 275) and (Gaspar, 1987, p. 57).

Table 10. Specific sampling schedule for a karst terrane^a.

Site No.	Distance, km	Sampling Interval, hours					
		Days 1–2	Days 3–4	Days 5–7	Days 8–14	Days 15–21	Days 22–49
1	0.60	2	4	6	12	24	56
2	0.95	2	4	6	12	24	56
3	1.40	4	6	12	24	24	56
4	2.90	4	6	12	24	24	56
5	5.00	4	6	12	24	24	56
6	11.00	12	12	24	24	24	56

^a Source: Adapted from Käß (1998, p. 333).

average concentration then provides a theoretical basis for an estimate of necessary tracer mass. Application of the predicted tracer mass with the hydraulic and geometric parameters in the ADE allows for an approximation of initial sample-collection time and subsequent sample collection frequency where 65 samples have been empirically determined to best describe the predicted BTC.

2.2.2. Range of Capabilities of EHTD

Although most of the tracer mass estimation equations listed in Table 3 were designed for tracing in solution conduits in karstic terranes, there appears to be no logical reason to exclude porous media systems. The fact that solute transport processes in hydrologic systems all follow the same basic theoretical principles suggests that an appropriate model for estimating tracer mass would function effectively for all hydrological systems. However, such a model would need to be able to account for slight differences in the nature of the flow systems (e.g., effective porosity) and the manner in which the tracer test is conducted (e.g., tracer release mode).

Breakthrough curves predicted using the tracer test design program EHTD for various hydrological conditions have been shown to be very reliable (Field, 2002c). The hydrologic conditions used to evaluate EHTD ranged from flowing streams to porous media systems so that the range of capabilities of EHTD could be assessed. The flowing streams used to evaluate EHTD included tracer tests conducted in small and large surface-water streams, a solution conduit, and a glacial-meltwater stream. The porous media systems used to evaluate EHTD included natural gradient, forced gradient, injection withdrawal, and recirculation tracer tests. Comparisons between the actual tracer tests and the results predicted by EHTD showed that EHTD adequately predicted tracer breakthrough, hydraulic characteristics, and sample collection frequency in most instances.

2.3. TRACER-TEST DESIGN RESULTS USING PREVIOUS METHODS

Tracer-test design examination parameters provided by Parriaux et al. (1988) and reprinted in Käb (1998, p. 324) have previously been applied to a small set of the 33 equations listed in Table 3. Unfortunately, only a few of these equations were examined using the test examination parameters. Although not stated it is likely that one of the reasons for the limited examination is that additional parameters are necessary for testing the equations.

2.3.1. Examination of Tracer-Mass Estimation Equations

The tracer-test design examination parameters originally listed in Parriaux et al. (1988)—and reprinted in Table 11 with additional parameters—were applied to 32 of the 33 equations in Table 3. Liquid Na-fluorescein, which is considered to be the tracer material used, is conventionally available as a 30% solution ($T_p = 0.3$) and has a density of 1.2 g cm^{-3} . Equation (33) was not evaluated because it was designed for conditions other than those listed in Table 11. Tracer mass estimates using the tracer test design examination parameters and Equations (1)–(32) resulted in tracer mass estimates that ranged from a fraction of a gram of tracer to tens of thousands of grams of tracer (Table 12). Large tracer mass ranges are probable using the same equation when variable hydrologic conditions and/or tracer-dependent coefficients T_{C_i} are applied. Equation (25) is expected to produce greater tracer mass estimates than the other equations because it is based on a long-pulse release ($t_2 > \bar{t}$), which will also cause a much later real value for t_p than the one listed in Table 11.

For perspective, the results of Equations (1)–(32) may be compared to similar results produced by

$$M = \frac{T_p Q 10^6}{\delta(t)} \quad (39)$$

for an impulse release and

$$M = T_p Q t_2 10^6 \quad (40)$$

for a pulse release. Although Equations (39) and (40) were not found in any of the references listed in Table 3, it is likely that they are commonly used because they exhibit mass balance. However, there appears to be no reason to believe that either would yield reasonable results because Q is the only included flow system parameter.

2.3.1.1. Porous Media. Application of Equations (1)–(32) to the porous media examination parameters listed in Table 11 resulted in tracer mass estimates that ranged from $2.5 \times 10^{-8} \text{ g}$ to $4.75 \times 10^8 \text{ g}$, or a difference of >16 orders of magnitude (Table 12). If Equations (5b), (9), and (20) are removed from consideration, the difference is 3 orders of magnitude. Equations (5b) and (9) may legitimately be removed from consideration on the assumption that T_{C_4} was misprinted in Milanović (1981, p. 276). Equation (20) may also include a misprint (volume rather than discharge). A range of 3 orders of magnitude for tracer mass is difficult to resolve without additional information or site-specific experience.

Table 11. Tracer test design parameters.

Parameter	Porous Media	Karst
Q , $\text{m}^3 \text{h}^{-1}$	7.20×10^1	3.60×10^2
L , m	5.00×10^2	3.00×10^3
W , m	1.00×10^2	1.00×10^2
V , m^3	1.00×10^5	3.00×10^5
b , m	1.00×10^1	1.00×10^2
n_e	1.00×10^{-2}	1.00×10^1
v , m h^{-1}	4.17×10^{-1}	4.17×10^1
q^{a} , $\text{m}^3 \text{h}^{-1}$	7.20×10^{-1}	3.60×10^1
t_d , h	3.60×10^3	2.16×10^2
t_p^{b} , h	1.20×10^3	7.20×10^1
C_p , mg m^{-3}	1.00×10^1	1.00×10^1
A_d , mg m^{-3}	1.00×10^0	1.00×10^0
θ^{c} , rad	5.24×10^{-1}	5.24×10^{-1}
S_f	1.00×10^0	1.00×10^0
t_2^{d} , h	1.56×10^3	9.63×10^1
T_{C_1}	5.00×10^0	2.00×10^0
T_{C_2}	3.00×10^3	5.00×10^3
T_{C_3}	2.50×10^{-1}	2.50×10^{-1}
T_{C_4}	2.50×10^{-9}	2.50×10^{-9}
T_{C_5}	5.00×10^{-1}	5.00×10^{-1}
T_{C_6}	1.00×10^0	1.00×10^0
T_{C_7}	5.00×10^{-1}	5.00×10^{-1}
T_{M_1} , g	2.00×10^3	2.00×10^3
T_{M_2} , g	2.40×10^4	2.40×10^4
T_ρ , g cm^{-3}	1.20×10^0	1.20×10^0
T_p	3.00×10^{-1}	3.00×10^{-1}
A_{pp}	5.00×10^0	1.00×10^0
I	1.00×10^{-1}	1.00×10^{-1}
S_m	1.00×10^0	1.00×10^0

^a $q = Q/100$ ^b $t_p = t_d/3$ ^c $\theta = 30^\circ$ ^d $t_2 = 1.3 t_p$

Adapted from Parriaux et al. (1988, p. 9).

Table 12. Tracer-mass estimates.

Equation ^a	Porous Media, g	Karst, g
(1a)	2.63×10^2	8.80×10^1
(2)	2.00×10^0	4.72×10^1
(3)	2.50×10^2	6.00×10^2
(4)	3.00×10^3	1.56×10^2
(5a)	2.50×10^0	7.50×10^1
(5b)	2.50×10^{-8}	7.50×10^{-7}
(6)	1.30×10^3	3.89×10^2
(7a)	2.92×10^3	1.77×10^5
(7b)	2.92×10^3	1.76×10^5
(8)	1.00×10^1	3.00×10^2
(9)	1.25×10^{-4}	7.50×10^{-4}
(10)	2.50×10^2	1.50×10^3
(11)	3.50×10^3	1.50×10^3
(12)	5.12×10^2	3.36×10^3
(13)	1.00×10^3	3.00×10^4
(14)	3.00×10^0	9.00×10^{-1}
(15)	4.00×10^1	2.00×10^2
(16)	4.80×10^0	2.40×10^1
(17)	9.00×10^2	2.70×10^4
(18)	4.15×10^2	1.24×10^2
(19)	3.60×10^2	1.80×10^3
(20)	4.75×10^8	8.55×10^9
(21)	9.84×10^1	2.95×10^3
(22)	2.29×10^2	1.25×10^2
(23)	3.05×10^2	9.15×10^1
(24)	4.16×10^2	1.24×10^2
(25)	1.35×10^3	4.04×10^2
(26)	6.24×10^2	1.87×10^2
(27)	4.83×10^2	1.56×10^2
(28)	1.80×10^3	5.40×10^4
(29)	7.05×10^1	8.46×10^1
(30)	5.00×10^2	3.00×10^3
(31)	1.00×10^3	3.00×10^3
(32)	5.00×10^2	1.50×10^3

^a From Table 3.

For comparison purposes, Equations (39) and (40) would yield 2.16×10^7 g and 3.37×10^{10} g for the impulse and pulse releases, respectively. The results of Equation (39) appear to be the greatest of all except for those of Equation (20) and the results of Equation (40) are greater than those of all 32 examined equations (Table 12). Equations (20), (39), and (40) likely represent an absolute upper range of tracer mass to release, and releases in this range would probably be excessive and possibly harmful (Field et al., 1995; Behrens et al., 2001).

2.3.1.2. Karstic Media. Results of the karstic media examination parameters listed in Table 11 in Equations (1)–(29) produced tracer mass estimates that ranged from 7.50×10^{-7} g to 8.55×10^9 g, a difference also of >16 orders of magnitude. Removing Equations (5b), (9), and (20) results in a difference of 5 orders of magnitude. As in the case with porous media, such a large range is difficult to resolve without additional information or site-specific experience.

Equations (39) and (40) resulted in 1.08×10^8 g and 1.01×10^{10} g for the impulse and pulse releases, respectively. Equation (39) resulted in an estimated mass greater than all but that of Equation (20) (Table 12) and the results of Equation (40) are greater than those of all 32 examined equations (Table 12). As with the porous media estimates, Equations (20), (39), and (40) likely represent an upper limit for tracer mass to release, and such a release would probably be excessive and possibly harmful (Field et al., 1995; Behrens et al., 2001).

2.4. EHTD ANALYSIS OF THE TWO TRACER TESTS

As with the 33 equations listed in Table 3, use of the EHTD methodology requires that specific flow-system parameters be measured or reasonably estimated. A subset of parameters from Table 11 that represent the required parameters necessary for evaluation by EHTD are shown in Table 13. From Table 13 it is apparent that only measurable parameters related to the hydraulics of the flow system are required for EHTD analysis. However, the two tracer-specific parameters, retardation and decay, and the sinuosity factor are not required. The sinuosity factor is an adjustable multiplier ≤ 1.5 that is similar to the one used in Equation (26) except that Equation (26) requires the inclusion of $S_n = 1.5$. It is also used by EHTD to increase the measured straight-line distance by an appropriate distance, because natural solution conduits are not constrained to perfectly straight channels.

Although not presented in Table 13, EHTD also requires identification of the type of flow system tracer test, the type of release, and the time for tracer injection, in an attempt

Table 13. EHTD tracer test design parameters.

Parameter	Porous Media	Karst
Q , $\text{m}^3 \text{h}^{-1}$	7.20×10^1	3.60×10^2
A^{a} , m^2	\dots	8.63×10^0
L , m	5.00×10^2	3.00×10^3
W , m	1.00×10^2	\dots
b , m	1.00×10^1	\dots
n_e	1.00×10^{-2}	\dots
q , $\text{m}^3 \text{h}^{-1}$	7.20×10^{-1}	3.60×10^0
C_p , mg m^{-3}	1.00×10^1	1.00×10^1
t_2^{b} , h	1.56×10^3	9.63×10^1
C_i^{c} , mg m^{-3}	0.00×10^0	0.00×10^0
γ_1^{c} , dimen.	0.00×10^0	0.00×10^0
γ_2^{c} , dimen.	0.00×10^0	0.00×10^0
S_n^{c}	\dots	1.00×10^0
R_d^{c}	1.00×10^0	1.00×10^0
μ^{c} , h^{-1}	0.00×10^0	0.00×10^0

^a For this analysis, $A = Q/v$ for the karstic spring. Normally Q and A would be measured concurrently and the solution $v = Q/A$ used by EHTD.

^b Parameter required by EHTD for pulse and continuous releases.

^c These parameters not required by EHTD but must be listed in the input file.

to ensure universality. The type of flow system tracer test can be simply a flowing stream (open-channel or closed-conduit flow = surface-water stream or solution conduit) or it can be porous media. EHTD analysis of porous media systems additionally requires consideration of any one of the following hydraulic conditions:

1. Natural gradient tracer test,
2. Forced gradient tracer test (extraction well),
3. Injection/withdrawal test (injection well rate = pumping well rate), or
4. Recirculation test (injection well rate = pumping well rate while recirculating the tracer back to the injection well).

The tracer test parameters listed in Table 13 relate to a solution conduit tracer test and a

forced gradient porous media tracer test, the latter assumed because of the relatively high discharge rate ($72 \text{ m}^3 \text{ h}^{-1}$) provided by Parriaux et al. (1988, p. 9).

Type of tracer release refers to three methods of tracer injection; impulse, pulse, and continuous. Impulse (instantaneous) releases are the most common tracer injection method for karstic systems, whereas pulse releases (slow releases over some period of time) are the most common tracer injection method for porous media systems. Continuous releases are rarely employed in either system, primarily because of cost. For the porous media and karstic tracer test parameters listed in Tables 11 and 13, impulse releases were assumed except for Equation (22), in which a long-pulse release was assumed.

Time for tracer injection refers specifically to tracer injection time, but it also may include pre- and post-tracer injection flush water to account for additional dilution effects. Total dilution volume V_D is obtained from

$$V_D = (q + Q)\bar{t}, \quad (41)$$

which should not be considered a technically correct approach. However, it does yield good approximations for dilution effects, which will usually be equal to or greater than the system volume V calculated from the total discharge for the duration of the tracer test. For this analysis, V_D was of some significance because q was fairly significant.

2.4.1. EHTD Results

Application of EHTD to the parameters listed in Table 13 resulted in tracer mass estimates of 525 g for the impulse release and 1950 g for the pulse release for the porous media tracer test and 102 g for the impulse release and 631 g for the pulse release for the karstic tracer test (Table 14). To obtain these results, EHTD uses an average concentration \bar{C} rather than a peak concentration C_p . For this analysis, the peak concentration used in Equations (1)–(32) was taken as the average concentration. The effect of taking $C_p = \bar{C}$ was relatively insignificant, because $R_d = 1.0$ and $\mu = 0.0 \text{ h}^{-1}$ (Field, 2002a).

Hydraulic parameters from EHTD simulations of the porous media and karstic tracer tests are shown in Table 14. Tracer breakthrough curves for the porous media and karstic systems tracer tests are shown in Figures 1 and 2, respectively. All the parameters listed in Table 14 were calculated by EHTD using the parameters listed in Table 13. Some of the EHTD-calculated parameters listed in Table 14 (e.g., v) approximate the same parameters listed in Table 11. However, important transport parameters such as axial dispersion D_L and Péclet number P_e are uniquely calculated by EHTD. Although these parameters may

Table 14. EHTD tracer test analysis results.

Parameter	Porous Media	Karst
M^a, g	5.25×10^2	1.02×10^2
M^b, g	1.95×10^3	6.31×10^2
\bar{t}, h	1.09×10^3	7.19×10^1
t_p^a, h	9.82×10^2	6.90×10^1
t_p^b, h	1.93×10^3	1.31×10^2
$v, \text{m h}^{-1}$	4.58×10^{-1}	4.17×10^1
$v_p^a, \text{m h}^{-1}$	5.09×10^{-1}	4.35×10^1
$v_p^b, \text{m h}^{-1}$	2.59×10^{-1}	2.30×10^1
$D_L^a, \text{m}^2 \text{h}^{-1}$	7.99×10^0	1.52×10^3
$D_L^b, \text{m}^2 \text{h}^{-1}$	2.09×10^1	2.44×10^3
α^a, m	1.74×10^1	3.64×10^1
α^b, m	4.56×10^1	5.86×10^1
P_e^a	2.87×10^1	8.25×10^1
P_e^b	1.10×10^1	5.12×10^1
t_1^a, h	1.92×10^2	2.90×10^1
t_1^b, h	2.16×10^2	1.80×10^1
t_f^a, h	4.80×10^1	3.00×10^0
t_f^b, h	9.60×10^1	5.00×10^0
t_d^a, h	3.27×10^3	2.00×10^2
t_d^b, h	6.56×10^3	3.41×10^2
$C_p^a, \text{mg m}^{-3}$	1.09×10^1	1.04×10^1
$C_p^b, \text{mg m}^{-3}$	1.63×10^1	1.87×10^1
V_D, m^3	7.93×10^4	2.61×10^4
V, m^3	7.85×10^4	2.59×10^4

^a Impulse release results.

^b Pulse release results.

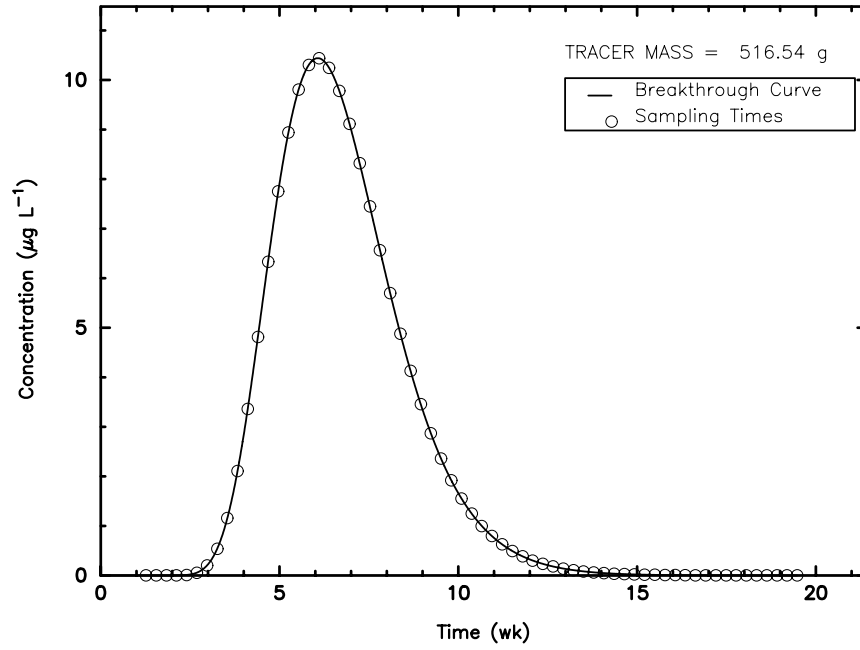


Figure 1. EHTD results for an impulse release for the porous media test parameters.

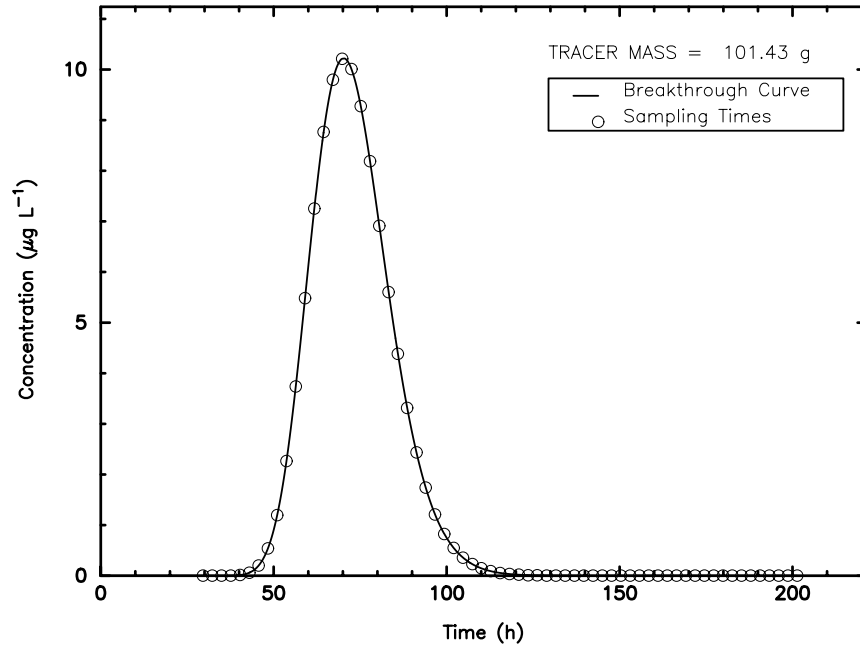


Figure 2. EHTD results for an impulse release for the karstic test parameters.

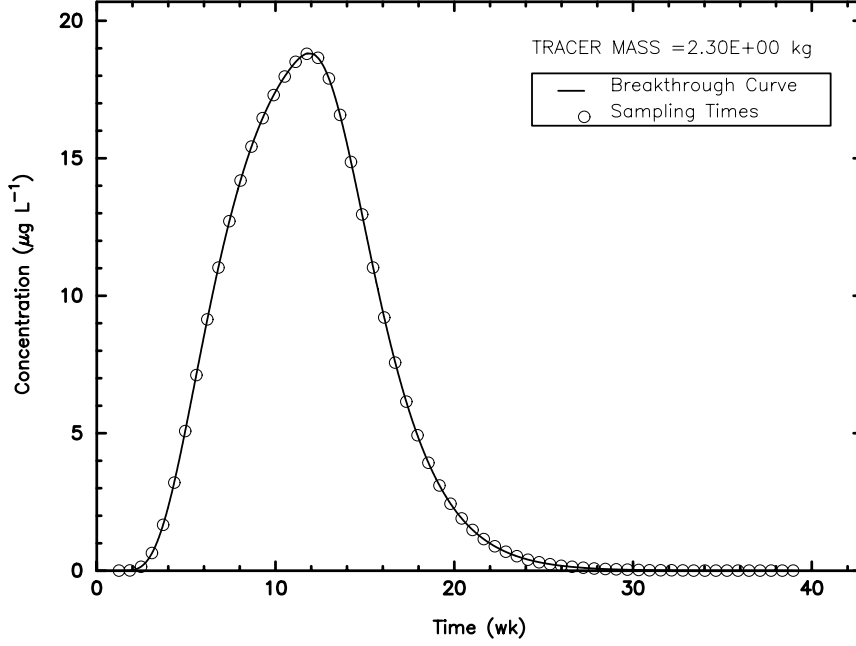


Figure 3. EHTD results for a pulse release for the porous media test parameters.

be only crudely approximated by EHTD, it has been shown that these parameter estimates are generally reasonable (Field, 2002c). Also, although \bar{t} remained unchanged regardless of the type of tracer release employed, t_p and C_p were greatly increased when a long-pulse release was employed (Table 14) (Figures 3 and 4) for the respective hydrologic systems. A long-pulse release also causes an earlier t_1 but a greater t_f (Table 14).

It will be noted that $V = 7.85 \times 10^4 \text{ m}^3$ and $V = 2.59 \times 10^4 \text{ m}^3$ for the porous media and karstic tracer tests, respectively. These volumes are much greater than the volumes listed in Table 11. The difference is a result of arbitrarily choosing of V (Parriaux et al., 1988, p. 9) as opposed to calculating V using an accepted approach such as

$$V = \frac{Q L}{v} \quad (42)$$

Applying Equation (42) results in $V = 8.64 \times 10^4 \text{ m}^3$ and $V = 2.59 \times 10^4 \text{ m}^3$ for the porous media and karstic tracer tests, respectively. Using these recalculated volumes in the equations listed in Table 3 did not significantly change the results of Equation (4), but it caused a slight decrease in the results of Equations (20) and (31) and a substantial decrease in the results of Equation (32) (Table 15). Although not expected, the estimated mass using Equation (32) with the improved estimates for V was in better agreement with the EHTD-predicted mass for the karstic media tracer test.

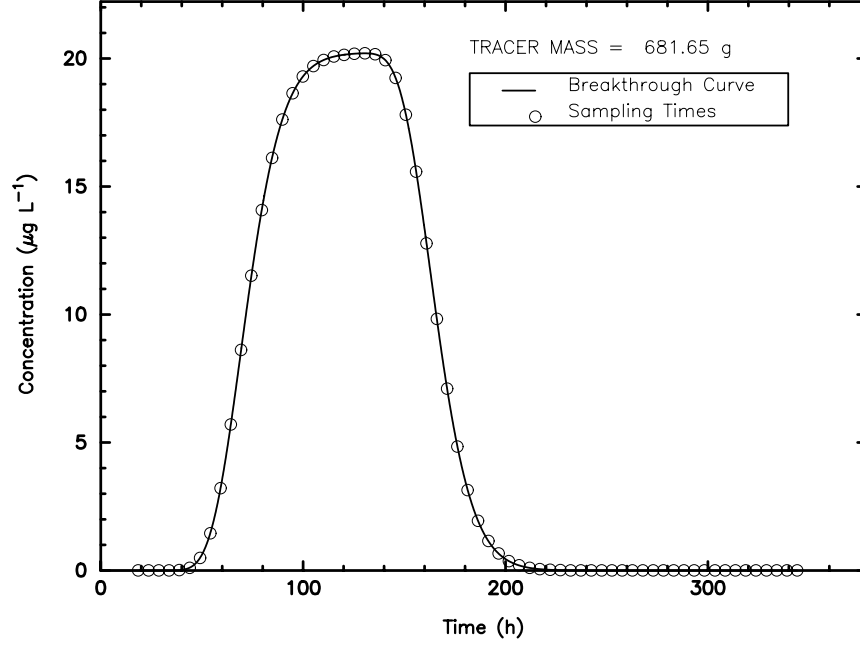


Figure 4. EHTD results for a pulse release for the karstic test parameters.

Table 15. Tracer-dye mass per 1000 m of traced distance.

Equation ^a	Porous Media, g	Karst, g
(4)	3.00×10^3	1.51×10^2
(20)	4.10×10^8	7.38×10^8
(31)	8.64×10^2	2.59×10^2
(32)	4.32×10^2	1.30×10^2

^a From Table 3.

2.4.1.1. EHTD Porous-Media Analysis Results. Comparisons with EHTD-estimated tracer mass for the impulse release for the porous media tracer test suggest that only Equations (12), (18), (23), (26), (30), and (32) can reasonably be considered for estimating tracer mass. Of these, only Equation (26) gave a greater result that was greater than the EHTD-estimated tracer mass, the other values being relatively low. Interestingly, Equation (12) is considered invalid for these conditions ($L < 12$ km), whereas Equation (30) is considered valid for tracing solution conduits. Equations (18), (23), (26), and (32) were all intended for tracing surface water. For the pulse release, Equation (25) underestimated M slightly relative to EHTD, probably as a result of the lack of consideration for additional dilution effects caused by q .

2.4.1.2. EHTD Karstic-Media Analysis Results. Comparisons with EHTD-estimated tracer mass for the karstic tracer test suggest that only Equations (1a), (4), (5a), (18), (22), (23), (26), (27), and (29) reasonably estimate the appropriate mass of tracer to release. The results of equations (1a), (5a), and (29) are low relative to the EHTD-estimated tracer mass, whereas those for Equations (4) and (18), (22), (23), (26), (27) are relatively high. Equations (4), (5a), and (29) all require the use of multipliers representing tracer-dependent factors controlled by aquifer conditions. These multipliers may also assume a range of values, but only Equation (29) is reasonably specific regarding which multiplier value to use for the given conditions. As with the porous media tracer test, the pulse release described by Equation (25) underestimated M slightly relative to EHTD, again probably as a result of the lack of consideration for additional dilution effects caused by q .

2.4.2. Mass Required as Related to Sorption by Detectors

Several of the 33 equations listed in Table 3, for example, Equations (5a), (21), (22), and (29), were specifically intended for sorption onto detectors, allowing for reduced tracer-dye concentrations. For the porous media tracer test, Equation (5a), (19), (22), and (29) all resulted in a lower estimated tracer mass than the mass suggested by EHTD. For the karstic tracer test, Equations (5a), (19)–(22), (29) all resulted in greater tracer mass estimates than suggested by EHTD.

In general, the vast majority of the 32 of 33 equations listed in Table 3 and tested resulted in much greater tracer mass estimates than suggested by EHTD for either the porous media system or the karstic system. Tracer dye concentration enhancement by activated carbon should allow for much lower tracer mass estimates than predicted by EHTD. However,

the lack of a measurable and distinct BTC that is normally obtained when water samples are collected and analyzed prevents clear determination that the dye of interest has been recovered.

2.5. TRAVEL TIMES AND SAMPLING FREQUENCIES

Typically, users of Equations (1)–(33) would initiate sample collection frequencies according to flow rates estimated using Darcy’s law for porous-media aquifers. Unfortunately, because hydraulic conductivity, hydraulic gradient, and effective porosity may not be available, Darcy’s law is difficult to apply. For karstic aquifers, weekly or biweekly sample collection schedules for qualitative tracer tests are conventionally employed. Alternatively, schedules shown in Tables 9 and 10 may be considered if water samples are to be collected. Rarely, an assumed karstic-flow velocity of 0.02 m s^{-1} may be considered in defining a sampling schedule.

2.5.1. Travel Times

The suggested time of arrival for peak concentration t_p for the tracer test design examination parameters (Table 11) of 50 days and 72 hours for the porous media case and the karstic media case, respectively, really represent \bar{t} . Because of the difficulty in estimating t_p prior to conducting a tracer test, $t_p \approx \bar{t}$ was taken as a necessary approximation. EHTD predicted $t_p = 41$ days and 81 days for the impulse release and the pulse release for the porous media tracer test, respectively, and $t_p = 70$ hours (3 days) and 131 hours (6 days) for the pulse release and the impulse release for the karstic media tracer test, respectively (Table 14). Clearly the t_p was very well approximated by EHTD for both example tracer tests.

The use of $t_d = 3L/v$ suggests durations of 150 days and 9 days for the porous media and karstic system, respectively (Table 11). EHTD, however, suggested 136 and 8 days for the porous-media and karstic system tracer tests, respectively, for an impulse release (Figs. 1 and 2) and 274 and 14 days for the porous-media and karstic system tracer tests, respectively, for a pulse release (Figs. 3 and 4) (Table 14). These differences occurred because EHTD employs a slightly different process for estimating t_d . These latter times are relatively insignificant.

2.5.2. Sampling times

EHTD suggests appropriate sampling frequencies based on the type of flow system and the type of release. In all instances, sampling-frequency suggestions are determined by the

expected times of travel and the need to adequately define the BTC. Early detection of tracer breakthrough requires that sampling be initiated prior to initial tracer breakthrough. Sixty-five samples are recommended for adequate BTC definition, especially for instances in which BTCs may be multimodal or long tailed (Field 2001a). Application of weekly or biweekly sampling schedules or the sampling schedules listed in Tables 9 and 10 would fail to adequately define either BTC.

Collecting samples for the EHTD-suggested durations t_d listed in Table 14 would clearly define the entire BTC should the tracer tests conform to the ADE. If tracer recoveries were still strong beyond the EHTD-suggested durations, sampling analyses could continue unimpeded at the EHTD-suggested frequencies.

2.5.2.1. Porous Media Sampling Times. Figures 1 and 3 depict the recommended sampling times for 65 samples that correspond, for impulse and pulse releases, respectively for the porous-media case. Suggested sampling frequencies were 48 hours for the impulse case and 96 hours for a pulse release (Table 14). Initial suggested sample-collection times were eight days and nine days after tracer injection for the impulse and pulse releases, respectively (Table 14).

2.5.2.2. Karstic Media Sampling Times. Recommended sampling times for the karstic test, for impulse and pulse releases are shown in Figures 2 and 4. Suggested sampling frequencies were three hours for the impulse case and five hours for a pulse release (Table 14). Initial suggested sample-collection times were 29 hours and 18 hours after tracer injection for the impulse and pulse releases, respectively (Table 14).

2.6. NOTATIONS FOR SECTION 2.

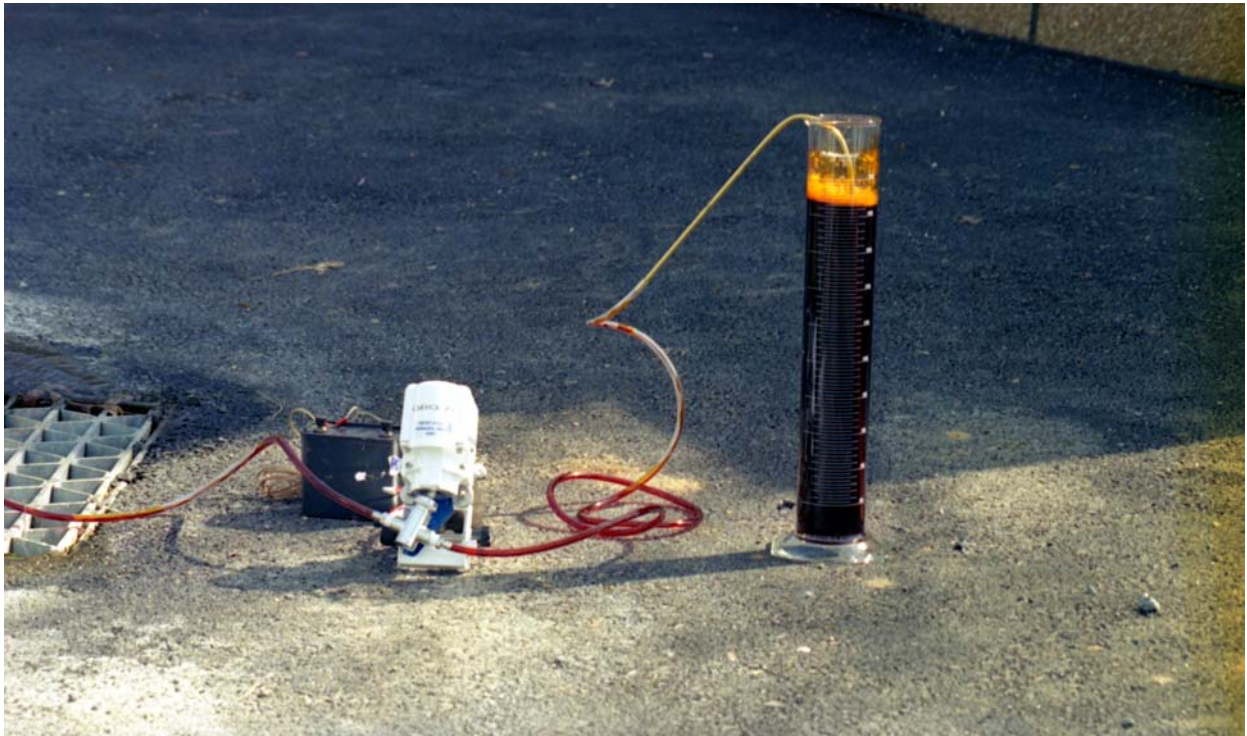
A	cross-sectional area of a spring (m^2)
A_{b_d}	absorbance of dye sample (nm)
A_{b_s}	absorbance of dye at 100% strength (nm)
A_{d_1}	tracer adsorption coefficient >1.0 ($\text{mg m}^{-3}[\text{?}]$) (Note: adsorption is normally identified as a distribution coefficient in $\text{mL}^3 \text{g}^{-1}$)
A_{d_2}	tracer adsorption coefficient ≥ 1.0 (mg m^{-3}) (Note: adsorption is normally identified as a distribution coefficient in $\text{mL}^3 \text{g}^{-1}$)
A_{pp}	multiplier for Appalachian karst = 5.0
α	dispersivity = $\frac{D}{v}$ (m)

b	aquifer thickness (m)
C_o	initial (stock) dye concentration (g m^{-3})
C_p	expected peak tracer concentration (mg m^{-3})
D_L	axial dispersion ($\text{m}^2 \text{h}^{-1}$)
g	gravitational acceleration = 978.039 at 0° Latitude[?] (cm s^{-2} [?])
I	multiplier for instrumental analysis = 0.01 to 1.0
K	aquifer hydraulic conductivity (m h^{-1} [?])
L	expected tracer transport distance (m)
M	calculated tracer mass to inject (g)
M_p	number of phage to be release ($N_p \text{ m}^3$)
n_e	effective porosity (dimen.)
θ	expected tracer entrance angle for transverse spread (degrees)
P	expected ratio of injected tracer to recovered tracer (In-EDTA) representing tracer loss = 1.0 to 3.0 (dimen.)
P_e	Péclet number = $\frac{vL}{D}$ (dimen.)
P_h	phage factor and count $\approx 2.0 \times 10^{10}$ to 5.0×10^{10} (dimen.)
ψ	tracer scattering angle (degrees)
q	inflow rate at injection point ($\text{m}^3 \text{h}^{-1}$)
Q	well or spring discharge ($\text{m}^3 \text{h}^{-1}$)
R_d	tracer retardation (dimen.)
S_f	safety factor to ensure adequate peak concentration for detection (dimen.)
S_m	multiplier for tracer mass = 1.0 to 2.0 (dimen.)
S_n	sinuosity factor = 1.0× to 1.5× (dimen.)
t_d	expected duration of tracer test (h)
$t_{d_{10}}$	expected tracer test duration at 10% of the peak concentration (s)
t_1	time for first sample to be collected (h)
t_2	tracer injection time for a pulse injection (h)
t_f	time interval for sample collection (h)
t_p	expected time to peak tracer arrival (h)
$t_{t_{10}}$	trailing edge to 10% level (h)
T_{C_i}	aquifer and tracer-dependent coefficients [Tables 4–7] (dimen.)
T_{M_1}	tracer dye (Na-fluorescein) mass to inject per spring discharge = 2.0×10^3 to 5.0×10^3 (g)
T_{M_2}	tracer dye (Na-fluorescein) mass to inject per inflow rate at injection point = 2.4×10^4

	(g)
T_{M_3}	tracer dye [Table 8] mass for 1000 m transport distance (g)
T_p	tracer purity = $\frac{A_{b_d}}{C_o A_{b_s}} \times 100$ (dimen.)
T_ρ	tracer density (g c ⁻¹ m)
μ	tracer decay (h ⁻¹)
v	average velocity for tracer migration (m h ⁻¹)
v_p	expected velocity for peak tracer migration (m s ⁻¹)
V	flow system volume (m ³)
V_D	dilution volume for a spring or well (m ³)
W	transverse spread of tracer (m)

Part II

MODEL THEORY AND METHOD DEVELOPMENT



Controlled release of slightly diluted uranine (Acid Yellow 73) into a storm drain to test for leakage. Tracer release is accomplished using a small, valveless, variable-rate, positive-displacement, fluid-metering pump operating on a 12-volt dc battery withdrawing fluid from a graduated cylinder. The decline in tracer in the graduated cylinder with respect to time provides a check on the rate of tracer release.

3. TRACER-TEST DESIGN METHODOLOGY

Previous efforts aimed at estimating tracer mass to be released for a tracer test focused primarily on expected dilution and drew upon the originators experience. None of the previous efforts appear to have been derived according to solute-transport theory. It would also appear that solute-transport theory was seldom considered in designing tracer-sampling schedules. Solute-transport theory in natural and controlled systems has been investigated extensively and is well-understood. It would seem appropriate then to consider solute-transport theory as a tool for determining the optimal tracer mass for release and sample-collection frequency.

3.1. SOLUTE-TRANSPORT MODELING

Numerous model variations designed to describe solute transport have been developed. A general one-dimensional advection-dispersion equation (ADE) typically appears as (see Notations section)

$$R_d \frac{\partial C}{\partial t} = D \frac{\partial^2 C}{\partial z^2} - v \frac{\partial C}{\partial z} - \mu C + \gamma(z) \quad (43)$$

The retardation factor R_d can represent retardation in porous media by (Freeze and Cherry, 1979, p. 404)

$$R_d = 1 + \frac{\rho_b K_d}{\theta} \quad (44)$$

or R_d can represent retardation in fractured media by (Freeze and Cherry, 1979, p. 411)

$$R_d = 1 + \frac{2K_a}{b_f} \quad (45)$$

or R_d can represent retardation in a solution conduit by (Field and Pinsky, 2000)

$$R_d = 1 + \frac{2K_a}{r} \quad (46)$$

The first-order rate coefficient for tracer decay μ in porous media is given as (Toride et al., 1995, p. 3)

$$\mu = \mu_l + \frac{\rho_b K_d \mu_s}{\theta} \quad (47)$$

in fractured media may be taken as

$$\mu = \mu_l + \frac{2K_a \mu_s}{b_f} \quad (48)$$

and in solution conduits may be taken as

$$\mu = \mu_l + \frac{2K_a\mu_s}{r} \quad (49)$$

If tracer decay for the liquid phase μ_l equals tracer decay for the sorbed phase μ_s then the combined first-order decay μ is equal to $\mu_l R_d$ (Toride et al., 1995, p. 4) which is a reasonable assumption commonly employed (Toride et al., 1995, p. 35).

The zero-order production coefficient $\gamma(z)$ in porous media is given as (Toride et al., 1995, p. 3)

$$\gamma(z) = \gamma_l(z) + \frac{\rho_b \gamma_s(z)}{\theta} \quad (50)$$

It is applicable to fractured media and solution conduits with $\theta = 1$ (100%).

3.2. TRACER MASS ESTIMATION

The most straightforward method for estimating tracer mass is to obtain a solution to Equation (43) and then solve for average concentration or its real root $f(x^*) \approx 0$. As a basic control, it is necessary to include a desired average concentration \bar{C} that corresponds to average time \bar{t} or peak concentration C_p that corresponds to peak time t_p .

A simple solution to Equation (43) for a Dirac (δ) function for obtaining the maximum tracer concentration that ignores tracer retardation and decay is

$$f(x^*) = C_p - \frac{M}{A n_e \sqrt{4\pi D_z t_p}}, \quad (51)$$

which may be solved explicitly for tracer mass M . Equation (51) will generally provide a reasonable estimate for M , provided reasonable estimates are available for the other parameters. However, Equation (51) may be oversimplified for many applications because it deals only with peak concentration and lacks consideration of tracer retardation and tracer decay. Applying Equation (51) may result in excessive tracer mass estimates, which is neither desirable from a hydrologic, aesthetic, economic, human health, or ecological perspective, nor is it necessary to achieve positive tracer recovery. Alternatively, actual tracer retardation and/or tracer decay may result in tracer mass estimates that are too small for adequate tracer recovery.

Application of more comprehensive solutions to Equation (43) will provide a more reasonable and reliable estimate for the tracer mass to be injected. Some solutions to Equation (43) can be evaluated explicitly for M , but other solutions for (43) may require evaluation for its real root for some $x^* \in [a_1, a_2]$, where x^* represents the estimated mass M .

3.2.1. Model Solutions

Solutions for Equation (43) for impulse and pulse releases are most appropriate for estimating tracer mass. A continuous release is less relevant because most tracer tests involve a finite time period for release. Although not a physical reality, it is probable that most tracer tests, especially in karstic aquifers, attempt to achieve an impulse release that may be described as a Dirac (δ) pulse. However, many attempts at an impulse release are actually pulse releases due to the time involved for the tracer to reach the flow system under investigation (Field, 1997; Field and Pinsky, 2000).

Applying the dimensionless parameters listed in the Notations section to Equation (43) result in (Toride et al., 1995, p. 4)

$$R_d \frac{\partial C_r}{\partial T} = \frac{1}{P_e} \frac{\partial^2 C_r}{\partial Z^2} - \frac{\partial C_r}{\partial Z} - \mu^E C_r + \gamma^E(Z), \quad (52)$$

which may be solved for the boundary value problem (BVP), the initial value problem (IVP), and the production value problem (PVP) by the law of superposition for resident concentration using a third-type inlet condition as (Toride et al., 1995, p. 6)

$$C^E(Z, \bar{T}) = C^B(Z, \bar{T}) + C^I(Z, \bar{T}) + C^P(Z, \bar{T}), \quad (53)$$

where the B , I , and P superscripts denote boundary, initial, and production value problems, respectively. A third-type inlet boundary condition for resident concentration is used because it conserves mass (Toride et al., 1995, p. 5) and it is the most physically realistic (Silebi and Schiesser, 1992, pp. 418–431).

EHTD considers only uniform constant initial concentration $C^I(Z, \bar{T})$ for background concentrations. EHTD considers only exponential production for $C^P(Z, \bar{T})$ and is intended to relate only to bacterial growth for release of a living bacterial agent. For tracer mass estimation, $C^I(Z, \bar{T})$ and $C^P(Z, \bar{T})$ can usually be taken as zero, so that $C^E(Z, \bar{T}) = C^B(Z, \bar{T})$.

3.2.1.1. Impulse Release for BVP. which when solved for the boundary value problem is (modified from Toride et al., 1995, p. 13)

$$f(x^*) = \bar{C}^E(Z, \bar{T}) - M_B \Gamma_1^E(Z, \bar{T}), \quad (54)$$

where $\bar{C}^E(Z, \bar{T})$ is a preset mean volume-averaged concentration that corresponds to dimensionless distance Z and dimensionless mean residence time \bar{T} . The auxiliary function

Γ_1^E is defined as (Toride et al., 1993, 1995, p. 14)

$$\Gamma_1^E(Z, \bar{T}) = e^{\frac{-\mu^E \bar{T}}{R_d}} \sqrt{\frac{P_e}{\pi R_d \bar{T}}} e^{\frac{-P_e(R_d Z - \bar{T})^2}{4 R_d \bar{T}}} \frac{P_e}{2 R_d} e^{P_e Z} \operatorname{erfc} \left(\frac{R_d Z + \bar{T}}{\sqrt{4 R_d \bar{T} / P_e}} \right). \quad (55)$$

Solving Equation (54) explicitly for M or for its real root as it relates to $\bar{C}^E(Z, \bar{T})$ limits the solution to the concentration corresponding with average travel time, which will be less than the peak concentration.

3.2.1.2. Pulse Release for BVP. The solution to Equation (52) for a pulse release for the case where $\mu^E = 0$ is (modified from Toride et al., 1995, p. 14)

$$f(x^*) = \bar{C}^E(Z, \bar{T}) - \sum_{i=1}^2 (g_i - g_{i-1}) \Gamma_2^E(Z, \bar{T} - \hat{T}_i), \quad (56)$$

and for the case where $\mu^E \neq 0$ is (modified from Toride et al., 1995, p. 14)

$$f(x^*) = \bar{C}^E(Z, \bar{T}) - \sum_{i=1}^2 (g_i - g_{i-1}) \Gamma_3^E(Z, \bar{T} - \hat{T}_i), \quad (57)$$

where (56) and (57) are again solved for the real root as related to $\bar{C}^E(Z, \bar{T})$, in which the result will be less than the peak concentration. The auxiliary functions Γ_2^E and Γ_3^E are defined as (Toride et al., 1993, 1995, p. 14)

$$\begin{aligned} \Gamma_2^E(Z, \bar{T}) &= \frac{1}{2} \operatorname{erfc} \left(\frac{R_d Z - \bar{T}}{\sqrt{4 R_d \bar{T} / P_e}} \right) \sqrt{\frac{P_e}{\pi R_d}} e^{\frac{-P_e(R_d Z - \bar{T})^2}{4 R_d \bar{T}}} \\ &- \frac{1}{2} \left(1 + P_e Z + \frac{P_e \bar{T}}{R_d} \right) e^{P_e Z} \operatorname{erfc} \left(\frac{R_d Z + \bar{T}}{\sqrt{4 R_d \bar{T} / P_e}} \right) \end{aligned} \quad (58)$$

when $\mu^E = 0$ and

$$\begin{aligned} \Gamma_3^E(Z, \bar{T}) &= \frac{1}{1+u} e^{\frac{P_e(1-u)Z}{2}} \operatorname{erfc} \left(\frac{R_d Z - u \bar{T}}{\sqrt{4 R_d \bar{T} / P_e}} \right) \\ &+ \frac{1}{1-u} e^{\frac{P_e(1+u)Z}{2}} \operatorname{erfc} \left(\frac{R_d Z + u \bar{T}}{\sqrt{4 R_d \bar{T} / P_e}} \right) \\ &- \frac{2}{1-u^2} e^{P_e Z + \frac{P_e(1-u^2)\bar{T}}{4 R_d}} \operatorname{erfc} \left(\frac{R_d Z + u \bar{T}}{\sqrt{4 R_d \bar{T} / P_e}} \right) \end{aligned} \quad (59)$$

where $u = \sqrt{1 + \frac{4\mu^E}{P_e}}$ when $\mu^E \neq 0$ (i.e., $\mu^E > 0$).

3.2.1.3. Uniform Initial Concentration (IVP). The IVP may be solved for uniform initial concentration by (Toride et al., 1995, p. 10)

$$C^I(Z, \bar{T}) = C_i \Gamma_4^E(Z, \bar{T}). \quad (60)$$

The auxiliary function Γ_4^E is defined as

$$\begin{aligned} \Gamma_4^E(Z, \bar{T}) = & e^{\frac{-\mu^E \bar{T}}{R_d}} \left\{ 1 - \frac{1}{2} \operatorname{erfc} \left[\frac{R_d(Z - Z_i) - \bar{T}}{\sqrt{4R_d \bar{T}/P_e}} \right] \sqrt{\frac{P_e \bar{T}}{\pi R_d}} e^{P_e Z - \frac{P_e [R_d(Z + Z_i) + \bar{T}]^2}{4R_d \bar{T}}} \right. \\ & \left. + \frac{1}{2} \left[1 + P_e(Z + Z_i) + \frac{P_e \bar{T}}{R_d} \right] e^{P_e Z} \operatorname{erfc} \left[\frac{R_d(Z + Z_i) + \bar{T}}{\sqrt{4R_d \bar{T}/P_e}} \right] \right\}. \end{aligned} \quad (61)$$

3.2.1.4. Exponential Production (PVP). The PVP may be solved for solute production that changes exponentially with distance by (Toride et al., 1995, p. 12)

$$\gamma^E(Z) = \gamma_1 + \gamma_2 e^{-\lambda^P Z}, \quad (62)$$

which gives the solution as (Toride et al., 1995, p. 12)

$$C^P(Z, \bar{T}) = \frac{1}{R_d} \int_0^{\bar{T}} \gamma_1 \Gamma_4^E(Z, \bar{T}; 0) + \gamma_2 \Gamma_5^E(Z, \bar{T}; \lambda^P) dT \quad (63)$$

$$= \begin{cases} \frac{\gamma_1}{\mu^E} [1 - \Gamma_4^E(Z, \bar{T}; 0) - \Gamma_3^E(Z, \bar{T}; \mu^E)] + \frac{\gamma_2}{R_d} \int_0^{\bar{T}} \Gamma_5^E(Z, \bar{T}; \lambda^P) dt & (\mu^E > 0) \\ \frac{\gamma_1}{R_d} \Gamma_6^E(Z, \bar{T}) + \frac{\gamma_2}{R_d} \int_0^{\bar{T}} \Gamma_4^E(Z, \bar{T}; \lambda^P) dt & (\mu^E = 0) \end{cases} \quad (64)$$

$$= \begin{cases} \frac{\gamma_1}{\mu^E} [1 - \Gamma_4^E(Z, \bar{T}; 0) - \Gamma_3^E(Z, \bar{T}; \mu^E)] + \frac{\gamma_2}{R_d} \int_0^{\bar{T}} \Gamma_5^E(Z, \bar{T}; \lambda^P) dt & (\mu^E > 0) \\ \frac{\gamma_1}{R_d} \Gamma_6^E(Z, \bar{T}) + \frac{\gamma_2}{R_d} \int_0^{\bar{T}} \Gamma_4^E(Z, \bar{T}; \lambda^P) dt & (\mu^E = 0) \end{cases} \quad (65)$$

where the auxiliary functions Γ_5^E and Γ_6^E are defined as

$$\begin{aligned} \Gamma_5^E(Z, \bar{T}) = & e^{\frac{-\mu^E \bar{T}}{R_d} + \frac{\lambda^P \bar{T}}{R_d P_e} + \frac{\lambda^P \bar{T}}{R_d} - \lambda^P Z} \left\{ 1 - \frac{1}{2} \operatorname{erfc} \left[\frac{R_d Z - (1 + 2\lambda^P/P_e) \bar{T}}{\sqrt{4R_d \bar{T}/P_e}} \right] \right. \\ & + \frac{1}{2} \left(1 + \frac{P_e}{\lambda^P} \right) e^{P_e Z + 2\lambda^P Z} \operatorname{erfc} \left[\frac{R_d Z + (1 + 2\lambda^P/P_e) \bar{T}}{\sqrt{4R_d \bar{T}/P_e}} \right] \\ & \left. - \frac{P_e}{2\lambda^P} e^{-\frac{\mu^E \bar{T}}{R_d} + P_e Z} \operatorname{erfc} \left[\frac{R_d Z + \bar{T}}{\sqrt{4R_d \bar{T}/P_e}} \right] \right\} \end{aligned} \quad (66)$$

and

$$\begin{aligned}
\Gamma_6^E(Z, \bar{T}) &= \bar{T} + \frac{1}{2} \left(R_d Z - \bar{T} + \frac{R_d}{P_e} \right) \operatorname{erfc} \left(\frac{R_d Z - \bar{T}}{\sqrt{4R_d \bar{T}/P_e}} \right) \\
&- \sqrt{\frac{P_e \bar{T}}{4\pi R_d}} \left(R_d Z + \bar{T} + \frac{2R_d}{P_e} \right) e^{-\frac{P_e(R_d Z - \bar{T})^2}{4R_d \bar{T}}} \\
&+ \left[\frac{\bar{T}}{2} - \frac{R_d}{2P_e} + \frac{P_e(R_d Z - \bar{T})^2}{4R_d} \right] e^{P_e Z} \operatorname{erfc} \left(\frac{R_d Z + \bar{T}}{\sqrt{4R_d \bar{T}/P_e}} \right). \quad (67)
\end{aligned}$$

3.2.2. Tracer Retardation and Tracer Decay

Application of any solution to Equation (43) or Equation (52) for instances where tracer retardation and tracer decay are significant ($R_d > 1; \mu > 0$) can have profound effects on the shape of the BTC. Commonly, increasing R_d tends to cause a flattening, lengthening, and spreading of the BTC, whereas increasing μ causes only a flattening of the BTC.

Conversely, increasing R_d when using Equations (54), (56), or (57) results in a steepening, lengthening, and spreading of the BTC. An increase in R_d has the effect of reducing the calculated value for \bar{C}^E , which causes a concomitant increase in estimated mass M so that the set value for \bar{C}^E can be maintained. A lengthening and spreading of the BTC continues in a normal manner because the time of travel t is not considered in the root determination.

Increasing μ when solving for the root also causes a steepening of the BTC because it also has the effect of reducing the calculated value for \bar{C}^E . The net effect is to cause an increase in estimated mass M so that the preset value for \bar{C}^E can be maintained.

3.3. SOLUTE TRANSPORT

Preliminary estimates for tracer mass in conjunction with travel time estimates and related hydraulic parameters may be applied to any particular solution to Equation (52) to obtain a BTC. Inverse analysis using the estimated parameters M , R_d , and/or μ and the predicted BTC can be conducted to observe the sensitivity of the model to any one of the three parameters.

The primary difficulty with application of any particular solution to the ADE is the need to estimate not only the tracer mass but the times of travel (\bar{t} , t_p , and t_i), which are related to flow velocity (v , v_p , v_i) and axial dispersion D_z . An inability on the part of the originators of previous tracer mass estimation equations (Field, 2002c) to estimate \bar{t} , v , and

D_z prior to initiating a tracer test is the most likely reason why solute transport theory was ignored when developing tracer mass estimation methods. Because \bar{t} and D_z can take on a wide range even when assuming steady-flow conditions, reasonable initial estimates for \bar{t} and D_z can be difficult to obtain and are most commonly acquired from a tracer test.

Estimates for hydraulic parameters can, however, be obtained from some basic flow-system measurements, functional relationships, and consideration of a simple conceptual model of the flow system. Although the simple model and functional relationships may be only approximations, they are likely to be sufficiently reliable as to lead to a good approximation of some basic hydraulic parameters that are necessary for a successful tracer test.

3.4. HYDRAULIC AND GEOMETRIC PARAMETERS

The use of Equations (54), (56), or (57) for assessing transport processes and predicting tracer mass requires that specific hydraulic and geometric parameters measured in the field be combined in simple functional relationships. These measured parameters and functional relationships can then be applied in a simple hypothetical model as a precursor to application of the ADE.

3.4.1. Measured Parameters

For flowing streams in surface channels or solution conduits, measurements for discharge Q , cross-sectional area A , and transport distance L need to be taken. These three parameters are the most important measurable field parameters necessary for establishing basic hydraulic and geometric controls in any hydrologic system.

For porous media, additional measurements or estimates for specific parameters must also be taken. These additional parameters are expected transverse spread W and vertical spread H of the tracer plume and effective porosity n_e . Moreover, it is necessary that the type of tracer test be identified as either a natural gradient test or a forced gradient test in which a radially symmetric flow field is created by an extraction well.

3.4.2. Functional Relationships

Discharge, cross-sectional area, and transport distance can each be measured at a downstream location such as a spring if a karst aquifer or estimated from Darcy's law if a porous-media aquifer. Transport distance in solution conduits may be corrected for sinuosity by

multiplying by a sinuosity factor ≤ 1.5 (Sweeting, 1973, p. 231). Surface stream or solution conduit volume V may be estimated by

$$V = AL. \quad (68)$$

Aquifer volume for porous media with regional gradient is estimated by

$$V = LWH, \quad (69)$$

and aquifer volume for porous media under forced-gradient conditions is estimated by

$$V = \pi L \left(\frac{H}{2} \right)^2. \quad (70)$$

Average flow velocity v for a surface stream or solution conduit may be estimated from

$$v = \frac{Q}{A} \quad (71)$$

or, for a natural gradient tracer test in porous media, by application of Darcy's law. Initial average flow velocity for a natural gradient tracer test will conform to the basic form of Equation (71) when n_e is included

$$v = \frac{Q}{WHn_e}, \quad (72)$$

although width W may be difficult to estimate. If W cannot reasonably be estimated, then velocity is estimated from

$$v = \frac{Q}{L/2Hn_e}, \quad (73)$$

which is not theoretically correct but may result in an acceptable approximation.

For a forced gradient tracer test in porous media in which the gradient is influenced by either a single extraction well or by a combination of an injection well and a withdrawal well, velocity may be estimated from (Käb, 1998, p. 377)

$$v = \frac{Q}{\pi L H n_e}, \quad (74)$$

and for an injection-withdrawal tracer test with recirculation from (Webster et al., 1970)

$$v = \frac{3Q}{\pi L H n_e}. \quad (75)$$

3.4.3. Travel Time Estimates

Estimates for transport velocities translate directly into transport times. Initial average time of travel \bar{t} is estimated from

$$\bar{t} = \frac{L}{v} \quad (76)$$

and tracer test duration from

$$t_d = \frac{n_m L}{v} \quad (77)$$

where $2 \leq n_m \leq 3$, depending on the type of tracer release. Parriaux et al. (1988, p. 8) recommend $n_m = 3$, but it has been experimentally established that setting $n_m = 2$ for impulse releases and $n_m = 3$ for pulse releases produces the best results.

Individual tracer travel time data points must also be estimated. A base time value t_b for initial time t_1 and subsequent time spacing Δt may be estimated up to \bar{t} by

$$t_b = \frac{n_m \bar{t}}{n}, \quad (78)$$

and a base time value t_m for subsequent time spacing $n_m \Delta t$ from \bar{t} may be estimated by

$$t_m = n_m t_b. \quad (79)$$

By assuming $\bar{t} = t_p$, individual time values t_i may be calculated up to \bar{t} from

$$t_i = t_b + \sum_{i=1}^{n/2} t_{n_i}, \quad (80)$$

and individual time values t_i from \bar{t} from

$$t_i = t_m + \sum_{i=n/2}^n t_{n_i}, \quad (81)$$

where n is a reasonable number of data points for obtaining a smooth BTC. Combining the values obtained from Equation (80) and Equation (81) results in a series of appropriately spaced time values that approximates initial tracer arrival and final tracer detection. Doubling or tripling time spacing after \bar{t} is not really necessary. However, it is essential that sufficiently early and late times be established to ensure adequate consideration of actual flow conditions.

3.5. CONTINUOUS STIRRED TANK REACTOR (CSTR)

Obtaining an estimate for M and D_z can be achieved for a predicted BTC on the basis of the theory of a completely mixed CSTR. A mass balance model that describes the dynamics of a simplified CSTR is (Silebi and Schiesser, 1992, p. 49–50)

$$\frac{d(VC)}{dt} = qC_0 - QC - VkC. \quad (82)$$

Setting $q = Q$ and using initial condition

$$C(0) = C_p, \quad (83)$$

the solution to Equation (82) is (Silebi and Schiesser, 1992, p. 50)

$$C(t) = C_p e^{-(Q+Vk)t/V}. \quad (84)$$

Equation (84) will produce an exponentially decaying BTC starting at the peak concentration C_p with a gradient that is dependent on the value of the reaction rate constant k and the space velocity Q/V (Levenspiel, 1999, p. 93). It is apparent from Equation (84) that whereas C_p may be preset, prior knowledge of discharge Q , reactor volume V , and transport times t must be determined.

Equation (84) is evaluated for C from $\bar{t} \approx t_p$ in a descending manner using $0.25 \leq k \leq 1.0$, although $k = 0$ would adequately suffice. The concentration values C obtained from Equation (84) leading from \bar{t} are then reversed to achieve an ascending limb leading to \bar{t} . Equation (84) is then resolved for C from \bar{t} in a descending manner using a $k \ll 1.0$. For $n = 200$, $k = 1/200$ represents a reasonable exponential decay for the descending limb.

The values for k were empirically determined such that $0.25 \leq k \leq 1.0$ represents a steeply ascending limb, whereas $k \ll 1.0$ represents a more gently decaying descending limb controlled by the number of data points. The result is a good approximation of a typically positively skewed BTC in which a cusp forms the peak concentration at the peak time of arrival. Although the values for k were empirically determined, the resulting BTC appears to reasonably represent a typical BTC based on observation and experience.

The BTC produced by the CSTR model is subsequently evaluated by

$$M = Q \int_0^\infty C(t) dt \quad (85)$$

to obtain the area under the BTC. The area represents an initial estimate for the tracer mass to be adjusted as required by Equations (54), (56), or (57).

3.5.1. Travel Times and Velocity

For the purpose of determining axial dispersion D_z , tracer travel time weighted for tracer mass for impulse and short-pulse releases is estimated from

$$\bar{t} = \frac{\int_0^\infty t C(t) dt}{\int_0^\infty C(t) dt}, \quad (86)$$

and tracer travel time variance σ_t^2 is estimated from

$$\sigma_t^2 = \frac{\int_0^\infty (t - \bar{t})^2 C(t) dt}{\int_0^\infty C(t) dt}, \quad (87)$$

where C is obtained from Equation (84). The CSTR-generated BTC is predicated on the assumption of an impulse or short-pulse release, so other forms of Equations (86) and (87) are not required.

3.5.2. Tracer Dispersion Estimates

Axial dispersion may be determined using the method of moments theory. Although statistically and theoretically valid, the method of moments has the tendency to overestimate dispersion. Alternatively, the effects of velocity variations, matrix diffusion, and immobile-flow regions can create the appearance of significant dispersion. These difficulties require that dispersion estimates be obtained in a manner that considers the method of moments while reducing the influence of long tails. This is most easily accomplished using the Chatwin (1971) method in conjunction with the method of moments.

3.5.2.1. *Estimating Dispersion by the Method of Moments.* Axial dispersion properly weighted for concentration may be estimated for an impulse release by

$$D_z = \frac{\sigma_t^2 v^3}{2z} \quad (88)$$

and for a short-pulse release by (Wolff et al., 1979)

$$D_z = \left(\sigma_t^2 - \frac{t_0}{12} \right) \frac{v^3}{2z}. \quad (89)$$

It should be recognized here that D_z solved by Equation (89) is based on the assumption of a BTC and does not represent the mean residence time distribution, as does Equation (88).

There will usually not be any major difference between D_z estimated from Equation (88) and D_z estimated from Equation (89). In addition, because the CSTR-generated BTC is based on an impulse release, Equation (89) may reasonably be ignored even though the subsequent tracer test may be a pulse or step test.

3.5.2.2. *Estimating Dispersion by the Chatwin Method.* Axial dispersion may be estimated using a modification of the method developed by Chatwin (1971), given by

$$\sqrt{t \ln \left(\frac{C_p \sqrt{t_p}}{C \sqrt{t}} \right)} = \frac{z}{2\sqrt{D_z}} - \frac{v t}{2\sqrt{D_z}}. \quad (90)$$

Subject to $t_\kappa \leq z/v$, Equation (90) is reduced to the general least-squares problem by solving

$$\min_x \|\mathbf{b} - \mathbf{A}\mathbf{x}\|_2^2, \quad (91)$$

where

$$\mathbf{A} = \begin{pmatrix} 1 & t_1 \\ 1 & t_2 \\ \vdots & \vdots \\ 1 & t_\kappa \end{pmatrix} \quad (92)$$

$$\mathbf{x} = (x_1, x_2)^T \quad (93)$$

$$\mathbf{b} = (b_1, b_2, \dots, b_\kappa)^T. \quad (94)$$

The parameters b_i are equal to the left-hand side of Equation (90)

$$b_i = \sqrt{t_i \ln \left(\frac{C_p \sqrt{t_p}}{C \sqrt{t_i}} \right)}, \quad (95)$$

and the parameters to be determined x_i are equal to the two factors on the right-hand side of Equation (90)

$$x_1 = \left(\frac{z}{2\sqrt{D_z}} \right) \quad (96)$$

$$x_2 = \left(\frac{v t}{2\sqrt{D_z}} \right), \quad (97)$$

where x_1 is the y intercept of the straight-line fit to the early-time data and x_2 is the gradient of the straight-line fit to the early-time data.

Equations (88) and (89) tend to overestimate D_z for nonporous-medium flow systems, which will generally result in an overestimation of tracer mass needed and a greater BTC spread than is likely to occur as a result of solute dispersion. Alternatively, Equation (90) tends to underestimate D_z for porous-medium flow systems, which will have an effect opposite that obtained from Equations (88) and (89).

For these two reasons, Equation (90) is used to estimate D_z for a nonporous-medium flow system and Equation (88) and/or Equation (89) are used to estimate D_z for porous-medium flow systems. Although not precise measures of D_z , these estimates are believed to be adequate for the purpose of obtaining an approximation of D_z for use in Equations (54), (56), or (57).

3.6. TRACER SAMPLE COLLECTION DESIGN

Solute transport parameter estimates are used in Equations (54), (56), or (57) with the initial estimate for tracer mass. Adjustments to the initial estimate for tracer mass are made iteratively on the basis of the estimated solute transport parameters, preset mean volume-averaged concentration \overline{C}^E , and any effects created by suggested tracer reactions. Final estimates are then used in the ADE to generate a BTC representative of the flow system to be traced.

3.6.1. Sample Collection

The ADE-generated BTC serves as the basis for determining an appropriate sampling frequency and an initial sample collection time. Rather than using guesswork, transport distance, or unmeasured estimates for tracer velocity, as is common (Field, 2002c), the BTC allows for realistic consideration of the times of travel.

3.6.1.1. *Sampling Frequency.* Sample collection frequency is based on an arbitrary number of samples to be collected that balances the cost of sample collection and analysis with the value of an ever-increasing number of samples. An adequate sampling frequency necessary for representing a continuous series by a discrete series must be determined for extracting optimal information while maximizing the accuracy of the results and minimizing the computational costs. The sampling frequency then is based on how rapidly tracer

concentration is changing, so that as the average $|dC/dt|$ increases, sampling frequency should also increase (Yevjevich, 1972, p. 2).

The number of samples n_s to be collected can be arbitrarily chosen initially. Novakowski (1992) suggested that n_s equal at least 20 to 30 samples, with the greatest concentration of samples occurring around C_p , which assumes that C_p is known, whereas (Kilpatrick and Wilson, 1989, p. 18) suggest that $n_s = 30$ samples will generally be necessary as a minimum for defining the BTC. To properly define rapid changes in the BTC, $n_s = 60$ was experimentally found to be more reliable if aliasing effects are to be avoided (Smart, 1988). Aliasing of a multimodal BTC is a common problem when an inadequate sampling frequency is applied to a tracer test that exhibits complex behavior.

Sampling frequency may then be determined from

$$t_{sf} = \frac{t_d - t_{sm}}{n_s}, \quad (98)$$

where t_{sm} corresponds to $C > 1.0^{-3} \text{ } \mu\text{g L}^{-1}$ for all tracer tests except recirculation tracer tests where $C > 1.0^{-6} \text{ } \mu\text{g L}^{-1}$. These values for t_{sm} are used on the assumption that lower concentrations are not readily detectable or necessarily relevant.

3.6.1.2. Initial Sample Collection. Once the sampling frequency has been determined, the initial sample collection time is adjusted backwards by an additional number of selected samples n_b . Initial sample collection time t_{s1} is then obtained by subtracting t_{sf} from t_{sm} for a selected number of additional samples n_b . For most instances, $n_b = 5$ may be taken as a reasonable number of additional samples to collect prior to the occurrence of $t_{s1} = t_{sm}$. All subsequent sampling times are found from

$$t_{si} = t_{sf} + \sum_{i=1}^{n_s} t_{si}. \quad (99)$$

The total number of samples to be collected with an associated sampling time spacing t_{sf} can be subsequently divided into fractions thereof as desired. Earlier sample collection than the recommended t_{s1} may be considered as appropriate. Sample collection ending times other than t_d may also be determined, depending on whether tracer detection has ceased prior to reaching t_d or is continuing beyond t_d .

3.7. METHODOLOGY EVALUATION

Application of this tracer estimation methodology provides a general sense of the appropriate tracer mass to release and the general hydraulics of the system to be traced. Because

the hydraulics of the system are approximated, sampling frequency and initial sample collection time can also be predicted. The computer code, EHTD, facilitates the tracer-design methodology for typical hydrological settings using measured hydrological field parameters to calculate functional relationships. The measured parameters and functional relationships are then applied to a hypothetical CSTR to develop a preliminary BTC that is then numerically evaluated by the method of moments for tracer mass and hydraulic parameter estimation. The calculated hydraulic parameters are then used in solving for estimated tracer mass and sampling times.

The CSTR-generated BTC is solved by the method of moments by developing a piecewise cubic Hermite function. That is, the interpolant is defined in terms of a set of cubic polynomials, each of which is defined between a pair of consecutive data points. The coefficients of these cubic polynomials are chosen so that the interpolant has continuous first derivatives, and the remaining freedom of choice is used to ensure that the interpolant is visually acceptable, meaning that monotonicity in the data results in monotonicity in the interpolant, which is defined by (Kahaner et al., 1989, p. 100–103 and 106–108)

$$g(t) \equiv \hat{h}(t) = \sum_{i=1}^n C_i \bar{h}_i(t) + d_i \hat{\bar{h}}_i(t). \quad (100)$$

A piecewise cubic Hermite function in effect produces the most reasonable interpolation of the data possible with excellent theoretical convergence properties. Integration is then accomplished by cubic Hermite quadrature as (Kahaner et al., 1989, p. 161–162)

$$I \approx I' = \int_{t_1}^{t_d} \hat{h}(t) dt = \sum_{i=1}^n C_i \int_{t_1}^{t_d} \bar{h}_i(t) + d_i \int_{t_1}^{t_d} \hat{\bar{h}}_i(t), \quad (101)$$

which is the compound trapezoid rule with appropriate end corrections. The compound trapezoid rule is exceptionally accurate when the integrand is a smooth periodic function given by equally spaced data points (Kahaner et al., 1989, p. 162).

Equations (54)–(57) may be solved directly or by using a combination of the bisection method and the secant method. The bisection method ensures certainty and the secant method ensures rapid convergence. This is very efficient and accurate and is guaranteed to produce reasonable results (Kahaner et al., 1989, p. 248–250).

For instances where tracer mass is expected to be adversely affected by retardation or decay, EHTD employs a constrained nonlinear least-squares optimization routine to adjust the tracer mass, retardation, and decay estimates relative to the BTC produced by the hypothetical CSTR. The nonlinear optimization routine searches for a vector \mathbf{y} of

Table 16. Tracer test design parameters.

Parameter	Value
<i>Measured Parameters</i>	
Release Mode	Impulse
Q , $\text{m}^3 \text{h}^{-1}$	3.63×10^2
z^a , m	2.74×10^3
A , m^2	2.23×10^0
\overline{C}^E , $\mu\text{g L}^{-1}$	5.00×10^1
<i>Functional Relationships</i>	
t_p , h	1.64×10^1
\bar{t} , h	1.69×10^1
v_p , m h^{-1}	1.68×10^2
v , m h^{-1}	1.63×10^2
V , m^3	6.12×10^3
<i>Axial Dispersion</i>	
D_z , $\text{m}^2 \text{h}^{-1}$	4.50×10^3
P_e	9.90×10^1
<i>Tracer Reaction</i>	
R_d	1.00×10^0
μ , h^{-1}	0.00×10^0

^a Transport distance = straight-line distance, $1.83 \times 10^3 \text{ m}$ \times sinuosity factor, 1.5.

p components that minimizes the sum of the squares function $f(y) = \frac{1}{2} \sum_{i=1}^n \hat{r}_i(y)^2$ that is constrained by $\underline{\gamma}_i \leq y_i \leq \overline{\gamma}_i$, $1 \leq i \leq p$ where the $\hat{r}_i(y)$ are twice continuously differentiable functions of y (Dennis et al., 1981).

3.7.1. Simulation

The methodology described was tested for Prospect Hill Spring located in Clarke County, Va., using the measured field parameters and functional relationships listed in Table 16. Figure 5 is a plot of time versus concentration produced by a hypothetical CSTR using the measured field parameters and functional relationships listed in Table 16. Integrating Figure 5 produced a preliminary estimate for tracer mass of $M = 111 \text{ g}$. Of particular

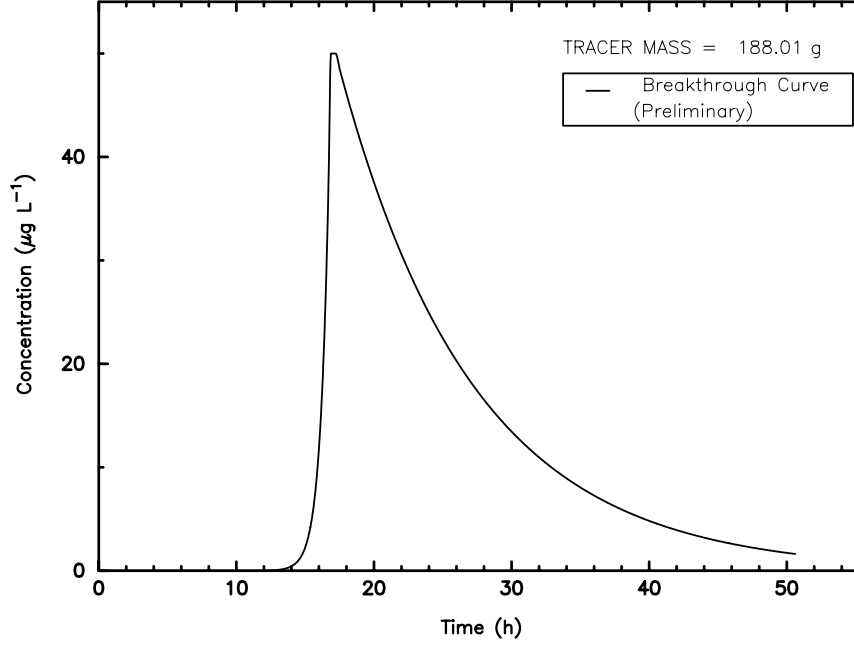


Figure 5. Preliminary tracer-breakthrough curve generated from a hypothetical CSTR.

significance are the variable effects created by the measured field parameters when combined in functional relationships. Increasing Q , decreasing A , or decreasing L all have the effect of shifting the curve to the left and decreasing the mass estimate. Decreasing Q , increasing A , or increasing L all have the effect of shifting the curve to the right and increasing the mass estimate.

Figure 6 is a plot of time versus concentration produced by the ADE using the measured field parameters and functional relationships listed in Table 16 with varying tracer retardation ($R_d = 1$, $R_d = 2$, $R_d = 3$) and no tracer decay ($\mu = 0 \text{ h}^{-1}$). The predicted tracer mass necessary for a successful tracing test and the resulting average and peak tracer concentrations are shown in Table 17 for varying tracer reaction conditions. From Figure 6 and Table 17 it is apparent that although \bar{C}^E remains the same for each BTC for varying values of R_d , \bar{t} and D_z appear to increase and v to decrease as R_d increases. In fact, these hydrologic parameters have not physically changed, but increasing R_d creates just such an appearance.

Table 17 also includes four instances of tracer decay ($\mu > 0 \text{ h}^{-1}$) without retardation ($R_d = 1.0$), the effects of which are shown in Figure 7 for three of the instances ($\mu = 0.0 \text{ h}^{-1}$, $\mu = 0.05 \text{ h}^{-1}$, $\mu = 0.1 \text{ h}^{-1}$), because $\mu = 0.01 \text{ h}^{-1}$ would not be readily distinguishable from

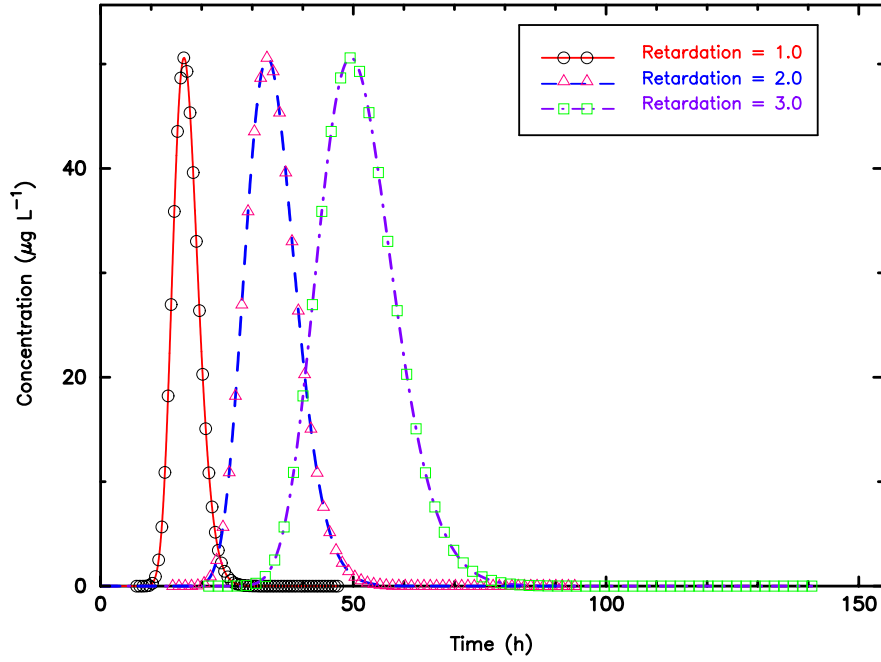


Figure 6. Predicted BTC for Prospect Hill Spring for increasing values for retardation. Symbols represent recommended sampling times.

Table 17. Predicted tracer mass and tracer concentration.

Tracer Reaction			M , g	\overline{C}^E , $\mu\text{g L}^{-1}$	C_p , $\mu\text{g L}^{-1}$
R_d	K_a^a , m	μ , h^{-1}			
1.0	0.0	0.0	113.99	50.00	50.59
1.0	0.0	0.01	134.94	50.00	50.77
1.0	0.0	0.05	265.00	50.00	51.92
1.0	0.0	0.1	616.07	50.00	54.02
2.0	0.42	0.0	227.98	50.00	50.59
3.0	0.84	0.0	341.97	50.00	50.59

^a K_a obtained for an assumed cylindrical solution conduit using Equations (46) and (68).

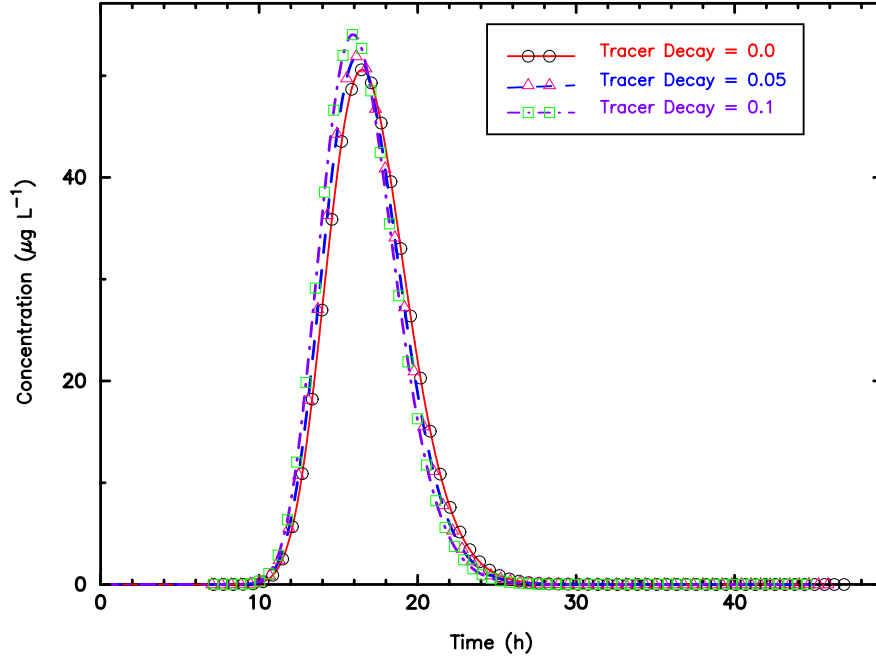


Figure 7. Predicted BTC for Prospect Hill Spring for increasing values for tracer decay. Symbols represent recommended sampling times.

$\mu = 0.0 \text{ h}^{-1}$. It is obvious from Figure 7 that as tracer decay is allowed to increase, C_p also increases (Table 17) because of the necessity of maintaining \bar{C}^E . This effect was not observed for increasing tracer retardation. In addition, because C_p increases, the BTC is steepened, causing an apparent decrease in tracer transport times. However, whereas t_p clearly decreases (Figure 7), \bar{t} remains unchanged regardless of the proposed tracer reactions.

Increasing tracer reaction effects causes a concomitant increase in tracer-mass estimates. The increase in tracer mass estimates reflects the need to match the set value for \bar{C}^E while including factors that have the net effect of decreasing tracer mass estimates, so that the overall effect is an estimate for tracer mass that approximates that which should be used in a tracer test.

Included in Figures 6 and 7 is an indication of appropriate sampling times for each BTC (Table 18).

Table 18. Recommended sampling times for selected tracer reaction conditions.

Sample Number	Sampling Time, hours					
	$R_d^a = 1.0$	$R_d^b = 1.0$	$R_d^c = 1.0$	$R_d^d = 1.0$	$R_d^e = 2.0$	$R_d^f = 3.0$
	$\mu = 0.0$	$\mu = 0.01$	$\mu = 0.05$	$\mu = 0.1$	$\mu = 0.0$	$\mu = 0.0$
1	7.13	7.15	7.02	7.11	14.26	21.39
2	7.75	7.77	7.63	7.69	15.51	23.26
3	8.37	8.39	8.23	8.28	16.75	25.12
4	9.00	9.00	8.84	8.86	17.99	26.99
5	9.62	9.62	9.45	9.45	19.24	28.85
6	10.24	10.23	10.06	10.03	20.48	30.72
7	10.86	10.85	10.66	10.62	21.72	32.58
8	11.48	11.47	11.27	11.20	22.96	34.45
9	12.10	12.08	11.88	11.79	24.21	36.31
10	12.73	12.70	12.49	12.37	25.45	38.17
11	13.35	13.31	13.09	12.96	26.69	40.04
12	13.97	13.93	13.70	13.54	27.94	41.90
13	14.59	14.54	14.31	14.13	29.18	43.77
14	15.21	15.16	14.92	14.71	30.42	45.63
15	15.83	15.78	15.52	15.30	31.66	47.50
16	16.45	16.39	16.13	15.88	32.91	49.36
17	17.08	17.01	16.74	16.47	34.15	51.23
18	17.70	17.62	17.35	17.05	35.39	53.09
19	18.32	18.24	17.95	17.64	36.64	54.95
20	18.94	18.86	18.56	18.22	37.88	56.82
21	19.57	19.47	19.17	18.81	39.12	58.68
22	20.18	20.09	19.78	19.39	40.37	60.55
23	20.80	20.70	20.38	19.98	41.61	62.41
24	21.43	21.32	20.99	20.56	42.86	64.28
25	22.05	21.93	21.60	21.15	44.09	66.14
26	22.67	22.55	22.20	21.73	45.34	68.01
27	23.29	23.17	22.81	22.32	46.58	69.87
28	23.91	23.78	23.42	22.90	47.82	71.73
29	24.53	24.40	24.03	23.49	49.07	73.60
30	25.15	25.01	24.63	24.07	50.31	75.46
31	25.78	25.63	25.24	24.66	51.55	77.33
32	26.40	26.25	25.85	25.24	52.79	79.19
33	27.02	26.86	26.46	25.83	54.04	81.06
34	27.64	27.48	27.06	26.41	55.28	82.92
35	28.26	28.09	27.67	27.00	56.52	84.79
36	28.88	28.71	28.28	27.58	57.77	86.65

continued on next page

Table 18. Recommended sampling times for selected tracer reaction conditions (*continued*).

Sample Number	Sampling Time, hours					
	$R_d^a = 1.0$ $\mu = 0.0$	$R_d^b = 1.0$ $\mu = 0.01$	$R_d^c = 1.0$ $\mu = 0.05$	$R_d^d = 1.0$ $\mu = 0.1$	$R_d^e = 2.0$ $\mu = 0.0$	$R_d^f = 3.0$ $\mu = 0.0$
37	29.51	29.33	28.89	28.17	59.01	88.51
38	30.13	29.94	29.49	28.75	60.25	90.38
39	30.75	30.56	30.10	29.34	61.50	92.24
40	31.37	31.17	30.71	29.92	62.74	94.11
41	31.99	31.79	31.32	30.51	63.98	95.97
42	32.61	32.40	31.92	31.09	65.22	97.84
43	33.23	33.02	32.53	31.68	66.47	99.70
44	33.86	33.64	33.14	32.26	67.71	101.56
45	34.48	34.25	33.75	32.85	68.95	103.43
46	35.10	34.87	34.35	33.43	70.20	105.29
47	35.72	35.48	34.96	34.02	71.44	107.16
48	36.34	36.10	35.57	34.60	72.68	109.02
49	36.96	36.72	36.18	35.19	73.92	110.89
50	37.58	37.33	36.78	35.77	75.17	112.75
51	38.21	37.95	37.39	36.36	76.41	114.62
52	38.83	38.56	38.00	36.94	77.65	116.48
53	39.45	39.18	38.60	37.53	78.90	118.34
54	40.07	39.79	39.21	38.11	80.14	120.21
55	40.69	40.41	39.82	38.69	81.38	122.07
56	41.31	41.03	40.43	39.28	82.63	123.94
57	41.93	41.64	41.03	39.86	83.87	125.80
58	42.56	42.26	41.64	40.45	85.11	127.67
59	43.18	42.87	42.25	41.03	86.35	129.53
60	43.80	43.49	42.86	41.62	87.60	131.40
61	44.42	44.11	43.46	42.20	88.84	133.26
62	45.04	44.72	44.07	42.79	90.08	135.12
63	45.66	45.34	44.68	43.37	91.33	136.99
64	46.28	45.95	45.29	43.96	92.57	138.85
65	46.91	46.57	45.89	44.54	93.81	140.72

^aRecommended sampling frequency = 37.12 minutes.

^bRecommended sampling frequency = 37.29 minutes.

^cRecommended sampling frequency = 36.95 minutes.

^dRecommended sampling frequency = 36.45 minutes.

^eRecommended sampling frequency = 1.24 hours.

^fRecommended sampling frequency = 1.86 hours.

Note that tracer decay has units of h^{-1} .

Sixty-five sampling times were developed to adequately determine when the first sample should be collected and to properly define the BTC. Breakthrough curve definition requires that the BTC peak be correctly identified and that a potentially long tail be detected. Further, in order to avoid the effects of data aliasing, a substantial number of samples are required (Smart, 1988). Although 20 to 30 samples have been suggested by others as adequate for BTC definition (Novakowski, 1992; Kilpatrick and Wilson, 1989, p. 18), these researchers were not concerned with problems associated with long tails or data aliasing. To ensure that data aliasing is avoided, 60 sample-collection times are developed by EHTD which allows for better BTC definition without excessive sampling. However, should 60 samples prove to be excessive, it is always possible to choose to collect some fraction of 60. To ensure that initial tracer breakthrough is not missed, $n_b = 5$ was included as an appropriate number of samples to collect prior to expected tracer breakthrough.

Part III

BASIC PROGRAM USAGE



Injection of 1 kg of uranine (Acid Yellow 73) at a sinkhole that receives flow from Bebec Creek on the Norville chalk plateau of Haute-Normandie, France. Dye recoveries were obtained ~2200 m away at a spring and well located in the Seine river alluvial plain (photo courtesy of Nicolas Massei).

4. USING EHTD TO DESIGN A TRACER TEST

EHTD is an easy-to-use program for the design of tracer tests in flowing water (e.g., open-channel flow or closed-conduit flow in surface streams, caves, sewers, etc.) and porous media (e.g., gravel aquifer). Using just a few field hydrological measurements, it estimates the “correct” tracer mass to release for a tracer study and predicts the hydraulic parameters that define solute migration. It also provides a reasonable sampling schedule for the proposed tracer test. A graphic BTC and A detailed output file provide substantial details necessary for implementing the proposed tracer test.

As with published (and some unpublished) tracer mass estimation equations, this program relies primarily on perceived travel distance, flow discharge, and flow cross-sectional area to estimate tracer mass. Unlike previously published equations, this program is somewhat more elaborate in that it attempts to rigorously apply solute transport theory by use of various forms of the advection-dispersion (equilibrium) model. Attempts at mass conservation and mass balance were essential to the method. Initial estimates for times of travel, related factors, and tracer mass are based on the concept of a hypothetical CSTR as a surrogate for the flow system.

Selected error messages appear toward the end of the whereas output file. Many of these error messages will not be of any great significance to the user, others are important. It is recommended that the error messages be checked to ensure proper EHTD functioning.

4.1. EHTD PROGRAM USAGE AND EXAMPLE DATA FILES

NOTE: This program functions best with a display equal to 1024×768 pixels, adequately with a display equal to 800×600 pixels, and not so well for further reduced display settings.

Before running the program, all EHTD files to his(her) should be copied to the PC's hard drive and the supplied CD-ROM disk stored in a safe location. Although plenty of storage space is available on the CD-ROM disk for the creation of data-output files and graphics files, the possibility of damage to the EHTD program file from excess use cannot be ignored.

4.1.1. Loading EHTD and Example Data Files

1. After booting up the computer, place the CD-ROM disk into the computer's CD-ROM disk drive.

2. At the computer desk top, place the mouse pointer (arrow) on the “My Computer” icon and click the *Right* mouse button (*Right Click*).
3. *Left Click* on the word “Explore” in the pop-up menu. Alternatively, just hit the letter “E” on the keyboard.
4. Place the mouse pointer on the CD-ROM disk drive icon (e.g., D: or E:) and *Left Double-Click*.
5. *Left Click* “Edit” at the top of the Window Screen and *Left Click* on “Select All” in the pull-down menu. Alternatively, just hit the letter “A” on the keyboard.
6. *Left Click* on the “Copy” icon on the “Tool Bar” near the top of the Window Screen (second row). Alternatively, *Left Click* on “Edit” at the top of the Window Screen and *Left Click* on “Copy” or just hit “C” on the keyboard.
7. *Left Click* on the preferred hard drive (e.g., C:).
8. *Left Click* on the “Paste” icon on the “Tool Bar” near the top of the Window Screen (second row). Alternatively, *Left Click* on “Edit” at the top of the Window Screen and *Left Click* on “Paste” or just hit “P” on the keyboard.

A folder named EHTD will be created on the chosen hard drive and all the appropriate files copied accordingly to the appropriate file folders².

4.2. EHTD EXECUTION

EHTD is very easy to use. After the appropriate data files are created (which are nearly self-explanatory), EHTD, for the most part, requires nothing more than hitting <ENTER> as requested or manipulating the mouse and clicking with the left mouse button. (See Section 5. on page 83 for a detailed discussion of EHTD data-input files.)

²EHTD was not designed for MSDOS[®] use, which requires that the files be moved according to the following instructions:

- At the C:\> prompt, type “MKDIR EHTD” (without the quotes — whenever quotes appear in this section type the requested information without the quotes).
- Next, copy the executable and data files stored in the file Ehtd_dos on the CD to the hard disk (for example, if C is the disk drive: “COPY D:*.* C:\EHTD*.*”).
- Repeat the above commands for the other files on the CD.
- Put the CD in a safe location.

```

*****
*
*
*   PROGRAM TO OPTIMIZE TRACER MASS TO BE INJECTED INTO A FLOW *
*   SYSTEM TO ENSURE RELIABLE TRACER-MASS RECOVERY AT THE      *
*   EXPECTED DOWNGRAIDENT SAMPLING STATIONS BASED ON THEORY.    *
*
*
*                               DEVELOPED                         *
*
*                               BY                                *
*
*                               MALCOLM S. FIELD                 *
*                               U.S. ENVIRONMENTAL PROTECTION     *
*                               AGENCY                            *
*
*****

ENTER INPUT FILE NAME (DEFAULT = EHTD.IN):

ENTER OUTPUT FILE NAME (DEFAULT = EHTD.OUT):

ENTER PLOT FILE NAME (DEFAULT = NULL):

```

Figure 8. Initial EHTD screen title which appears at program start.

1. In the Windows Explorer, *Left Double-Click* the EHTD folder and then *Left Double-Click* the EHTD.EXE file to initiate program operation.³
2. At this point, EHTD will open the program initiation screen and title (Figure 8) and will prompt you to enter an input file name for the file to be evaluated (Figure 8) unless you specified a file when starting the program using a DOS prompt. One advantage of a subdirectory on your hard disk is that you will not be required to provide an obscure path for all subfiles; the program will find them automatically because they are all at the same location as the executable file. If the data files are in different locations

³If a command prompt is preferred, then at the C:\> prompt, type "CD\EHTD" without the quotes. You will then see a new prompt; C:\EHTD>. You may now type "EHTD" to run the program by just responding to the requested information, assuming that you have also copied the necessary data files or created your own. You may want to type "EHTD *filename*" such as "EHTD Ehtd.in", which will automatically load and begin running the EHTD default data set described in the journal article (Molz et al., 1986b). You may do the same with any of the other *.in data files, which will load the appropriate data files and begin processing.

from EHTD, you will need to provide the correct path to the *.in files. Alternatively, pressing <ENTER> will automatically run the default file, Ehtd.in.

3. Now enter a data output file name to be written or press <ENTER> for default name (EHTD.out) as requested (Figure 8). Be aware that previous output files can be overwritten if the same name is used for more than one. However, an input file cannot be overwritten if one is mistakenly entered.
4. Enter a plot file name to be written or press <ENTER> for NULL, which means that no plot file is to be written (Figure 8). As with the output file name, duplicate usage of plot file names will result in the overwriting of previous plot files, but exiting input file names will not be accepted. There is no default plot file name used (the default is no plot file). If a plot file name is given, then two plot files will be created; a TIME-CONCENTRATION data file and a PostScript plot file. The latter will have an appropriate name assigned (e.g., sampling station name) and a .ps extension added. The TIME-CONCENTRATION data file will consist of four columns of data as shown in Table 19.

It will be noted from Table 19 that much more data will appear in the first two columns than in the second two columns. This is because the first two columns define the BTC, whereas the second two columns represent suggested sampling times, which are necessarily reduced to a workable recommendation. It will also be noted that multiple sampling stations will necessarily be recorded in the same plot file one right after the other in the order in which they appear in the input file but with the header information separating each new sampling station data set. Individual sampling station PostScript files are created, however. A single sampling station file listing will result in just one set of data being recorded.

After the last file name has been entered, EHTD will respond for approximately one second with:

FILE NAMES HAVE BEEN READ

unless NULL was specified for no plot file to be generated in which case EHTD will respond for approximately one second with:

Table 19. Table illustrating the form of the EHTD-created plot file.

PLOT FILE: <i>Sampling Station File Name</i>			
TIME (h)	CONC. ($\mu\text{g/l}$)	TIME (h)	CONC. ($\mu\text{g/l}$)
-----	-----	-----	-----
...
:	:	:	:
:	:
:	:		
:	:		
...	...		
PLOT FILE: <i>Sampling Station File Name</i>			
TIME (h)	CONC. ($\mu\text{g/l}$)	TIME (h)	CONC. ($\mu\text{g/l}$)
-----	-----	-----	-----
...
:	:	:	:
:	:
:	:		
:	:		
...	...		
PLOT FILE: <i>Sampling Station File Name</i>			
TIME (h)	CONC. ($\mu\text{g/l}$)	TIME (h)	CONC. ($\mu\text{g/l}$)
-----	-----	-----	-----
...
:	:	:	:
:	:
:	:		
:	:		
...	...		

NO PLOT FILE SPECIFIED, RESULTS WILL NOT BE WRITTEN TO A PLOT FILE!

followed by:

FILE NAMES HAVE BEEN READ

4.3. USER-REQUESTED LATIN HYPERCUBE SAMPLING (LHS) ROUTINE

After the last file name has been read, EHTD will ask if you want to generate a series of input files using a Latin Hypercube Sampling (LHS) routine and the original input file parameters as initial parameters to be randomly selected within an appropriate range. This routine was added to allow the user to consider the effect of conditions that may differ from the measured conditions. At the end of each LHS-generated input file, a suggested solute mass to manually enter is provided (see Section 4.4.). A comprehensive discussion of LHS is provided in Iman and Helton (1988) and McKay et al. (1979).

The actual LHS query appears as:

DO YOU WANT TO RUN THE LATIN HYPERCUBE SAMPLING ROUTINE (Y=YES, N=NO)?

Pressing N causes the LHS routine to be ignored only for the particular sampling station currently being evaluated by EHTD. Subsequent sampling stations that are part of the overall input file will each be queried as to whether the user would like to run the LHS routine.

Pressing Y causes a second query:

DO YOU WANT TO GENERATE A SERIES OF INPUT FILES OR ONE FILE OF MEAN VALUES?

1=INPUT FILES

2=FILE OF MEANS

Entering 1 causes the following request:

ENTER THE NUMBER OF LHS-DEVELOPED INPUT FILES DESIRED (N > 12):

for a flowing stream system or:

ENTER THE NUMBER OF LHS-DEVELOPED INPUT FILES DESIRED (N > 14):

for a porous media system. The generation of LHS input files requires that a specific minimum number of input files be generated to satisfy the inequality (Blower and Dowlatabadi, 1994; McKay et al., 1979)

$$N > \frac{4k_L}{3}. \quad (102)$$

Alternatively, entering 2 causes the following request:

ENTER THE NUMBER OF LHS-DEVELOPED CALCULATIONS DESIRED (e.g., N = 1000):

which means that the LHS routine is expecting entry of a “large” number for development of a set of mean values for use in a single input file. Note, however, values in the range of $\geq 10,000$ will necessitate patience on the part of the user as EHTD runs the LHS routine. Also, note that for porous media systems with “DIST-Y” set to zero will cause an insignificant error report to the screen which can be ignored. (See Table 25 on page 86 for a discussion of “DIST-Y”.)

After determining whether a LHS routine is to be run, EHTD informs the user that input data are being read and that input errors are being evaluated:

INPUT FILE READ AND AND ERROR AND INPUT-ERROR CHECK PROCEEDING

from which the program quickly moves on to either informing the user of any data entry errors or processing the input file. Later in the program, if the user has requested that the LHS routine be run, EHTD will query the user for a LHS-generated output file name:

ENTER LATIN HYPERCUBE OUTPUT FILE NAME (DEFAULT = LHS_*n*.OUT):

where *n* represents the number of the LHS-generated output files or set of calculations to be developed. If a series of input files was selected above (1=INPUT FILES), one file is developed for each sampling station evaluated by the LHS routine. If the default is used, then *n* will increment automatically to correspond with each sampling station listed in the

Table 20. Variable parameter types used in the LHS routine.

Variable	Porous Media	Flowing Stream
1	Mass	Mass
2	Discharge	Discharge
3	Effective Porosity	Cross-Sectional Area
4	Aquifer Thickness	Lateral Transport Distance
5	Lateral Transport Distance	Initial Concentration
6	Transverse Transport Distance	First Production Coefficient
7	Initial Concentration	Second Production Coefficient
8	First Production Coefficient	Retardation
9	Second Production Coefficient	Decay
10	Retardation	
11	Decay	

original input file. This one file will contain all of the LHS-generated input files, which the user may then selectively enter into EHTD by copying and pasting the desired input file as a new file.

Alternatively, if one input file of mean values was selected (2=FILE OF MEANS), a single input file consisting of the mean values of the required parameters (e.g., discharge, Q) will be developed followed by a comprehensive set of univariate statistics that describe the parameters. The statistics listing is ignored by EHTD when this file is later processed (if processing is initiated by the user) because it appears after the “END OF FILES” input file statement. The univariate statistics, developed using the equations shown in the box in Figure 9 on the next page, provide a sense of the range and distribution of values produced by the LHS routine. Substitution of, for example, the minimum or maximum value of a selected parameter (e.g., Stat(6,*) and Stat(7,*), respectively in Figure 9 on the following page) may be a desirable change in some instances. It is necessary to note here that the parameters used in the univariate statistics are listed as individual variables identified in Table 20.

4.4. USER-SUGGESTED SOLUTE MASS

At this point the user will be queried by EHTD as to whether the user would like to suggest a solute mass (tracer or pollutant) for EHTD to use. This feature is useful for predicting the outcome of an accidental spill or a deliberate release of a highly toxic substance, as might occur from a terrorist attack. A similar type of approach was developed by Taylor

1. Mean, Stat(1,*)	$\bar{x}_w = \frac{\sum f_i w_i x_i}{\sum f_i w_i}$
2. Variance, Stat(2,*)	$\sigma_w^2 = \frac{\sum f_i w_i (x_i - \bar{x}_w)^2}{n-1}$
3. Standard Deviation, Stat(3,*)	$\sigma_w = \sqrt{\sigma_w^2}$
4. Skewness, Stat(4,*)	$\gamma_{x_w} = \frac{\frac{1}{n} \sum f_i w_i (x_i - \bar{x}_w)^3}{[\frac{1}{n} \sum f_i w_i (x_i - \bar{x}_w)^2]^{3/2}}$
5. Kurtosis, Stat(5,*)	$\kappa_{x_w} = \left\{ \frac{\frac{1}{n} \sum f_i w_i (x_i - \bar{x}_w)^4}{[\frac{1}{n} \sum f_i w_i (x_i - \bar{x}_w)^2]^2} \right\} - 3$
6. Minimum, Stat(6,*)	$x_{\min} = \min(x_i)$
7. Maximum, Stat(7,*)	$x_{\max} = \max(x_i)$
8. Range, Stat(8,*)	$x_r = x_{\max} - x_{\min}$
9. Coefficient of Variation, Stat(9,*)	$x_{cv} = \frac{\sigma_w}{\bar{x}_w} \quad \text{for } \bar{x}_w \neq 0$
10. Number of values processed, Stat(10,*)	$n = \sum f_i$

where the statistics are given in terms of a single variable x . The i -th datum is x_i , with corresponding frequencies set to unity ($f_i = 1$) and weights also set to unity ($w_i = 1$).^a

^aNote that none of the variables shown in this box are intended in any way to match similar variables used elsewhere in this document. For example, x_i here represents any required input parameter (e.g., discharge, Q) and n represents the the number of values requested (processed) by the LHS routine to develop the mean values for each of the required parameters.

Figure 9. Equations used to calculate the univariate statistics used to describe the LHS-generated mean values used in a single input file.

et al. (1986, p. 41–54), Kilpatrick and Taylor (1986), and Mull et al. (1988a, p. 75–79), but these methods are much more difficult to implement, they require a great deal more measured data acquired over a very long timeframe, and they tend to overestimate the peak downstream concentration. EHTD does not suffer from the limitations listed and reliably reproduces peak concentration. However, the previously developed methods do provide a better visual fit to an expected long BTC tail than does EHTD, but this better tail fit is useful primarily in estimating solute persistence.

This first EHTD query appears as:

DO YOU WANT TO SUGGEST AN INITIAL SOLUTE MASS (Y=YES, N=NO)?

Entering N represents a “no,” and EHTD will continue processing by adjusting the internally estimated solute mass to achieve the desired downstream \overline{C} . Entering Y represents a “yes,” which causes EHTD to pause a second time for the user to be further queried as to the actual solute mass to be considered. This second EHTD query appears as:

ENTER A SUGGESTED SOLUTE MASS IN GRAMS (g):

where the user would enter a solute mass that EHTD is to use for processing. The originally desired \overline{C} will be ignored by EHTD. EHTD will bypass all tracer mass estimation routines and proceed directly to the basic solute-transport modeling routine using the estimated hydraulic parameters (see Section 3.4.) and the user-supplied solute mass.

EHTD will respond by noting the user-suggested solute mass to be used in processing in milligrams (mg) and an appropriate error code, an explanation of which appears at the end of the EHTD output file. The EHTD response will appear as:

USER-SUGGESTED MASS = ... mg

ERROR CODE AVERAGE CONCENTRATION ESTIMATE = ...

where ... represents an appropriate numerical value.

4.5. SCREEN OUTPUT

Further processing by EHTD will result in a screen display of

1. INITIAL TRACER MASS ESTIMATE is an initial tracer mass estimate based on the CSTR analogy.
2. ADJUSTED TRACER MASS ESTIMATE is an adjusted tracer mass estimate based on factors such as tracer-reactivity effects such as tracer retardation and tracer decay.
3. FINAL TRACER MASS ESTIMATE is the final tracer mass estimate based on the use of the selected optimization routine.

These are presented so that the user can gain a sense of the workings produced by EHTD prior to going to a screen plot of the resulting BTC or reviewing the output file. (See Section 6. on page 97 for a detailed discussion of EHTD data output files.)

Table 21. Screen display of a typical EHTD warning message.

```
*** WARNING -- END OF FILE ASSUMED BECAUSE OF MISSING "END OF RUNS" FILE TERMINATOR ***

WARNING MESSAGE...THIS MESSAGE WILL ONLY BE PRINTED ONCE.
RECOVERABLE ERROR IN INPUT FILE
ERROR NUMBER =          -1

Press <RETURN> to continue program
```

In instances where the user is interested in the effects created by solute retardation and/or solute decay, the user may have EHTD run an optimization routine, which may result in a slight modification of the estimated tracer mass and/or retardation and decay, depending on whether one or the other or both are to be adjusted by EHTD. (See Section 3.7. on page 55, Line Numbers 10–14 listed in Table 25 on page 86, and related discussion on pages 93–95 for discussions related to EHTD optimization of the selected parameters.)

4.5.1. Screen Output of Error Messages

As EHTD progresses, various error messages may pop up from time to time. For the most part, these can be ignored if they are only listed as warnings. More serious errors will stop EHTD from any additional data processing.

4.5.1.1. *Warning Messages.* Warning messages are fairly common and are primarily an indication of some abnormality in the user-specified input file that EHTD has recognized. Usually, these warning messages can be ignored. For example, should the user construct an input file that is missing the last three lines (two comment lines and the input file ending command `END OF RUNS`), the warning message shown in Table 21 will appear. This message is stating nothing more than that the user inadvertently did not complete the input file in standard form (see Section 5. on page 83 for a detailed discussion of input file standard forms), but EHTD has recognized this error and will process the input file anyway, so the user is instructed to press `<RETURN>` to continue. The `ERROR NUMBER = -1` will appear in the output file with an explanation. Other basic warning messages are possible.

4.5.1.2. *Error Messages.* A more serious error, identified as fatal by EHTD, will also occur if a critical item is missing from the user-specified input file. For example, should the input file be missing the sampling station name (a required field), then EHTD will

respond with a screen display similar to the one shown in Table 22. The first line shown in Table 22 indicates that either the sampling station name or the ‘‘END OF RUNS’’ file terminator is missing. From the second line it is apparent that the sampling station name is missing, because this line indicates that the last sampling station name identified by EHTD (STATION NAME READ WAS:) appears nonsensical (i.e., DISCHARGE (m³/h) . . .). The listed station name on line 2 of Table 22 is actually just a comment line that should normally be ignored by EHTD (see Section 5. on page 83 for an description of comment lines in input files).

Also apparent from the first line in Table 22 is that a missing ‘‘END OF RUNS’’ file terminator may still cause a fatal error rather than just a warning error as shown in Table 21. This may sometimes occur if EHTD is unable to distinguish a “true end” to the user-supplied input file.

All the information shown in Table 22 up to the statement FATAL ERROR IN... will be printed in the named output file. The ERROR NUMBER = -5 will not appear in the output file because the necessary information will already have been produced. Following the listed error number, the statement, JOB ABORT DUE TO FATAL ERROR., is the last significant statement for a typical user. The additional information listed (i.e., MESSAGE START NERR . . .) are of no consequence to the user; this information is useful to programmers only. Other basic error messages are possible.

Table 22. Screen display of a typical EHTD warning message.

MISSING STATION NAME OR "END OF RUNS" FILE TERMINATOR				
LAST STATION NAME READ WAS: DISCHARGE (m ³ /h) DISTANCE (m) AREA (m ²) SINUOSITY FACTOR				
PROGRAM STOPPED DUE TO ERROR IN INPUT FILE				
CHECK INPUT FILE INCONSISTENT ERRORS				
FOR EXAMPLE --- DOES THE NUMBER OF RECOVERY STATIONS MATCH THE ACTUAL NUMBER OF RECORDED RECOVERY STATIONS?				
FATAL ERROR IN...				
FATAL ERROR IN INPUT FILE				
ERROR NUMBER = -5				
JOB ABORT DUE TO FATAL ERROR.				
0	ERROR MESSAGE SUMMARY			
MESSAGE START	NERR	LEVEL	COUNT	
FATAL ERROR	-5	2	1	

Table 23. Typical screen display of optimization results.

I	INITIAL X(I)	D(I)							
1	0.183887D+09	0.600D+00							
2	0.100000D+01	0.521D+05							
3	0.000000D+00	0.206D+05							
IT	NF	F	RELDX	PRELDF	RELDX	MODEL	STPPAR	D*STEP	NPRELDF
0	1	0.152D-70							
1	2	0.152D-70	0.00D+00	0.44D-77	0.0D+00	G	0.0D+00	0.3D-71	0.44D-77
***** X- AND RELATIVE FUNCTION CONVERGENCE *****									
FUNCTION	0.151871D-70	RELDX	0.000D+00						
FUNC. EVALS	2	GRAD. EVALS	3						
PRELDF	0.440D-77	NPRELRF	0.440D-77						
I	FINAL X(I)	D(I)	G(I)						
1	0.183887D+09	0.600D+00	0.165D-78						
2	0.100000D+01	0.521D+05	-0.306D-68						
3	0.000000D+00	0.206D+05	0.199D-69						
FINAL TRACER MASS ESTIMATE									
MASS = 1.84E+05 g									
Press <RETURN> to initiate plot routine									

4.5.2. Screen Output of Optimization Results

Selecting the optimization routine may result in a slight alteration of the estimated tracer mass, the tracer retardation, and/or the tracer decay. Prior to displaying the final tracer mass estimate, EHTD will display the results of the optimization routine, which will appear similar to the one shown in Table 23.

Most of the information provided in Table 23 will be of little use and may be ignored. However, at the top of Table 23 is a list of the parameter values (I) selected for optimization, their initial values (INITIAL X(I)), and the derivative of each (D(I)). For this example, three parameters are shown; the order will always be MASS, RETARDATION, and DECAY unless retardation is not included in the optimization routine, in which case the order would be MASS and DECAY.

The next row (IT NF F...) is an indication of the optimization iterations that will follow and related operations (only one iteration after an initial value for this example).

This can be a very large set of iterations if radical changes to the values are required, but this is unlikely.

Next is an indication of how well the optimization routine performed; in this instance the statement:

```
***** X- AND RELATIVE FUNCTION CONVERGENCE *****
```

indicates very positive optimization results. This same line appears in the final output file as an error message so that the user has a documented record of how well the optimization routine performed.

The next three rows also will not be of much use to the user, as they only indicate the function evaluations, gradient evaluations, *etc.* However, the next four rows are very useful, as they represent the final outcome of the optimization routine. The **FINAL X(I)** and **D(I)** are similar to those listed at the top of Table 23, and the **G(I)** represents the final gradient estimates.

Lastly, the screen displays the **FINAL TRACER MASS ESTIMATE** just as though the optimization routine had not been run. EHTD then informs the user to continue on to the plot routine to visualize the predicted BTC.

4.6. COMPUTER GRAPHICS

A high-quality color graphics algorithm, PGPLOT⁴ (Pearson, 1997) that allows cascading of graphics screens, direct printing, creation of screen files, and more using pull-down menus in the Windows environment is included in EHTD. It is particularly useful for evaluating the effect of interpolating and/or extrapolating the original data. Publication-quality plots may be generated as PostScript files from the graphics screen incorporated into the program. Alternatively, a screen dump using any type of printer is possible.

4.6.1. Features of the Interactive Graphics Loop

Running EHTD will start a conventional Windows screen with a series of pull-down menus (Table 24). Each underlined character in Table 24 indicates that the <Alt> key plus the underlined character implements the respective menu item. For example, <Alt+F> will initiate the pull-down menu items underneath the File heading. Of course the mouse pointer

⁴PGPLOT may be obtained from <http://www.astro.caltech.edu/~tjp/pgplot/>

can be used to access the menu items.

It is necessary to point out here that most users will not use the pull-down menus very often. Most of the more useful graphics functions have been built directly into EHTD so as to alleviate excess work on the part of the user. However, in some instances, the user may find particular functions of value. For example, selecting the Cascade function under the Window pull-down menu after a total five or six graphics plots have been produced in a series of child windows will cause the child windows to become stacked, but slightly offset to the right and down.

The items shown in Table 24 works whether the program is currently at the text-only screen (Graphic 1) where the user responds to queries posed by EHTD or if the program is currently at the data-plot screen (PGPlot Graphics, #1). However, there is little point in accessing any of the pull-down items from the text-only screen whereas in the data-plot screen the user may find some items of value. For example, the color data-plot screen can be printed as it appears, saved as it appears, resized to fit the whole screen, *etc.*

A brief description of each pull-down item shown in Table 24 is provided in the next six subsections. Because the items listed in Table 24 are relatively self explanatory, the items are only briefly described.

Table 24. Pull-down menu items available in EHTD.

<u>F</u> ile	<u>E</u> dit	<u>V</u> iew	<u>S</u> tate	<u>W</u> indow	<u>H</u> elp
<u>P</u> rint...	Select <u>T</u> ext	<u>S</u> ize To Fit	<u>P</u> ause Ctrl+S	<u>C</u> ascade	<u>C</u> ontents
<u>S</u> ave...	Select <u>G</u> raphics	<u>F</u> ull Screen Alt Enter		<u>T</u> ile	Using <u>H</u> elp
<u>E</u> xit Ctrl+C	Select <u>A</u> ll			<u>A</u> rrange Icons	<u>A</u> bout
	<u>C</u> opy Ctrl+Ins			<u>I</u> nput	
	<u>P</u> aste			<u>C</u> lear Paste	
				<u>S</u> tatus Bar	
				<u>1</u> Graphic 1	
				<u>2</u> PGPlot Graphics, # 1	
				\vdots	

4.6.1.1. File. Items listed under this heading in Table 24 are described as follows.

Print... *A screen dump to the local printer attached to the respective PC.*

Save... *Save the screen as a bitmapped (*.BMP) file.*

Exit Ctrl+C *Exit the program.*

4.6.1.2. Edit. Items listed under this heading in Table 24 are described as follows.

Select Text *Select text for pasting to the clipboard.*

Select Graphics *Select graphics for pasting to the clipboard.*

Select All *Select both text and graphics for pasting to the clipboard.*

Copy Ctrl+Ins *Copy selected items to the clipboard.*

Paste *Paste selected items to the screen.*

4.6.1.3. View. Items listed under this heading in Table 24 are described as follows.

Size To Fit *Fit the graphics screen to the view surface without scroll bars.*

Full Screen Alt+Enter *Fit the entire graphics screen to the view surface without the menu items displayed (a left-mouse click returns to the original screen).*

4.6.1.4. State. Items listed under this heading in Table 24 are described as follows.

Pause Ctrl+S *Pause the graphic display.*

Resume Ctrl+Q *Resume graphic display.*

Pause and Resume appear only as alternates of each other, so that only the one that is not currently functioning is accessible. The one that is currently in operation is not displayed in the pull-down menu.

4.6.1.5. Window. Items listed under this heading in Table 24 are described as follows.

Cascade *Allows for a cascading view of multiple child windows at one time.*

Tile *Allows for a tile display of multiple child windows at one time.*

Arrange Icons *Not currently used in EHTD.*

Input *Automatically displays the input screen (Graphic 1) for data input.*

Clear Paste *Clears an item pasted onto the screen.*

Status Bar *Displays the current operating mode of the displayed graphics screen in a bar at the bottom of the screen (when “check marked”).*

1 Graphic 1 *Name of the data input screen (“check marked”) if active.*

2 PGPlot Graphics, # 1 *Identifying name/number of all subsequently opened graphics screens (active when “check marked”).*

4.6.1.6. Help. Items listed under this heading in Table 24 are described as follows.

Contents *Listing of available help contents.*

Using Help *Description on the use of the Help.*

About *Identifies the EHTD program.*

4.7. EHTD SOURCE

The FORTRAN source for EHTD is included on the CD. It is a very large program and it had to be split into pieces to allow its use on a PC. It is not recommended that users to attempt to follow the logic or modify the program. Questions regarding the program’s functioning can be addressed to the author.

In addition, the graphics routine developed at the California Institute of Technology is included. However, it is not allowed for use in commercial products.

5. EHTD USE OF INPUT FILES

EHTD is written to work only with prepared data files because there is too much important data that needs to be entered correctly. Keyboard entry is typically very frustrating and usually results in typographical errors that are difficult to correct. If these errors are caught, it usually indicates that it is time to repeat the entire data entry process.

Good computer programs allow for created data files to be read directly by the program. These files can easily be corrected or modified as desired without a great deal of effort on the part of the user.

EHTD data files have been developed in a relatively simple manner to be as straightforward as possible. Each data file consists of a leading part that identifies the planned tracer test followed by any number of likely sample recovery stations. If more than a single sample recovery station is listed in the data file, then the projected tracer mass calculated by EHTD is an additive process.

This additive process is correct only if the multiple sample recovery stations are independent of each other. If the multiple sample recovery stations are in line with each other (e.g., they occur along the same stream line), then twice as much tracer will be estimated than may be necessary. This situation must be evaluated by the user on a case-by-case basis.

5.1. DESCRIPTION OF INPUT FILES

EHTD uses a straight-forward, standard format for data input files. Unnecessary “comment” or blank lines are interspersed with necessary lines that EHTD reads and processes. Although the comment lines may be left blank, adding descriptive comments is useful for keeping the file well organized.

Figure 10 illustrates the general form of a typical flowing stream input file, the components of which are briefly described, and Figure 11 illustrates the general form of a typical porous media input file, the components of which are briefly described in Table 25. Note that the ***Line*** numbers listed in Figures 10 and 11 correspond to the ***Line*** numbers listed in Table 25. No column numbers are provided because *free format* input is permitted (i.e., the placement of input items is irrelevant).

A cursory inspection of Figures 10 and 11 will show that the only significant difference between the two occurs at ***Line(s)*** 8 and ultimately ***Line(s)*** 9 (repeated as necessary in both figures and any real data-input file). Although not apparent in Figures 10 and 11

Line

Generic Flowing Stream Input File

```

1  PROJECT NAME
2  Name of Planned Tracer Test
3  FLOW      RELEAS      RTIM (h)      INFLOW (m^3/h)      UNITS
4  ...      ...      ...      ...      ...
5  *****
6  STATION NAME
7  Name of Sample Station 1
8  DISCHARGE (m^3/h)      DISTANCE (m)      AREA (m^2)      SINUOSITY FACTOR
9  ...      ...      ...      ...
10 INIT. CONC. (ug^3/L) GAMMA1      GAMMA2
11 ...      ...      ...
12 RETARDATION      DECAY (1/h)      OPTIM      AVE. CONC. (ug/L)
13 ...      ...      ...      ...
14 ...      ...
15 ...      ...
16 ...      ...
17 *****
6  STATION NAME
7  Name of sample station 2
8  DISCHARGE (m^3/h)      DISTANCE (m)      AREA (m^2)      SINUOSITY FACTOR
9  ...      ...      ...      ...
10 INIT. CONC. (ug^3/L) GAMMA1      GAMMA2
11 ...      ...      ...
12 RETARDATION      DECAY (1/h)      OPTIM      AVE. CONC. (ug/L)
13 ...      ...      ...      ...
14 ...      ...
15 ...      ...
16 ...      ...
17 *****
18 STOP PROCESSING
19 End of Runs

```

Figure 10. Generic example of an flowing stream input file illustrating the basic format used by EHTD for processing. Note that the *Line* numbers are not part of a typical input file and are listed here only for reference purposes for Table 25. Also note that *Lines* 6–17 are repeated for each individual sampling station considered for the particular study.

Line

Generic Porous Media Input File

```

1  PROJECT NAME
2  Name of Planned Tracer Test
3  FLOW      RELEAS      RTIM (h)      INFLOW (m^3/h)      UNITS
4  ...      ...      ...      ...      ...
5  *****
6  STATION NAME
7  Name of Sample Station 1
8  DISCHARGE (m^3/h)  POROSITY  THICKNESS (m)  DIST-X (m)  DIST-Y (m)
9  ...      ...      ...      ...      ...
10 INIT. CONC. (ug^3/L) GAMMA1  GAMMA2
11 ...      ...      ...
12 RETARDATION      DECAY (1/h) OPTIM      AVE. CONC. (ug/L)
13 ...      ...      ...      ...
14 ...      ...
15 ...      ...
16 ...      ...
17 *****
18 STATION NAME
19 Name of sample station 2
20 DISCHARGE (m^3/h)  POROSITY  THICKNESS (m)  DIST-X (m)  DIST-Y (m)
21 ...      ...      ...      ...      ...
22 INIT. CONC. (ug^3/L) GAMMA1  GAMMA2
23 ...      ...      ...
24 RETARDATION      DECAY (1/h) OPTIM      AVE. CONC. (ug/L)
25 ...      ...      ...      ...
26 ...      ...
27 ...      ...
28 ...      ...
29 *****
30 STOP PROCESSING
31 End of Runs

```

Figure 11. Generic example of an porous media input file illustrating the basic format used by EHTD for processing. Note that the *Line* numbers are not part of a typical input file and are listed here only for reference purposes for Table 25. Also note that *Lines* 6–17 are repeated for each individual sampling station considered for the particular study.

Table 25. Description of the input file components listed in Figures 10 and 11.

Line	Type	Identifier	Description
1	Comment line.
2	Character	TITLE1	Descriptive title for planned tracer test.
3	Comment line.
4	Integer	FLOW	Type of flow data code: 1 Open-channel or closed-conduit flow. 2 Porous media flow and a natural-gradient tracer test. 3 Porous media flow and a forced-gradient tracer test. 4 Porous media flow and a injection/withdrawal test. 5 Porous media flow and a recirculation test.
4	Integer	RELEAS	Tracer release method data code: 1 Impulse tracer release (<i>i.e.</i> , Dirac δ function). 2 Pulse tracer release (time dependent). 3 Continuous tracer (step) release.
4	Real	RTIME (h)	Time in hours for pulse release (RELEAS = 2) only, but a place holder is required (automatically converted to zero for RELEAS \neq 2).
4 or	Real Real	INFLOW (m ³ /t) INFLOW (ft ³ /t)	Injection flow rate (m ³ h ⁻¹ or ft ³ h ⁻¹).
4	Integer	UNITS	Units used in the input file. 1 Metric units (e.g., m, m ² , m ³ h ⁻¹). 2 English units (e.g., ft, ft ² , ft ³ h ⁻¹).
5	Comment line.
6	Comment line.
7	Character	TITLE2	Descriptive title for sampling station.
8	Comment line (Note the Line 8 differences between Figure 10 and Figure 11).

continued on next page

Table 22. Description of the input file components (*continued*).

Line	Type	Identifier	Description
<i>Flowing Stream Entry for Line 9</i> (see Figure 10)			
9 or	Real Real	DISCHARGE (m ³ /T) DISCHARGE (ft ³ /T)	Sampling station discharge (m ³ h ⁻¹ or ft ³ h ⁻¹). estimated from surface discharge (e.g., spring[s]; surface-water stream) if FLOW = 1. Estimated from Darcy's law for porous media discharge if FLOW = 2. Estimated from pumping well if FLOW = 3 or 4.
9 or	Real Real	DISTANCE (m) DISTANCE (ft)	Estimated longitudinal distance from release point to expected recovery point (m or ft).
9 or	Real Real	AREA (m ²) AREA (ft ²)	Cross-sectional area of discharge point (e.g., spring or surface-water stream cross-sectional area) (m ² or ft ²).
9	Real	SINUOSITY FACTOR	DISTANCE multiplier (≤ 1.5) to account for sinuosity. Applicable to solution conduits primarily when a straight-line distance between tracer injection and recovery points is listed for DISTANCE.
<i>Porous Media Entry for Line 9</i> (see Figure 11)			
9 or	Real Real	DISCHARGE (m ³ /T) DISCHARGE (ft ³ /T)	Sampling station discharge (m ³ h ⁻¹ or ft ³ h ⁻¹). estimated from surface discharge (e.g., spring[s]; surface-water stream) if FLOW = 1. Estimated from Darcy's law for porous media discharge if FLOW = 2. Estimated from pumping well if FLOW = 3 or 4.
9	Real	POROSITY	Estimated effective porosity of the porous medium.
9 or	Real Real	THICKNESS (m) THICKNESS (ft)	Estimated porous medium thickness (m or ft).
9 or	Real Real	DIST-X (m) DIST-X (ft)	Estimated longitudinal distance from release point to expected recovery point (m or ft).
9 or	Real Real	DIST-Y (m) DIST-Y (ft)	Estimated transverse spread of tracer at the expected recovery point (m or ft).

continued on next page

Table 22. Description of the input file components (*continued*).

Line	Type	Identifier	Description
10	Comment line.
11	Real	INIT. CONC. (ug/L)	Initial (background) tracer concentration (≥ 0.0) ($\mu\text{g L}^{-1}$).
11	Real	GAMMA1	First exponential production (growth) constant (≥ 0.0).
11	Real	GAMMA2	Second exponential production (growth) constant (≥ 0.0).
12	Comment line.
13	Real	RETARDATION	Factor to account for possible tracer retardation (≥ 1.0).
13	Real	DECAY	Factor to account for possible tracer decay (≥ 0.0).
13	Integer	OPTIM	Global program optimization data code: 0 No optimization. 1 Optimization.
13	Real	AVE. CONC. (ug/L)	Desired average concentration at the sampling station ($\mu\text{g L}^{-1}$).
14	Integer	...	Optimization for tracer retardation. 0 No optimization. 1 Optimization.
14	Integer	...	Optimization for tracer decay. 0 No optimization. 1 Optimization.
15	Real	...	Minimum bound on tracer retardation optimization.
15	Real	...	Minimum bound on tracer decay optimization.
16	Real	...	Maximum bound on tracer retardation optimization.
16	Real	...	Maximum bound on tracer decay optimization.
17	Comment line.
18	Comment line.

continued on next page

Table 22. Description of the input file components (*continued*).

Line	Type	Identifier	Description
19	Character	END OF RUNS	Program termination code: Not required, but allows file notes to be included at the end of the input file (e.g., references).

^a**Lines** 6–17 may be repeated for any number of sampling stations.

because of the generic aspect of each is that the value to be entered for type of flow, **FLOW**, on **Line** 4 must correspond to the listing on **Line** 9. Correct representation of **Line** 9 is not required, but it is useful for clarity purposes, as pointed out in Table 25. Section 5.1.1. provides a detailed line-by-line explanation of Figures 10 and 11 in reference to Table 25.

5.1.1. Line-by-Line Description of Input Files

Figure 10, Figure 11, and Table 25 each include a **Line** number to identify the line on which a particular item must be supplied in a data input file. These **Line** numbers are provided here only as a guide to the user and are never to be included in any actual data input file. Below is a detailed description of each line for a typical data input file. In most instances, the description provided refers to Figure 10 and refers specifically to Figure 11 only when necessary because of the similarity of most data entry lines for the two types of data input files.

Line 1 is a comment statement provided to the user to enter a clarifying statement that is ignored by EHTD. It is generally used as a convenient label for **Line** 2, which is READ by the program. For example, Figure 10 lists **Line** 1 as:

PROJECT NAME

which is stating that the **Line** 2 is a name to be READ by EHTD. **Line** 1 can be left blank if desired.

Line 2 is a *user-supplied name* that is required and is READ by EHTD. It intended to be an identifier for the specific tracer test being designed. For example, Figure 10 lists **Line** 2 as:

Name of Planned Tracer Test

which should match all references to the eventual tracer test.

Line 3 is also a comment statement provided so that the user may enter a clarifying statement, which is ignored by EHTD. It is generally used as a convenient label for **Line 4** which is READ by the program. For example, Figure 10 lists **Line 3** as:

FLOW	RELEAS	RTIME (h)	INFLOW (m ³ /h)	UNITS
------	--------	-----------	----------------------------	-------

which is stating that control codes and data listed on **Line 4** are to be READ by EHTD. **Line 3** best serves as a header listing for **Line 4**.

Line 4 is a *user-specified input*, the specifics of which are as follows:

FLOW = 1 if open-channel or closed-conduit flow (surface-water stream or solution conduit).

FLOW = 2 if porous media flow and a natural-gradient tracer test.

FLOW = 3 if porous media flow and a forced-gradient tracer test (extraction well).

FLOW = 4 if porous media flow and an injection/withdrawal test (injection well rate = pumping well rate).

FLOW = 5 if porous media flow and a recirculation test (injection well rate = pumping well rate).

RELEAS = 1 for impulse (instantaneous) tracer release (i.e., Dirac δ function).

RELEAS = 2 for pulse tracer release (time dependent).

RELEAS = 3 for continuous (step) tracer release.

RTIME (h) is time for a pulse release (RELEAS = 2). It is meaningless for a nonpulse tracer release (i.e., RELEAS \neq 2), but some value must be entered as a place holder (automatically converted to zero for RELEAS \neq 2).

INFLOW (m³/h) or (ft³/h) is the rate of injection, and it can have significant effects on the extent of predicted dilution. For pulse and continuous releases into porous media systems, a value for INFLOW should definitely be included. No value should be listed for impulse releases. The user must also decide whether pre- and post-tracer injection flush water should be included to account for additional dilution effects. However, for flowing streams (e.g., surface-water streams), upstream discharges entering the injection point should not be included as INFLOW.

UNITS = 1 for metric units (meters, square meters, cubic meters per hour).

UNITS = 2 for English units (feet, square feet, cubic feet per hour).

For example, **Line** 4 in Figure 10 might, for an actual tracer test, appear as:

```
1          1          0.0          0.0          1
```

which states that FLOW = 1, RELEAS = 1, RTIME (h) = 0.0 h, INFLOW (m³/h) = 0.0 m³ h⁻¹, and UNITS = 1. It will be noted that the values listed for RTIME and INFLOW are merely place holders. Alternatively, **Line** 4 in Figure 10 might appear as:

```
1          2          3.0          0.0          1
```

which represents a 3-hour pulse release in which flush or inflow water should be excluded, such as might occur with a tracer test in a surface-water stream.

As yet another alternative, **Line** 4 might be the listing for FLOW as any integer greater than 1 and less than 6 ($2 \leq x \leq 5$), which requires a proper corresponding entry in **Line** 9. In this instance, **Line** 4 in Figure 11 might appear as:

```
4          2          76.56          5.688E01          1
```

which represents a porous media injection/withdrawal tracer test in which tracer was injected into a well over a period of 76.56 hours coupled with an injection flow rate and downgradient withdrawal rate equal to $5.688 \times 10^1 \text{ m}^3 \text{ h}^{-1}$.

NOTE: Time values are always in hours!

Line 5 is also a comment statement provided so that the user may enter a clarifying statement, which is ignored by EHTD. It is generally used as a convenient breaking point before listing the sample station name(s). For example, Figure 10 lists **Line** 5 as:

```
*****
```

which has no real meaning and is ignored by EHTD. **Line** 5 can be left blank if desired.

Line 6 is also a comment statement provided so that the user may enter a clarifying statement, which is ignored by EHTD. It is generally used as a convenient indicator that

Line 7 will contain the *sample station name*. For example, Figure 10 lists **Line 6** as:

STATION NAME

which is ignored by EHTD but is useful for recognizing **Line 7**, which is READ by EHTD. **Line 6** can be left blank if desired.

Line 7 is a *user-supplied name* that is required and is READ by EHTD. It intended to be an identifier for a specific sample station. For example, Figure 10 lists **Line 7** as:

Name of Sample Station 1

where the number 1 is used in this example as an indicator that there is more than one sampling station for the example tracer test. The actual name can be anything, but one must be listed.

Line 8 is another comment statement provided so that the user may enter a clarifying statement, which is ignored by EHTD. It is intended as a convenient indicator for appropriate input to be listed on **Line 8**. For example, Figure 10 lists **Line 8** as:

DISCHARGE (m³/h) DISTANCE (m) AREA (m²) SINUOSITY FACTOR

Alternatively, Figure 11 lists **Line 8** as:

DISCHARGE (m³/h) POROSITY THICKNESS (m) DIST-X (m) DIST-Y (m)

Both of these examples serve as indicators of data input for **Line 9** and to be READ by EHTD. **Line 8** best serves as a header listing for **Line 9**.

Line 9 is a series of *user-supplied data* representing either field measurements or estimates for the parameters identified on **Line 8** of Figure 10 or Figure 11, as appropriate. For example, **Line 9** (with **Line 8** added for clarity) in Figure 10 might, for an actual tracer test, appear as:

DISCHARGE (m ³ /h)	DISTANCE (m)	AREA (m ²)	SINUOSITY FACTOR
6.408E3	8000.0	18.8	1.0

which states that DISCHARGE (m³/h) = 6.408×10³ m³ h⁻¹, DISTANCE (m) = 8000.0

m, AREA (m²) = 18.8 m², and SINUOSITY = 1.0 or no sinuosity adjustment. Alternatively, **Line 9** (with **Line 8** added for clarity) in Figure 11 might appear as:

DISCHARGE (m ³ /h)	POROSITY	THICKNESS (m)	DIST-X (m)	DIST-Y (m)
5.688E1	0.35	21.6	38.3	0.0

which states that DISCHARGE (m³/h) = 5.688×10^1 m³ h⁻¹, POROSITY = 0.35, THICKNESS (m) = 21.6 m, DIST-X (m) = 38.3 m, and DIST-Y (m) = 0.0 m.

Of particular significance in the second example is the lack of an estimated transverse spread (DIST-Y (m) = 0.0). Transverse spread needs to be estimated only for a natural-gradient porous media tracer test (FLOW = 2). All subsequent cases (FLOW = 3–5) will result in an automatic transverse spread estimate by EHTD according to Equations (72) – (75).

Line 10 is a comment statement provided so the user may enter a clarifying statement, which is ignored by EHTD. It is intended as a convenient indicator for appropriate input to be listed on **Line 11**. For example, Figure 10 lists **Line 10** as:

INIT. CONC. (ug/L)	GAMMA1	GAMMA2
--------------------	--------	--------

Line 11 is a series of *user-supplied input* representing a desire on the part of the user to allow for initial (background) tracer concentration and exponential (growth) production. Initial concentration and production values to be entered must always conform to ≥ 0.0 . So, for example, **Line 11** in Figure 10 might appear as:

0.02	0.1	0.2
------	-----	-----

which states that INIT. CONC. (ug/L) = 0.02 $\mu\text{g L}^{-1}$, GAMMA1 = 0.1, GAMMA2 = 0.2.

It is essential that estimated values for initial concentration > 0.0 and the exponential production parameters > 0.0 not be excessively large. Very large values for either initial concentration (relative to set average concentration) or exponential production parameters may result in nonsense results from EHTD.

Line 12 is a comment statement provided so the user may enter a clarifying statement, which is ignored by EHTD. It is intended as a convenient indicator for appropriate

input to be listed on **Line** 13. For example, Figure 10 lists **Line** 12 as:

RETARDATION	DECAY (1/h)	OPTIM	AVE. CONC. (ug/L)
-------------	-------------	-------	-------------------

Line 13 is a series of *user-supplied input* representing a desire on the part of the user to allow for tracer retardation in the system, tracer-specific decay (in reciprocal hours only), to turn on program optimization, and to set a required average tracer concentration. Retardation values to be entered must always conform to ≥ 1.0 , decay values must always conform to ≥ 0.0 , and average concentration must conform to > 0.0 for obvious reasons (i.e., from solute transport theory, retardation can never be less than one, decay can never be negative, and average concentration can never be less than or equal to zero). So, for example, **Line** 13 in Figure 10 might appear as:

1.0	0.0	0	20.0
-----	-----	---	------

which states that RETARDATION = 1.0, DECAY (1/h) = 0.0 h⁻¹, OPTIM = 0, AVE. CONC. (ug/L) = 20.0 µg L⁻¹. Note that setting optimization to zero (OPTIM = 0) informs EHTD not to perform an optimization routine. However, setting optimization to one (OPTIM = 1) informs EHTD to perform an optimization on the estimated tracer mass, retardation, and decay if appropriate (see **Line** 14 description in Table 25 and below.

It is essential that estimated values for retardation > 1.0 and decay > 0.0 h⁻¹ not be excessively large. Very large values for either retardation or decay may result in nonsense results from EHTD.

Line 14 is a series of two *user-supplied input* switches to inform EHTD whether retardation and/or decay estimates are to be estimated. For example, if OPTIM = 1 (**Line** 13) and **Line** 14 in Figure 10 is represented by

1	1
---	---

EHTD, is informed to perform a full optimization (mass, retardation, and decay). Setting **Line** 14 to

0	1
---	---

informs EHTD to optimize mass and decay only, whereas

1 0

informs EHTD to optimize mass and retardation only. If **OPTIM** = 0 (**Line** 13) and **Line** 14 is represented by

1 1

EHTD is informed to not perform any optimization because the main optimization control switch is set to off.

Line 15 sets the minimum bounds to be considered by EHTD on the optimization of retardation and decay. Values for **Line** 15 for retardation cannot be less than one, and for decay they cannot be less than zero. For example, **Line** 15 in Figure 10 will commonly appear as

1.0 0.0

which informs EHTD of the minimum bounds allowed according to the user.

Line 16 sets the maximum bounds to be considered by EHTD on the optimization of retardation and decay. Values for **Line** 15 for retardation can be any number greater than one, and for decay they can be any number greater than zero. For example, **Line** 15 in Figure 10 will commonly appear as

10.0 5.0

which informs EHTD of the maximum bounds allowed according to the user.

Line 17 is a comment statement provided so that the user may enter a clarifying statement, which is ignored by EHTD. It is generally used as a convenient breaking point before listing the sample station name(s). For example, Figure 10 lists **Line** 17 as:

which has no real meaning and is ignored by EHTD. **Line** 17 can be left blank if desired.

Line 18 is also a comment statement provided so that the user may enter a clarifying statement, which is ignored by EHTD. It is generally used as a convenient indicator that **Line** 17 will contain the *End of Runs* indicator. For example, Figure 10 lists

Line 18 as:

STOP PROCESSING

which is ignored by EHTD but is useful for recognizing ***Line*** 19, which is READ by EHTD if included. ***Line*** 18 can be left blank if desired.

Line 19 is a stopping criterion that is specifically listed *End of Runs* and that is READ by EHTD. It intended to facilitate EHTD processing, but it is not required. *Line 19* may be left blank without any expected processing difficulties, but a warning message to the user is returned. Using the stopping criterion *End of Runs* is useful for allowing the inclusion of file notes to be included at the end of the data input file. For example, Figure 10 lists ***Line*** 19 as:

End of Runs

Karstic site

Tracer injection to occur in a sinking stream

Tracer recovery expected at two springs

Discharge measurements made on *date*

where the informational statements following ***Line*** 19 are not processed by EHTD but are useful notes. In particular, the date when discharge measurements were taken is very valuable, because discharges can change radically over very short time periods.

6. EHTD OUTPUT FILES

EHTD produces only minimal screen output. For the most part, screen output is limited to estimates for tracer mass and warning and/or error messages related to the respective input file and processing. Most of this information can be ignored by the user, as all of the screen text output is reproduced in much greater detail in the EHTD output file.

Upon completion of input file processing, EHTD automatically develops a screen plot of the likely BTC according to the data contained in the input file. As noted in Section 3.1. the BTC developed by EHTD is based on the conventional ADE using any one of the three solutions listed in Section 3.2.1., Equations (54) – (57). It will be noted that unless the user specifically informs EHTD to produce a Plot File during program initiation or saves the screen plot as a *.bmp file (see Section 4.6.1.), no final screen plot will be produced for later viewing.

6.1. DESCRIPTION OF OUTPUT FILES

Entering the name of a typical EHTD data input file when requested by EHTD (see Section 4.2.), the requested data output file name, and the requested plot file name, if desired, results in rapid data processing by EHTD. Figure 12 represents a typical data input file. It consists of measured data developed for the Lost River Cave System in Kentucky, in which recovery was expected at the Lost River Rise [see Field and Pinsky (2000) for a brief discussion of the site]. Upon completion of input file processing by EHTD, a conventional BTC is plotted on the CRT screen (Figure 13). This plot displays the recommended tracer mass necessary to generate the particular BTC displayed. If multiple recovery stations were listed in the input file (see Figure 10 for a general example), then the final output file will recommend a tracer mass that is developed by summing the masses recommended for each individual sampling station.

If a plot file is requested of EHTD by the user, then a standard plot file in ASCII format will be produced. Figure 14 depicts the plot file developed by EHTD from the Lost River Cave System data input file (Figure 12). The first two columns of data in Figure 14 are much longer than the second two columns and represent the data points generated by EHTD to produce the BTC. The second two columns of data never exceed 65 data points and represent the recommended sampling times and likely concentration values.

Data processing completion by EHTD also completes the development of data output files that describe the results of EHTD analysis. The data output files are quite long because

```

PROJECT NAME
KARST EXAMPLE -- LOST RIVER CAVE SYSTEM
FLOW      RELEAS      RTIM (h)      INFLOW (m^3/h)      UNITS
1          1          0.0          0.0                1
*****
STATION NAME
LOST RIVER RISE
DISCHARGE (m^3/h)  DISTANCE (m)  AREA (m^2)  SINUOSITY FACTOR
6.408E3           8000.0    18.8        1.0
INIT. CONC. (ug/L)  GAMMA1      GAMMA2
0.0              0.0        0.0
RETARDATION        DECAY (1/h)  OPTIM      AVE. CONC. (ug/L)
1.0               0.0        0          18.3
1                 1
1.0               0.0
10.0              5.0
*****
STOP PROCESSING
END OF RUNS

```

Figure 12. Typical example input file to illustrate how an example EHTD-generated output file appears after processing.

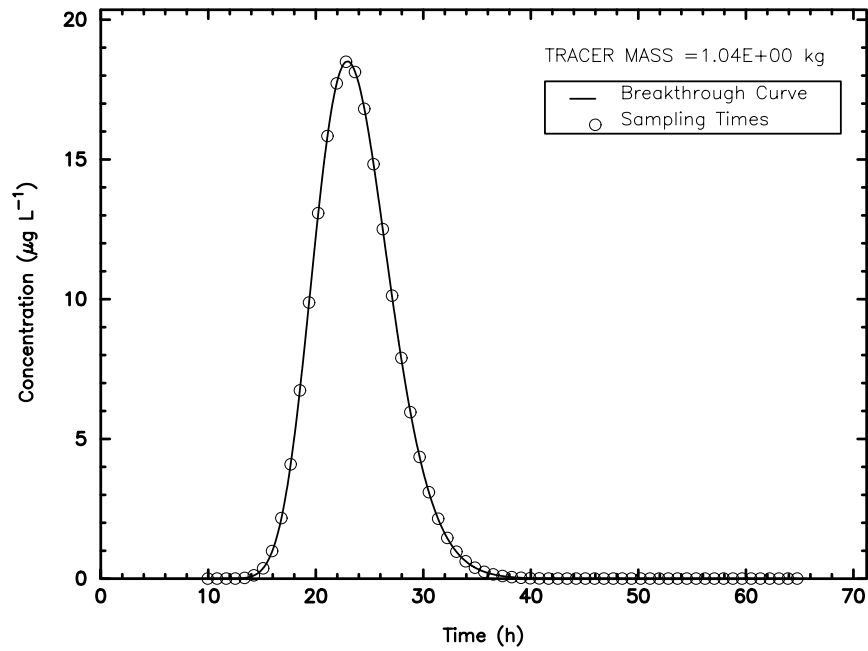


Figure 13. Standard-form example BTC generated by EHTD from a typical input file (see Figure 12). Note that recommended sampling times are shown (open circles), as is recommended tracer mass to inject. In addition, time and concentration units are adjusted automatically to their most readable values according to the tracer test design parameters.

PLOT FILE: LOST RIVER RISE

BREAKTHROUGH CURVE		SAMPLE TIMES AND CONC.	
TIME	CONC.	TIME	CONC.
(h)	($\mu\text{g/L}$)	(h)	($\mu\text{g/L}$)
-----	-----	-----	-----
.23471	0.0000	9.9516	.15918E-05
.46941	0.0000	10.808	.39299E-04
.70412	0.0000	11.665	.53591E-03
.93883	0.0000	12.522	.45611E-02
1.1735	0.0000	13.378	.26531E-01
1.4082	0.0000	14.235	.11300
1.6429	0.0000	15.092	.37166
1.8777	0.0000	15.948	.98432
2.1124	0.0000	16.805	2.1701
2.3471	0.0000	17.662	4.0911
2.5818	0.0000	18.518	6.7403
2.8165	0.0000	19.375	9.8809
3.0512	0.0000	20.232	13.082
3.2859	0.0000	21.088	15.839
3.5206	0.0000	21.945	17.723
3.7553	0.0000	22.802	18.492
3.9900	0.0000	23.658	18.130
4.2247	0.0000	24.515	16.813
4.4594	0.0000	25.372	14.830
4.6941	0.0000	26.228	12.505
4.9288	0.0000	27.085	10.123
5.1635	0.0000	27.942	7.8980
5.3983	0.0000	28.799	5.9579
5.6330	0.0000	29.655	4.3585
5.8677	0.0000	30.512	3.1001
6.1024	0.0000	31.369	2.1490
6.3371	0.0000	32.225	1.4548
6.5718	0.0000	33.082	.96361
6.8065	0.0000	33.939	.62552
7.0412	0.0000	34.795	.39855
7.2759	0.0000	35.652	.24959
7.5106	0.0000	36.509	.15381
7.7453	0.0000	37.365	.93383E-01

Figure 14. Data file generated by EHTD used to produce Figure 13.

7.9800	0.0000	38.222	.55912E-01
8.2147	.17967E-09	39.079	.33045E-01
8.4494	.79528E-09	39.935	.19294E-01
8.6841	.32080E-08	40.792	.11138E-01
8.9189	.11880E-07	41.649	.63619E-02
9.1536	.40652E-07	42.505	.35976E-02
9.3883	.12931E-06	43.362	.20154E-02
9.6230	.38444E-06	44.219	.11191E-02
9.8577	.10733E-05	45.075	.61624E-03
10.092	.28266E-05	45.932	.33669E-03
10.327	.70494E-05	46.789	.18260E-03
10.562	.16710E-04	47.645	.98335E-04
10.797	.37773E-04	48.502	.52608E-04
11.031	.81676E-04	49.359	.27968E-04
11.266	.16940E-03	50.215	.14781E-04
11.501	.33788E-03	51.072	.77675E-05
11.735	.64959E-03	51.929	.40601E-05
11.970	.12065E-02	52.786	.21115E-05
12.205	.21689E-02	53.642	.10928E-05
12.439	.37810E-02	54.499	.56295E-06
12.674	.64030E-02	55.356	.28874E-06
12.909	.10550E-01	56.212	.14748E-06
13.144	.16937E-01	57.069	.75026E-07
13.378	.26531E-01	57.926	.38023E-07
13.613	.40602E-01	58.782	.19200E-07
13.848	.60777E-01	59.639	.96614E-08
14.082	.89084E-01	60.496	.48455E-08
14.317	.12800	61.352	.24224E-08
14.552	.18044	62.209	.12074E-08
14.787	.24981	63.066	.60003E-09
15.021	.33995	63.922	.29736E-09
15.256	.45506	64.779	.14697E-09
15.491	.59966		
15.725	.77846		
15.960	.99620		
16.195	1.2575		
16.429	1.5667		
16.664	1.9275		
16.899	2.3431		

Figure 14. Data file generated by EHTD used to produce Figure 13 *continued*.

17.134	2.8157
17.368	3.3463
17.603	3.9350
17.838	4.5803
18.072	5.2795
18.307	6.0284
18.542	6.8214
18.777	7.6518
19.011	8.5115
19.246	9.3916
19.481	10.282
19.715	11.173
19.950	12.054
20.185	12.913
20.419	13.741
20.654	14.527
20.889	15.262
21.124	15.936
21.358	16.543
21.593	17.075
21.828	17.528
22.062	17.897
22.297	18.180
22.532	18.376
22.767	18.484
23.001	18.505
23.236	18.443
23.471	18.300
23.940	17.790
24.409	17.018
24.879	16.033
25.348	14.891
25.818	13.643
26.287	12.341
26.757	11.028
27.226	9.7425
27.695	8.5131
28.165	7.3621
28.634	6.3044

Figure 14. Data file generated by EHTD used to produce Figure 13 *continued*.

29.104	5.3482
29.573	4.4967
30.042	3.7489
30.512	3.1001
30.981	2.5439
31.451	2.0722
31.920	1.6760
32.390	1.3465
32.859	1.0748
33.328	.85268
33.798	.67246
34.267	.52733
34.737	.41128
35.206	.31911
35.675	.24635
36.145	.18927
36.614	.14475
37.084	.11021
37.553	.83550E-01
38.022	.63081E-01
38.492	.47439E-01
38.961	.35539E-01
39.431	.26527E-01
39.900	.19730E-01
40.370	.14625E-01
40.839	.10805E-01
41.308	.79569E-02
41.778	.58418E-02
42.247	.42762E-02
42.717	.31212E-02
43.186	.22719E-02
43.655	.16492E-02
44.125	.11941E-02
44.594	.86240E-03
45.064	.62133E-03
45.533	.44659E-03
46.002	.32026E-03
46.472	.22916E-03

Figure 14. Data file generated by EHTD used to produce Figure 13 *continued*.

46.941	.16362E-03
47.411	.11658E-03
47.880	.82901E-04
48.350	.58834E-04
48.819	.41675E-04
49.288	.29465E-04
49.758	.20796E-04
50.227	.14652E-04
50.697	.10305E-04
51.166	.72362E-05
51.635	.50731E-05
52.105	.35511E-05
52.574	.24820E-05
53.044	.17322E-05
53.513	.12071E-05
53.983	.84008E-06
54.452	.58385E-06
54.921	.40523E-06
55.391	.28089E-06
55.860	.19447E-06
56.330	.13447E-06
56.799	.92868E-07
57.268	.64064E-07
57.738	.44144E-07
58.207	.30384E-07
58.677	.20891E-07
59.146	.14349E-07
59.615	.98452E-08
60.085	.67484E-08
60.554	.46212E-08
61.024	.31615E-08
61.493	.21608E-08
61.963	.14756E-08
62.432	.10067E-08
62.901	.68627E-09
63.371	.46742E-09
63.840	.31809E-09
64.310	.21630E-09
64.779	.14696E-09

Figure 14. Data file generated by EHTD used to produce Figure 13 *continued*.

of the large amount of information developed by EHTD to produce a reliable prediction of results.

6.1.1. EHTD-Produced Data Output Files

EHTD-produced data output files are very detailed and organized. Each data output file is organized in a manner that allows the user to follow how EHTD progressed from initial input data to preliminary transport estimates to final transport estimates. Consistency of output in terms of units (SI only) and form are maintained regardless of type of trace planned or input units (English vs. SI). Using a typical input file (Figure 12), EHTD generates a standard-form data output file, which is shown in Figures 15.

6.1.1.1. *Data Output File Header Material.* Initial output by EHTD is a boxed file (Figure 15, page 106) that identifies the file and developer, when the file was last modified, and the data input file read by EHTD to produce the output file. The critical information listed is the last modified data, because this ensures that the most up-to-date version is being used, and the input file name, because this ensures identification of which data input file conforms with which data output file.

6.1.1.2. *Input Data Units.* A typical data input file allows both English and SI units (Figure 15, page 106). However, EHTD data-output files only appear with SI units because of convenience, consistency, and the fact that SI units represent “better” science.

6.1.1.3. *Initial Data Input Reprise.* EHTD next repeats the initial design data (Figure 15, page 106) listed in the data input file (see Figure 15). This ensures that the opportunity to review the input data is provided so that the user can check that the tracer test design matches expected field conditions. This information is not repeated regardless of how many sampling stations are listed in the data input file because this information represents the tracer injection aspects of the project.

6.1.1.4. *Sampling Station Name.* EHTD identifies the expected tracer recovery station to which the following data refer (Figure 15, page 106). As a new sampling station is read by EHTD, new expected recovery data are produced in the data output file.

```

*****
*
*          TRACER-TEST DESIGN PROGRAM          *
*          -----                            *
*
*          LAST MODIFIED:          JUNE 19 2002  *
*
*  EQUILIBRIUM MODEL FOR ROOTS AND NONLINEAR OPTIMIZATION *
*  FOR TRACER MASS, TRACER RETARDATION, TRACER DECAY, INITIAL *
*  SAMPLE COLLECTION TIME, AND SUBSEQUENT SAMPLING FREQUENCY *
*
*          MALCOLM S. FIELD          *
*          USEPA -- NCEA-W          *
*          WASHINGTON, DC 20460      *
*
*  DATA INPUT FILE:  LOST.IN      *
*
*****

```

```

          INPUT DATA
=====

  ALL DATA ARE IN "CONSISTENT UNITS"

      LENGTH [L]    (m)
      TIME    [T]    (h)
      CONC.   [M/T]  (mg/m^3 = µg/L)
=====

```

Figure 15. Standard-form example output file generated by EHTD from a typical input file (see Figure 12).

```

                                PROJECT NAME AND TRACER-TEST CONDITIONS
=====

                                PROJECT NAME
                                -----
                                KARST EXAMPLE -- LOST RIVER CAVE SYSTEM

FLOW TYPE      STATIONS      RELEASE MODE      RELEASE TIME
                                (h)
-----
              1              1              IMPULSE              0.00E+00
=====

FLOWING STREAM TRACER TEST

*****
*
*  STATION: LOST RIVER RISE
*
*
*****

```

Figure 15. Standard-form example output file generated by EHTD from a typical input file (see Figure 12) *continued*.

TABLE 1.1. INPUT FACTORS THAT INFLUENCE TRACER MASS ESTIMATION

MEASURED PARAMETERS OF INFLUENCE				
DISCHARGE (m^3/h)	DISTANCE (m)	X-SEC. AREA (m^2)	SINUOUS FACTOR	
6.4080E+03	8.00E+03	1.88E+01	1.00E+00	
TRACER-SPECIFIC FACTORS OF INFLUENCE				
FACTOR	VALUE	LOWER BOUND	UPPER BOUND	ADJUSTABLE
RETARDATION	1.00E+00	0.00E+00	0.00E+00	0
DECAY (1/h)	0.00E+00	0.00E+00	0.00E+00	0
SET AVERAGE CONCENTRATION (µg/L = mg/m^3)				
1.83E+01				

OUTPUT DATA

ALL DATA ARE IN "CONSISTENT UNITS"

LENGTH [L] (m)
 TIME [T] (h)
 CONC. [M/T] (mg/m³ = μg/L)
 MASS [M] (mg, g, kg)

Figure 15. Standard-form example output file generated by EHTD from a typical input file (see Figure 12) *continued*.

TABLE 2.1.1. INITIAL ESTIMATED HYDRAULIC FACTORS

ESTIMATED STATISTICAL TIMES OF TRAVEL			
AVERAGE TIME (INI. EST.) (h)	AVERAGE TIME (ADJ. EST.) (h)	AVERAGE TIME VARIANCE (h ²)	PEAK TIME (INI. EST.) (h)
2.3471E+01	3.6943E+01	1.3812E+02	2.3471E+01
ESTIMATED TRANSPORT VELOCITIES AND DISCHARGE VOLUME			
AVE. VELOCITY (INI. EST.) (m/h)	AVE. VELOCITY (ADJ. EST.) (m/h)	PEAK VELOCITY (INI. EST.) (m/h)	SYSTEM VOLUME (INI. EST.) (m ³)
3.4085E+02	2.3685E+02	3.3417E+02	3.0080E+05
ESTIMATED DISPERSION PARAMETERS			
DISPERSION (m ² /h)	PECLET NUMBER (DIMEN.)	DISPERSIVITY (m)	
3.1336E+04	8.7018E+01	9.1935E+01	

Figure 15. Standard-form example output file generated by EHTD from a typical input file (see Figure 12) *continued*.

TABLE 2.1.2. FINAL ESTIMATED HYDRAULIC FACTORS WITHOUT RETARDATION
(NONREACTIVE TRANSPORT)

ESTIMATED STATISTICAL TIMES OF TRAVEL		
AVERAGE TIME (h)	TIME VARIANCE (h ²)	PEAK TIME (h)
2.3471E+01	1.3812E+02	2.2767E+01
ESTIMATED TRANSPORT VELOCITIES AND DISCHARGE VOLUME		
AVE. VELOCITY (m/h)	PEAK VELOCITY (m/h)	
3.4085E+02	3.5139E+02	
ESTIMATED DISPERSION PARAMETERS		
DISPERSION (m ² /h)	PECLET NUMBER (DIMEN.)	DISPERSIVITY (m)
3.1336E+04	8.7018E+01	9.1935E+01

Figure 15. Standard-form example output file generated by EHTD from a typical input file
(see Figure 12) *continued*.

TABLE 3.1. FINAL TRACER-MASS ESTIMATE CALCULATIONS

=====			
TRACER-MASS ESTIMATES			

TRACER MASS (INI. EST.) (g)	TRACER MASS (ADJ. EST.) (g)	TRACER MASS (REA. EST.) (g)	TRACER MASS (FIN. EST.) (g)

2.0723E+03	1.0400E+03	---	1.0400E+03
ERROR CODE =>	4		4

FINAL TRACER-MASS REDUCTION FACTORS			

SYSTEM VOL. (m ³)	DILUTION VOL. (m ³)	RETARDATION (DIMEN.)	DECAY (1/h)

1.50E+05	1.50E+05	1.00E+00	0.00E+00

TRACER CONCENTRATIONS			

SET CONC. (μg/L)	AVERAGE CONC. (μg/L)	PEAK CONC. (μg/L)	

1.83E+01	1.8300E+01	1.8505E+01	
=====			

Figure 15. Standard-form example output file generated by EHTD from a typical input file (see Figure 12) *continued*.

TABLE 4.1. ESTIMATED SAMPLING FREQUENCY

SAMPLING TIME INTERVAL			

	EXACT (min)	CONVENIENT (min)	

	5.1401E+01	51.	

RECOMMENDED SAMPLING TIMES SINCE TRACER RELEASE			

SAMPLE NUMBER	EXACT (h)	CONVENIENT (h)	CONVENIENT (min)

1	9.9516E+00	9.	57.
2	1.0808E+01	10.	48.
3	1.1665E+01	11.	40.
4	1.2522E+01	12.	31.
5	1.3378E+01	13.	23.
6	1.4235E+01	14.	14.
7	1.5092E+01	15.	5.
8	1.5948E+01	15.	57.
9	1.6805E+01	16.	48.
10	1.7662E+01	17.	40.
11	1.8518E+01	18.	31.
12	1.9375E+01	19.	23.
13	2.0232E+01	20.	14.
14	2.1088E+01	21.	5.
15	2.1945E+01	21.	57.
16	2.2802E+01	22.	48.
17	2.3658E+01	23.	40.
18	2.4515E+01	24.	31.
19	2.5372E+01	25.	22.
20	2.6228E+01	26.	14.

Figure 15. Standard-form example output file generated by EHTD from a typical input file (see Figure 12) *continued*.

21	2.7085E+01	27.	5.
22	2.7942E+01	27.	57.
23	2.8799E+01	28.	48.
24	2.9655E+01	29.	39.
25	3.0512E+01	30.	31.
26	3.1369E+01	31.	22.
27	3.2225E+01	32.	14.
28	3.3082E+01	33.	5.
29	3.3939E+01	33.	56.
30	3.4795E+01	34.	48.
31	3.5652E+01	35.	39.
32	3.6509E+01	36.	31.
33	3.7365E+01	37.	22.
34	3.8222E+01	38.	13.
35	3.9079E+01	39.	5.
36	3.9935E+01	39.	56.
37	4.0792E+01	40.	48.
38	4.1649E+01	41.	39.
39	4.2505E+01	42.	30.
40	4.3362E+01	43.	22.
41	4.4219E+01	44.	13.
42	4.5075E+01	45.	5.
43	4.5932E+01	45.	56.
44	4.6789E+01	46.	47.
45	4.7645E+01	47.	39.
46	4.8502E+01	48.	30.
47	4.9359E+01	49.	22.
48	5.0215E+01	50.	13.
49	5.1072E+01	51.	4.
50	5.1929E+01	51.	56.
51	5.2786E+01	52.	47.
52	5.3642E+01	53.	39.
53	5.4499E+01	54.	30.
54	5.5356E+01	55.	21.
55	5.6212E+01	56.	13.
56	5.7069E+01	57.	4.
57	5.7926E+01	57.	56.
58	5.8782E+01	58.	47.
59	5.9639E+01	59.	38.

Figure 15. Standard-form example output file generated by EHTD from a typical input file (see Figure 12) *continued*.

60	6.0496E+01	60.	30.
61	6.1352E+01	61.	21.
62	6.2209E+01	62.	13.
63	6.3066E+01	63.	4.
64	6.3922E+01	63.	55.
65	6.4779E+01	64.	47.

=====

```

*****
*
*      CALCULATED TRACER-MASS:      1.040E+00 kg      *
*                                  1.040E+03 g        *
*                                  1.040E+06 mg        *
*
*****

```

ERROR CODE	DESCRIPTION
-----	-----
4	No change in sign of F(X*) was found although the interval (A,B) collapsed to the requested tolerance. The user must examine this case and decide whether A is near a local minimum of F(X*) or A is near a zero of even multiplicity, or neither of these.

```

*****
*
*      RECOMMENDED TRACER-MASS:      1.040E+00 kg      *
*                                  1.040E+03 g        *
*                                  1.040E+06 mg        *
*
*****

```

TRACER-TEST DESIGN PROGRAM RESULTS AS OF: 1/18/2002
2:39:20:30 pm

Figure 15. Standard-form example output file generated by EHTD from a typical input file (see Figure 12) *continued*.

6.1.1.5. Table 1.1. Input Factors. EHTD prints results in a standardized tabular form, the first of which is labeled TABLE 1.1 INPUT FACTORS THAT INFLUENCE TRACER-MASS ESTIMATION (Figure 15, page 106). This table represents a reprise of specific sampling station measured or input data listed in Table 12.

6.1.1.6. Output Data Units. The results of a typical data output file are only in SI units (Figure 15, page 106). EHTD data output files appear only with SI units for convenience and consistency and because SI units represent “better” science.

6.1.1.7. Table 2.1.1. Initial Hydraulic Factors. The next output table (TABLE 2.1.1. INITIAL ESTIMATED HYDRAULIC FACTORS) (Figure 15, page 106) describes the initial calculations essential for developing the preliminary BTC (see Figure 5, page 58). Although mostly self-explanatory, some items do need to be clarified. For example, AVERAGE TIME is listed twice, once as an “initial estimate” and once as an “adjusted estimate.” The initial estimate relates directly to the measured discharge and expected travel distance. The adjusted estimate relates to moment analysis of the preliminary BTC, which has a “connecting bar” to the AVERAGE TIME VARIANCE to show that these two are related only to each other.

6.1.1.8. Table 2.1.2. Final Hydraulic Factors. This table reflects final calculations developed by EHTD. Figure 15, page 106 does not show any significant differences from Table 2.1.1. (Figure 15, page 106) because ‘‘NONREACTIVE TRANSPORT’’ was specified, the result of which is no retardation effects.

6.1.1.9. Table 3.1. Final Tracer Mass Estimate. Table 3.1. (Figure 15, page 106) reflects the “initial tracer mass estimate” obtained from the preliminary BTC (see Figure 5, page 58), the “adjusted tracer mass estimate” obtained from the BTC and developed according to Equations (54) – (57), the “readjusted tracer mass estimate” obtained when OPTIMIZATION is requested, and the “final tracer-mass estimate” resulting from the complete EHTD processing. An ERROR CODE is included as appropriate; its meaning is described at the end of the output file.

This table also lists the “set,” “average,” and “peak” tracer concentrations (Figure 15, page 106) associated with the data input file (Figure 12). Very rarely will the average concentration not match the set concentration and the peak concentration not be greater

than either the set or the average concentration. Should the average concentration not equal the set concentration or the peak concentration be less than either the average or the peak concentrations, a clear error in either data input or EHTD processing is indicated.

6.1.1.10. *Table 4.1. Estimated Sampling Frequency.* A particularly useful aspect of EHTD is its ability to recommend when the first sample should be collected and an appropriate sampling frequency thereafter. This information is reflected in Table 4.1. (Figure 15, page 106) in terms of “exact times” (decimal years, decimal weeks, decimal days, decimal hours, and decimal minutes) and “convenient time” (i.e., 12-hour clock). This information provides the user with a helpful file for either programming an automatic data recorder or for determining when to collect grab samples at a sufficient frequency for adequately defining the BTC.

6.1.1.11. *Calculated Tracer-Mass.* A boxed final estimate for tracer mass in kilograms, grams, and milligrams (Figure 15, page 106) follows Table 4.1. for each sampling station listed in the data input file (Figure 12).

6.1.1.12. *Error Codes.* Following the results of each sampling station calculation, a list of error codes (Figure 15, page 106) are reprinted and a basic description of each is provided. Often these will be fairly insignificant, as is the case shown in Figure 15.

6.1.1.13. *Recommended Tracer-Mass.* Completion of processing of the entire project (e.g., all listed sampling files in the data input file, Figure 12) will result in a summed estimate for tracer mass in kilograms, grams, and milligrams. For multiple sampling station listings in a data input file, the recommended tracer mass may greatly exceed any individual sampling station, which can be problematic if subsurface pathways do not connect to all the listed sampling stations. In this latter instance, it is possible that more tracer than is desired could be recovered at selected sampling stations although this is much less of a problem than with the conventional conjecture method (see Section 2.1.1.).

6.1.1.14. *Date and Time of Processing.* EHTD prints out the time when EHTD processed the data input file because the results of EHTD are highly temporal-dependent. That is, flows are likely to be higher in wet seasons than during dry seasons. To obtain reasonable results, EHTD should be run soon after basic field measurements are taken and

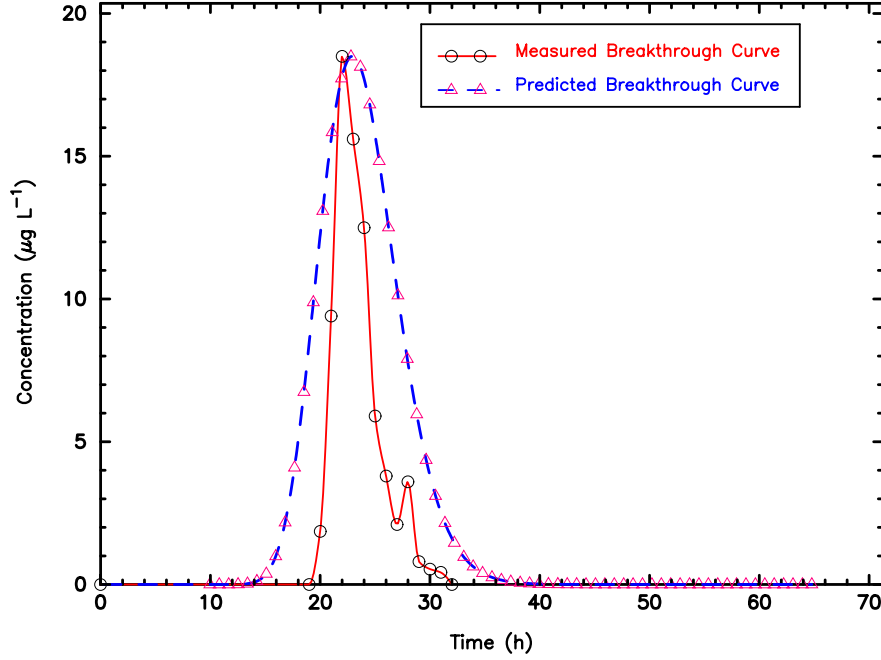


Figure 16. Comparison of EHTD-predicted BTC to measured BTC for the Lost River Rise using a typical input file (see Figure 12). Note the good prediction for tracer arrival times developed by EHTD.

EHTD-suggested recommendations implemented shortly thereafter. Significant errors in calculations and in implementation are likely to occur if there is a delay in following up on field measurements.

6.2. THE QUALITY OF EHTD-PREDICTED RESULTS

A comparison of the EHTD-predicted BTC to the measured BTC for the Lost River Rise is shown in Figure 16. It will be noted that whereas EHTD predicted a greater spread than was actually measured, the estimated times for tracer arrival were very well predicted; therefore, it is likely that the measured BTC would have been given better definition had sampling proceeded according to the recommended sampling times (frequency) developed by EHTD.

Of particular significance is the estimate for tracer mass versus the actual tracer mass injected. EHTD recommended approximately twice as much tracer as was actually used for the project. The excess mass recommendation in this instance reflects the greater-than-expected longitudinal dispersion calculated by EHTD.

Section 7. contains a detailed examination of how well EHTD functions under a variety of conditions. It will be noted from Section 7. that EHTD appears to work extremely well for any the environmental condition or design consideration.

6.3. EFFECT OF INITIAL CONCENTRATION AND EXPONENTIAL PRODUCTION

The inclusion of an initial (background) concentration and exponential (growth) production can greatly influence the shape of the BTC and two final estimated parameters: average concentration and peak concentration. However, the EHTD-suggested tracer mass is not affected.

These two additional conditions will generally be most beneficial when used in conjunction with a user-supplied solute mass (see Section 4.4., page 72) and EHTD is used as a counterterrorism tool (see Section 8.). This may be especially true for exponential production for the release of a bacteria if adequate nutrients and respiratory conditions exist.

6.3.1. Effect of an Initial Concentration

An initial concentration will cause the BTC to begin at a concentration that is equal to the value entered by the user. This effect may or may not be evident depending upon the initial concentration entered relative to the final peak concentration (see Lines 10 and 11 of Table 25 and explanation on page 93).

6.3.2. Effect of Exponential Production

Exponential growth will cause the entire BTC to continue rising even as concentration is decreasing because of the growth factors included. This effect may or may not be evident, depending on the dimensionless exponential production constants (**GAMMA1**, **GAMMA2**) entered relative to the final peak concentration (see Lines 10 and 11 of Table 25 and explanation on page 93).

6.3.3. Breakthrough Curve Shape

The influence of an initial concentration ($C_i = 0.3 \mu\text{g L}^{-1}$) and exponential production ($\gamma_1 = \gamma_2 = 0.5$) (Figure 17) is reflected in Figure 18. A comparison of the data listed in Figure 18 with the data listed in Figure 14 (pages 100–104) shows that BTC time data and sample time data (columns 1 and 3 of Figures 14 and 18) are identical, but that BTC

```

PROJECT NAME
KARST EXAMPLE -- LOST RIVER CAVE SYSTEM
FLOW      RELEAS      RTIM (h)      INFLOW (m^3/h)      UNITS
1          1          0.0          0.0                1
*****
STATION NAME
LOST RIVER RISE
DISCHARGE (m^3/h)  DISTANCE (m)  AREA (m^2)  SINUOSITY FACTOR
6.408E3           8000.0    18.8        1.0
INIT. CONC. (ug/L)  GAMMA1      GAMMA2
0.3              0.5        0.5
RETARDATION        DECAY (1/h)  OPTIM      AVE. CONC. (ug/L)
1.0               0.0        0          18.3
1                 1
1.0               0.0
10.0              5.0
*****
STOP PROCESSING
END OF RUNS

```

Figure 17. Example input file with an initial concentration and exponential production constants.

PLOT FILE: LOST RIVER RISE

BREAKTHROUGH CURVE		SAMPLE TIMES AND CONC.	
TIME	CONC.	TIME	CONC.
(h)	($\mu\text{g/L}$)	(h)	($\mu\text{g/L}$)
-----	-----	-----	-----
.23471	.30500	9.9516	.51277
.46941	.31000	10.808	.53135
.70412	.31501	11.665	.55050
.93883	.32001	12.522	.57332
1.1735	.32501	13.378	.61428
1.4082	.33001	14.235	.71994
1.6429	.33502	15.092	.99791
1.8777	.34002	15.948	1.6297
2.1124	.34502	16.805	2.8337
2.3471	.35003	17.662	4.7708
2.5818	.35503	18.518	7.4328
2.8165	.36004	19.375	10.582
3.0512	.36504	20.232	13.785
3.2859	.37005	21.088	16.539
3.5206	.37505	21.945	18.415
3.7553	.38006	22.802	19.171
3.9900	.38507	23.658	18.794
4.2247	.39007	24.515	17.461
4.4594	.39508	25.372	15.463
4.6941	.40009	26.228	13.123
4.9288	.40510	27.085	10.729
5.1635	.41011	27.942	8.4939
5.3983	.41513	28.799	6.5459
5.6330	.42014	29.655	4.9405
5.8677	.42515	30.512	3.6778
6.1024	.43017	31.369	2.7235
6.3371	.43519	32.225	2.0271
6.5718	.44020	33.082	1.5345
6.8065	.44523	33.939	1.1954
7.0412	.45025	34.795	.96782
7.2759	.45527	35.652	.81845
7.5106	.46030	36.509	.72243
7.7453	.46533	37.365	.66184

Figure 18. Data file generated by EHTD used to produce Figure 19.

7.9800	.47036	38.222	.62428
8.2147	.47539	39.079	.60136
8.4494	.48043	39.935	.58757
8.6841	.48547	40.792	.57940
8.9189	.49052	41.649	.57461
9.1536	.49556	42.505	.57184
9.3883	.50062	43.362	.57025
9.6230	.50567	44.219	.56936
9.8577	.51074	45.075	.56885
10.092	.51581	45.932	.56857
10.327	.52089	46.789	.56842
10.562	.52598	47.645	.56833
10.797	.53109	48.502	.56829
11.031	.53623	49.359	.56826
11.266	.54143	50.215	.56825
11.501	.54671	51.072	.56824
11.735	.55215	51.929	.56824
11.970	.55784	52.786	.56824
12.205	.56396	53.642	.56824
12.439	.57073	54.499	.56824
12.674	.57853	55.356	.56824
12.909	.58787	56.212	.56824
13.144	.59947	57.069	.56824
13.378	.61428	57.926	.56824
13.613	.63359	58.782	.56824
13.848	.65902	59.639	.56824
14.082	.69260	60.496	.56824
14.317	.73679	61.352	.56824
14.552	.79452	62.209	.56824
14.787	.86919	63.066	.56824
15.021	.96461	63.922	.56824
15.256	1.0850	64.779	.56824
15.491	1.2349		
15.725	1.4189		
15.960	1.6418		
16.195	1.9082		
16.429	2.2224		
16.664	2.5882		
16.899	3.0085		

Figure 18. Data file generated by EHTD used to produce Figure 19 *continued*.

17.134	3.4857
17.368	4.0208
17.603	4.6137
17.838	5.2630
18.072	5.9659
18.307	6.7181
18.542	7.5142
18.777	8.3473
19.011	9.2094
19.246	10.091
19.481	10.984
19.715	11.876
19.950	12.757
20.185	13.617
20.419	14.444
20.654	15.230
20.889	15.963
21.124	16.636
21.358	17.241
21.593	17.771
21.828	18.221
22.062	18.587
22.297	18.867
22.532	19.059
22.767	19.163
23.001	19.181
23.236	19.115
23.471	18.967
23.940	18.449
24.409	17.667
24.879	16.674
25.348	15.523
25.818	14.268
26.287	12.958
26.757	11.639
27.226	10.347
27.695	9.1117
28.165	7.9558
28.634	6.8937

Figure 18. Data file generated by EHTD used to produce Figure 19 *continued*.

29.104	5.9339
29.573	5.0793
30.042	4.3287
30.512	3.6778
30.981	3.1197
31.451	2.6464
31.920	2.2490
32.390	1.9185
32.859	1.6460
33.328	1.4232
33.798	1.2425
34.267	1.0970
34.737	.98058
35.206	.88816
35.675	.81521
36.145	.75798
36.614	.71334
37.084	.67871
37.553	.65199
38.022	.63147
38.492	.61579
38.961	.60386
39.431	.59482
39.900	.58801
40.370	.58289
40.839	.57906
41.308	.57621
41.778	.57409
42.247	.57252
42.717	.57136
43.186	.57051
43.655	.56989
44.125	.56943
44.594	.56910
45.064	.56886
45.533	.56868
46.002	.56856
46.472	.56847

Figure 18. Data file generated by EHTD used to produce Figure 19 *continued*.

46.941	.56840
47.411	.56835
47.880	.56832
48.350	.56830
48.819	.56828
49.288	.56827
49.758	.56826
50.227	.56825
50.697	.56825
51.166	.56824
51.635	.56824
52.105	.56824
52.574	.56824
53.044	.56824
53.513	.56824
53.983	.56824
54.452	.56824
54.921	.56824
55.391	.56824
55.860	.56824
56.330	.56824
56.799	.56824
57.268	.56824
57.738	.56824
58.207	.56824
58.677	.56824
59.146	.56824
59.615	.56824
60.085	.56824
60.554	.56824
61.024	.56824
61.493	.56824
61.963	.56824
62.432	.56824
62.901	.56824
63.371	.56824
63.840	.56824
64.310	.56824
64.779	.56824

Figure 18. Data file generated by EHTD used to produce Figure 19 *continued*.

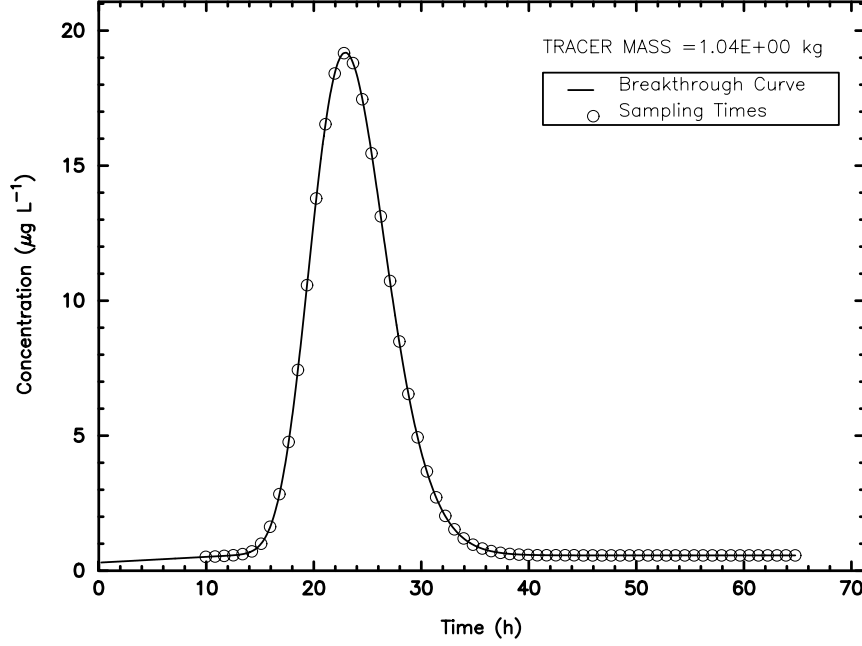


Figure 19. Effect of including an initial concentration and exponential production to the Lost River Cave System data. Note that the BTC does not begin at zero concentration and exhibits a gently rising slope prior to initiating a steep rise in response to tracer release.

concentration data and sample concentration data (columns 2 and 4 of Figures 14 and 18) are very different.

Using the data listed in Figure 18, Figure 19 depicts the Lost River Cave System with an $C_i = 0.3 \mu\text{g L}^{-1}$ and exponential production ($\gamma_1 = \gamma_2 = 0.5$) applied. It is evident from Figure 19 that these conditions have a significant influence on the final BTC when compared with the conditions of Figure 13, as shown in Figure 20.

6.3.4. Average and Peak Concentration Estimates

The general output file (Figure 15) will be slightly altered when an initial concentration and/or exponential production are supplied in an input file to specifically reflect changes in the estimated \overline{C} and C_p . Providing an initial concentration and/or exponential production will cause the bottom of EHTD-produced Table 3.1 to be altered to appear as Figure 21 (see Figure 15 on page 111 for comparison). In addition to producing a modified Table 3.1, EHTD will also produce a Table 5.1 immediately after Table 4.1. The EHTD-produced Table 5.1 will provide an estimate of \overline{C} and C_p (Figure 22).

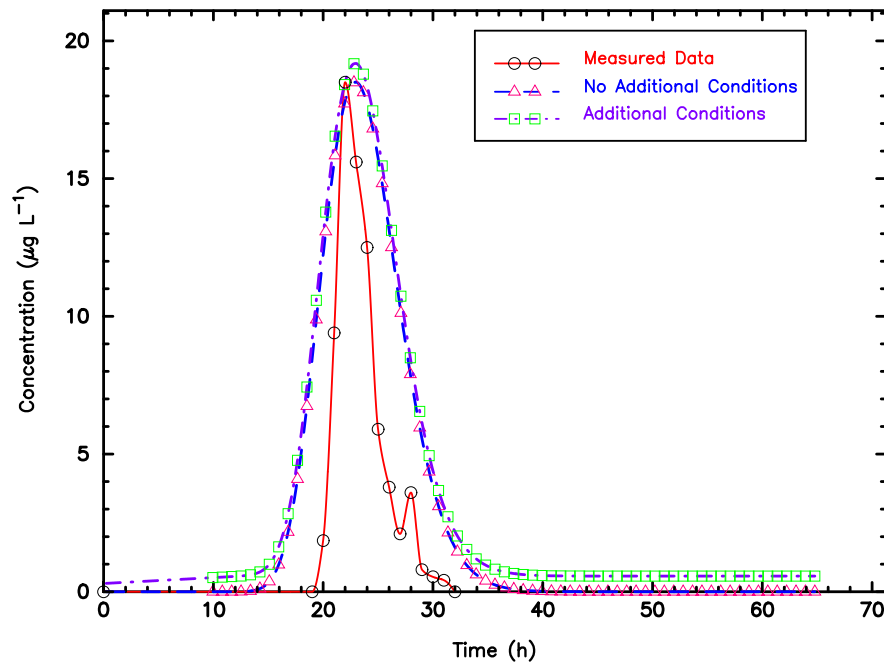


Figure 20. Comparison of the effect of including an initial concentration and exponential production to the Lost River Cave System data. The label **No Additional Conditions** indicates just the tracer release data and the label **Additional Conditions** indicates that an initial concentration and exponential production are included with the tracer release data.

FINAL TRACER-MASS REDUCTION FACTORS			
SYSTEM VOL. (m ³)	DILUTION VOL. (m ³)	RETARDATION (DIMEN.)	DECAY (1/h)
1.50E+05	1.50E+05	1.00E+00	0.00E+00
TRACER CONCENTRATIONS			
SET CONC. (μg/L)	AVERAGE CONC. (μg/L)	PEAK CONC. (μg/L)	
1.83E+01	1.8300E+01*	1.8505E+01*	
*PRELIMINARY ESTIMATES FOR AVERAGE CONC. AND PEAK CONC. SEE REVISED ESTIMATES LISTED IN TABLE 5.1.			

Figure 21. Modified EHTD-produced portion of Table 3.1 to reflect influence of an initial concentration and/or exponential production.

*** TABLE 5.1. REVISED TRACER CONCENTRATIONS ***		
SET CONC. (μg/L)	AVERAGE CONC. (μg/L)	PEAK CONC. (μg/L)
1.83E+01	1.8967E+01	1.9181E+01

Figure 22. Example EHTD-produced Table 5.1 to reflect influence of an initial concentration and/or exponential production.

7. TRACER TEST DESIGN EXAMINATION DATA SETS

Several hydrological tracer tests representing various environmental and design conditions are listed in Table 26. The results of each of the measured eight tracer tests were

Table 26. Example test data sets.

Test Name	Test Type
<i>Flowing Stream</i>	
Uvas Creek	Small Creek
Missouri River	Large River
Dyers Spring	Solution Conduit
Variegated Glacier	Meltwater Channel
<i>Porous Media</i>	
Test Site Wilerwald	Natural Gradient
Kirchdorf-Unteropfingen Site	Forced Gradient
Mobile Site	Injection Withdrawal
Chalk River	Recirculation

compared with forecasted results. For purposes of the type of analysis, flow through a solution conduit and glacial-meltwater channel are listed under the flowing stream category along with small surface-water creeks and large rivers. This is because flow through a solution conduit behaves more like surface-water flow than porous media flow even though flow through solution conduits is correctly classed as ground-water flow. Prediction of flow through solution conduits and glacial-meltwater channels requires treatment similar to that of surface-water flow.

7.1. FLOWING STREAMS

Two surface-water streams representing small and large flows were examined to evaluate the effect of extreme flow discharge ranges on prediction capabilities. Uvas Creek is a small stream that was traced in the mid 1970s. The Missouri River is a large river that was traced in the mid 1960s. Dyers Spring was chosen as a representative tracer test through a solution conduit to a potable-water spring. All three tracer tests were conducted and analyzed by the U.S. Geological Survey. A glacial-meltwater channel (Variegated Glacier) was also listed as a flowing stream because water flow through glacial meltwater channels behaves similarly to flow in surface-water streams.

7.1.1. Small Creek

Uvas Creek was traced in 1976 using a steady 3-hour injection of 1068 g of chloride in late summer during a low flow period (Bencala and Walters, 1983; Zand et al., 1976). The emphasis of the tracing test was to investigate the mass transport processes in a small stream. The experimental study was limited to a 610 m reach, with widths ranging from 0.3 to 4 m. Flow rate at the time of the study was $45.0 \text{ m}^3 \text{ h}^{-1}$. Tracer concentration measurements were taken at selected reaches where measured flow rates varied slightly from $45.0 \text{ m}^3 \text{ h}^{-1}$. For this evaluation, tracer recovery at reach 281 m was used. The channel was composed of a rough bed with alternating pools and riffles and a steep slope (0.03 m m^{-1}).

7.1.2. Large River

The Missouri River was traced along a 243 km reach between Sioux City, Iowa and Plattsmouth, Nebraska, in 1967. The purpose of the tracer test was to obtain sufficient data to simultaneously define axial dispersion, transverse mixing, cross-sectional geometry, and transverse velocity distribution. Approximately 54 kg of Rhodamine WT (C.I. Acid Red 388) were injected as a line source extending across the middle half of the channel (Yotsukura et al., 1970, pp. G3–G5).

Sampling stations were located in a manner such that cross-sectional areas could be divided into four increments with approximately equal discharges. Discharge measurements were taken at the four cross-sections by the current meter method. Sampling frequency varied from 15 minutes to 2 hours, depending on the expected rate of change of concentration (Yotsukura et al., 1970, pp. G5–G6).

7.1.3. Solution Conduit

Dyers Spring is a blue-hole rise pit that connects an impenetrable solution-conduit system with a nearby karst window developed in the St. Louis Limestone. It is an important water-supply spring in Elizabethtown, Kentucky (Mull and Lyverse, 1984, p. 21). Limestone is exposed at the bottom of the karst window, where a stream reportedly flows into a swallet. No other external drainage has been observed, so all water entering the karst window eventually drains into the swallet (Mull et al., 1988b, p. 58).

Several tracer tests to Dyers Spring using the karst window were performed by the U.S. Geological Survey with varying degrees of tracer mass recovery (Mull et al., 1988b, p. 71). The primary intent of the tracer tests was to assess the solute transport processes operative

in the system. Recoveries ranged from 54 to 172%, which is probably a function of flow conditions when the tracer tests were undertaken and discharge measurement errors.

The Dyers Spring tracer test considered here consisted of an impulse injection of 3.57 g of Rhodamine WT, which resulted in 63% mass recovery. Errors in discharge estimation, Rhodamine WT deaminoalkylation (Käb, 1998, pp. 33–35), and/or isomer-specific sorption (Sutton et al., 2001) may have partially affected tracer-mass recovery estimates. Moderate-flow conditions (Mull et al., 1988b, pp. 25, 69) may also have caused unknown tributary flow to or from the solution conduit and a consequent reduced tracer mass recovery (Field and Nash, 1997).

7.1.4. Meltwater Channel

A tracer test was conducted in 1983 at Variegated Glacier in southeastern Alaska immediately post-glacial surge, when meltwater discharge from the glacier increased greatly. An approximately 5.2 kg pulse ($t_2 = 10$ minutes) of Rhodamine WT was injected through a borehole at the base of the glacier (Brugman, 1987, p. 93) and recovered at Lower Stream, 10 km downstream. Hot water was injected into the borehole prior to dye injection to ensure good hydraulic connection with the basal water system (Brugman, 1987, pp. 91–91). Discrete samples were collected at the glacier terminus. Sample-collection frequency was initially set at 40 minutes but was lengthened after 8 hours (Brugman, 1987, p. 93).

7.2. POROUS MEDIA

Tracer tests are commonly conducted in porous media aquifers in a variety of forms. These tracer tests rarely include natural-gradient tracer tests because of the typically long travel times involved. To increase the rate of transport, forced-gradient tracer tests, injection-withdrawal tracer tests, and recirculation tracer tests are often employed. Table 26 lists four tracer tests representing each of these types of tracer tests.

7.2.1. Natural-Gradient Tracer Test

Natural-gradient tracer tests in porous media are difficult and generally aggravating to implement because of the design information required and the very long tracer transport times involved. Even so, natural-gradient tracer tests are desirable because the flow field is not distorted, as occurs with forced-gradient tracer tests. Test Site Wilerwald, located northeast of Berne, Switzerland, in the Swiss Central Plateau, was established to evaluate

solute transport processes in a porous media aquifer. The aquifer is in the Emme Valley and consists of postglacial Holocene sandy gravels that vary in thickness from a few meters to 88 m with ground-water depths that vary from 0.5 to 3 m (Leibundgut, 1992, pp. 230–231).

In September, 1985, 1 kg of sodium fluorescein (C.I. Acid Yellow 73) dissolved in 90 L of water was released over a one hour period into an injection well. Sampling commenced almost immediately and continued for 24 weeks at several downgradient wells. The furthest well sampled for tracer from the injection well was approximately 200 m to the northwest (Leibundgut and De Carvalho Dill, 1992, pp. 232–233). The basic transport parameters used to describe the aquifer consisted of a hydraulic conductivity $K = 8.64 \text{ m h}^{-1}$, aquifer thickness $b = 10 \text{ m}$, effective porosity $n_e = 12 - 17\%$, and hydraulic gradient $i = 0.4\%$ (Małoszewski et al., 1992b, p. 239).

7.2.2. Forced-Gradient Tracer Test

A tracer and aquifer test were simultaneously conducted over a period of several months at the Kirchdorf-Unteropfingen area within the Iller Valley in Germany. Alpine Rhine glacial materials consisting of well-rounded, stratified, fine to coarse gravel with intercalated sand fractions make up the valley aquifer. The extraction well was pumped at a rate of $1368 \text{ m}^3 \text{ h}^{-1}$. During the pumping test, 3 kg of sodium fluorescein were released immediately into an observation well situated 585 m from the extraction well. Initial tracer recovery occurred at the extraction well within about 3 days and continued for more than 100 days (Käb, 1998, pp. 515–516). The pump test yielded a transmissivity of $1019 \text{ m}^2 \text{ h}^{-1}$ ($K = 116 \text{ m h}^{-1}$) and specific yield = 0.14, which was taken to be the same as effective porosity (Käb, 1998, pp. 515–516) for this evaluation.

7.2.3. Injection-Withdrawal Tracer Test

An injection withdrawal two-well tracer test consists of injecting water containing tracer into an injection well and withdrawing water from an extraction well at an equal rate so that equilibrium may be established. Such a test was conducted in a soil borrow area at the Barry Steam Plant of the Alabama Power Company near Mobile, Alabama, in the late summer of 1984. The surface is composed of Quaternary-age, low-terrace deposits consisting of interbedded sands and clays down to a depth of 61 m. Below these deposits a Miocene series of undifferentiated sands, silty clays, and thin-bedded limestones extend to a depth of 305 m (Molz et al., 1986a, p. 38).

At the Mobile site bromide was injected into a well over a period of 3.19 days. The entire tracer test lasted 32.5 days (Molz et al., 1986b). The injection and withdrawal wells, separated by a distance of 38.3 m, were operated continuously at $57 \text{ m}^3 \text{ h}^{-1}$ (Molz et al., 1986a, p. 55) to cause steady-state conditions between the injection-withdrawal wells. Details of the test are described in Molz et al. (1986b) and Molz et al. (1986a, pp. 52–60, 71).

7.2.4. Recirculation

A two-well recirculation tracer test is the same as an injection/withdrawal tracer test except that the extracted water is recirculated back into the injection well. Such a tracer test was conducted at the Chalk River site. The basic tracer test design parameters for a recirculation tracer test conducted at the Chalk River site are listed in Huyakorn et al. (1986) and described in detail in Pickens and Grisak (1981). Two glaciofluvial sand aquifers are separated by a 1 m layer of silty clay, which was taken as the bottom confining layer for the aquifer being traced. This sand aquifer is 8.2 m thick and is confined above by a 17 cm-thick silty-clay layer. Aquifer tests at the site resulted in a K that ranged from 720 to 7200 m h^{-1} , but a single-well tracer test suggests $K = 5040 \text{ m h}^{-1}$ (Pickens and Grisak, 1981).

The recirculation tracer test consisted of two wells 8 m apart that were operated at a flow rate of $1.62 \text{ m}^3 \text{ h}^{-1}$. Tracer was injected for a period of 3.22 days with an initial concentration of $4.1 \times 10^{-3} \text{ } \mu\text{g L}^{-1}$ (Huyakorn et al., 1986), which translates into a tracer mass of 521 μg .

7.3. TRACER-TEST DESIGN RESULTS

The eight tracer tests listed in Table 26 were used to test EHTD. Because these tests represent a range of tracer test types, the robustness of EHTD could be examined. Simulations using these eight data sets consisted of using only those measured or estimated field parameters necessary for application of EHTD while excluding specific tracer test-determined parameters. Set average tracer concentration \overline{C} and possible tracer reactions, tracer retardation R_d and tracer decay μ were adjustable parameters so that measured peak tracer concentration C_p and measured tracer mass M could be matched. Normal use of EHTD to predict tracer test results prior to test implementation would not require adjustment to match C_p or M except as may be desired.

Table 27. Required flowing stream tracer test design specifics.

Parameter	Uvas Creek	Missouri River	Dyers Spring	Variegated Glacier
Q , $\text{m}^3 \text{h}^{-1}$	4.79×10^1	3.47×10^6	1.16×10^2	1.44×10^5
L , m	2.81×10^2	2.43×10^5	9.14×10^2	1.00×10^4
A , m^2	3.60×10^{-1}	5.23×10^2	1.84×10^0	6.15×10^1
t_2 , h	3.00×10^0	1.67×10^{-1}
t_V , m^3
\overline{C}^a , $\mu\text{g L}^{-1}$	3.12×10^3	1.62×10^0	4.14×10^0	3.69×10^1
\overline{C}^b , $\mu\text{g L}^{-1}$	3.19×10^3	1.62×10^0	4.12×10^0	1.94×10^1

^a Average tracer concentration for nonreactive tracer transport.

^b Average tracer concentration for reactive tracer transport.

7.3.1. Flowing Streams Results

Flowing stream tracer tests make up the first four tracer tests listed in Table 26. These four tests include small and large surface-water streams, karst solution conduit, and glacial-meltwater stream. The parameters required for EHTD simulation for these tests are listed in Table 27. EHTD simulation of flowing streams requires only measurement or estimates for discharge Q , longitudinal distance L , cross-sectional area A , tracer release mode t_2 , and set average tracer concentration \overline{C} . Two listings for \overline{C} appear in Table 27 because μ may cause the predicted C_p to fall below the measured C_p that occurs with no tracer decay. Of the four tracer tests listed in Table 27, a slightly decreased C_p was a problem only for the Uvas Creek tracer test.

Hydraulic results of the EHTD-predicted BTCs for the four flowing stream tracer tests are compared with the actual BTC results in Table 28. Tracer injection specifics are listed in Table 29 and include consideration tracer mass, injection concentration C_i , pulse injection volume t_V , injection rate q , flow system volume V , and dilution volume D_V , which represents the combined effect of the injection flow rate q with discharge Q .

7.3.1.1. Uvas Creek Tracer Test. The tracer test conducted at Uvas Creek was chosen as a test case to evaluate the ability of EHTD to predict tracer tests results in very small streams when t_2 is large. For instances where $t_2 \geq \bar{t}$, Yu et al. (1999) recommend the BTC be solved for a Heaviside condition up to C_p of the BTC. For the Uvas Creek injection, t_2 was 3.00 hours (Table 27), but tracer recovery occurred within several minutes at reach

Table 28. EHTD-predicted BTCs versus measured BTCs for the flowing stream tracer tests.

Data Set ^{a,b}	\bar{t} , hours	t_p , hours	v , m h ⁻¹	D , m ² h ⁻¹	P_e , dimen.	t_1 , hours	t_f , hours
<i>Uvas Creek Tracer Test</i>							
Measured	2.11×10^0	4.33×10^0	1.33×10^2	8.64×10^2	4.33×10^1	5.33×10^{-1}	1.67×10^{-1}
EHTD-N	2.11×10^0	4.03×10^0	1.33×10^2	4.52×10^2	8.26×10^2	7.56×10^{-1}	1.36×10^{-1}
EHTD-R	2.11×10^0	4.03×10^0	1.33×10^2	4.52×10^2	8.26×10^2	7.63×10^{-1}	1.34×10^{-1}
<i>Missouri River Tracer Test</i>							
Measured	4.20×10^1	4.00×10^1	5.78×10^3	5.35×10^6	2.62×10^2	3.40×10^1	1.00×10^0
EHTD-N	3.66×10^1	3.59×10^1	6.62×10^3	1.90×10^7	8.46×10^1	1.53×10^1	1.29×10^0
EHTD-R	3.66×10^1	3.59×10^1	6.62×10^3	1.90×10^7	8.46×10^1	1.73×10^1	1.46×10^0
<i>Dyers Spring Tracer Test</i>							
Measured	1.72×10^1	1.45×10^1	5.38×10^1	3.28×10^2	1.50×10^2	1.15×10^1	5.00×10^{-1}
EHTD-N	1.45×10^1	1.42×10^1	6.32×10^1	6.61×10^2	8.73×10^1	6.22×10^0	5.09×10^{-1}
EHTD-R	1.45×10^1	1.41×10^1	6.32×10^1	6.61×10^2	8.73×10^1	6.39×10^0	5.32×10^{-1}
<i>Variegated Glacier Tracer Test</i>							
Measured	5.00×10^0	4.30×10^0	2.00×10^3	2.09×10^5	9.57×10^1	1.90×10^0	7.00×10^{-1}
EHTD-N	4.27×10^0	4.23×10^0	2.34×10^3	3.58×10^5	6.55×10^1	1.53×10^0	1.93×10^{-1}
EHTD-R	4.27×10^0	3.59×10^0	2.34×10^3	3.58×10^5	6.55×10^1	1.76×10^0	1.80×10^{-1}

^a EHTD-N = nonreactive tracer test results. EHTD-R = reactive tracer test results.^b Reactive results are listed as though no tracer reactions have occurred.

Table 29. EHTD-predicted results versus measured results for the flowing stream tracer tests.

Data Set ^a	M , g	I_C , $\mu\text{g L}^{-1}$	C_p , $\mu\text{g L}^{-1}$	V_I , m^3	q , $\text{m}^3 \text{h}^{-1}$	V , m^3	D_V , m^3
<i>Uvas Creek Tracer Test</i>							
Measured	1.07×10^3	...	6.25×10^3	1.01×10^2	...
EHTD-N	8.97×10^2	6.24×10^3	6.24×10^3	1.44×10^2	4.79×10^1	1.01×10^2	1.01×10^2
EHTD-R	1.07×10^3	6.255×10^3	6.25×10^3	1.70×10^2	5.68×10^1	1.01×10^2	1.01×10^2
<i>Missouri River Tracer Test</i>							
Measured	5.44×10^4	...	1.64×10^0	1.46×10^8	...
EHTD-N	7.88×10^4	...	1.64×10^0	1.27×10^8	1.27×10^8
EHTD-R	8.91×10^4	...	1.64×10^0	1.44×10^8	1.44×10^8
<i>Dyers Spring Tracer Test</i>							
Measured	3.57×10^0	...	4.19×10^0	2.00×10^3	...
EHTD-N	2.63×10^0	...	4.19×10^0	1.68×10^3	1.68×10^3
EHTD-R	3.56×10^0	...	4.19×10^0	1.77×10^3	1.77×10^3
<i>Variegated Glacier Tracer Test</i>							
Measured	5.24×10^6	2.38×10^{11}	3.70×10^1	2.20×10^{-2}	1.32×10^{-1}	7.20×10^5	...
EHTD-N	9.76×10^3	4.43×10^8	3.70×10^1	2.20×10^{-2}	1.32×10^{-1}	6.15×10^5	6.15×10^5
EHTD-R	5.23×10^6	2.37×10^{11}	3.72×10^1	2.20×10^{-2}	1.32×10^{-1}	7.69×10^5	7.69×10^5

^a EHTD-N = nonreactive tracer test results. EHTD-R = reactive tracer test results.

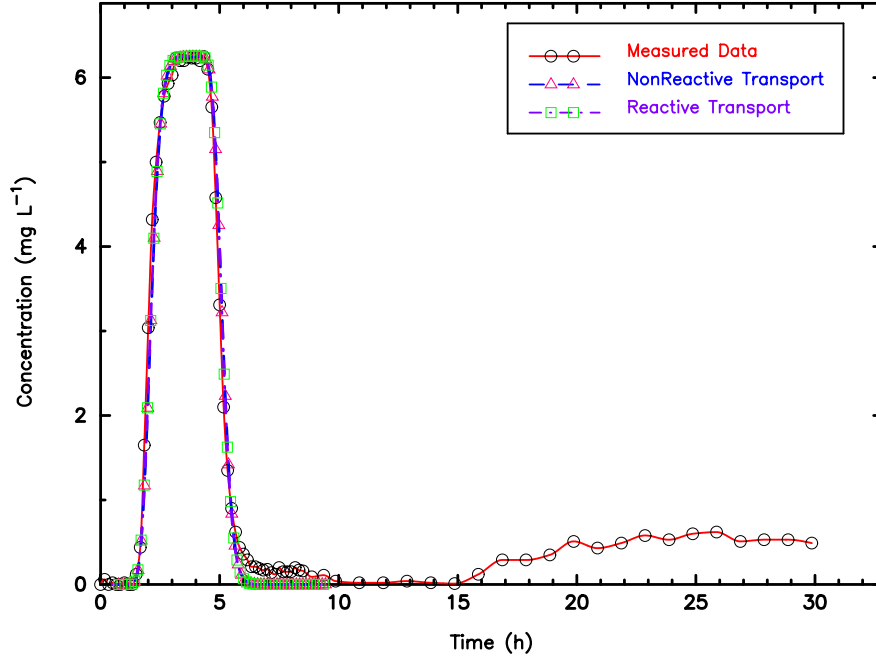


Figure 23. Comparison of measured data for the Uvas Creek site tracer test with EHTD-predicted results for nonreactive and reactive transport. For reactive transport, $R_d = 1.0$ and $\mu = 0.08 \text{ h}^{-1}$.

281 (281 m from injection site) and \bar{t} was 2.11 hours (Table 28).

Reach 281 was chosen to evaluate EHTD because the short travel distance coupled with the relatively long t_2 caused a plateau in the BTC (Figure 23). Setting $\bar{C} = 3.12 \text{ mg L}^{-1}$ for nonreactive transport (Table 27) resulted in an almost exact fit visually of the EHTD-predicted results to the actual BTC, but the EHTD-predicted tracer mass was slightly less than that injected during the actual tracer test (Figure 23). Setting $\bar{C} = 3.19 \text{ mg L}^{-1}$ and $\mu = 0.08 \text{ h}^{-1}$ for reactive transport also resulted in a nearly exact fit visually of the EHTD-predicted results to the actual BTC while matching the injected tracer mass (Figure 23). Only the measured long BTC tail was not predicted by EHTD. Both the nonreactive and the reactive EHTD-predicted BTC plateaus match the measured BTC plateau. Accounting for $\mu = 0.08 \text{ h}^{-1}$ had no measurable effect on the BTC or the estimated transport parameters. EHTD substantially underestimated D (Table 28), but any adverse effects appear to be insignificant because EHTD-recommended sampling times were appropriate for defining the BTC.

EHTD-generated BTCs for both nonreactive and reactive tracer tests predicted the

measured BTC in the sense that the initial sample collection time and sample collection frequency recommended by EHTD would have resulted in an accurate depiction of the actual BTC. The occurrence of the long tail may or may not have been detected, depending on whether sample collection continued after 11 hours.

The Uvas Creek travel times listed in Table 28 show average travel time \bar{t} to be less than the time to peak concentration t_p ($\bar{t} < t_p$), which appears contrary to typical tracer tests, where $\bar{t} > t_p$. The greater t_p for the Uvas Creek tracer test is an artifact of the long t_2 relative to actual tracer travel times. It should be noted that the measured \bar{t} and v were obtained from Q/A and related to L in Bencala and Walters (1983) is the same method used by EHTD (Field, 2002c), which explains the exact match by the EHTD-estimated \bar{t} and v . Breakthrough-curve analysis using QTRACER (Field, 2002b), modified to account for short-pulse releases (Wolff et al., 1979) and long-pulse releases (Sardin et al., 1991), resulted in a $\bar{t} = 2.08$ hours and $v = 135 \text{ m h}^{-1}$ which quite reasonably match the measured results. However, QTRACER estimated $D = 542 \text{ m}^2 \text{ h}^{-1}$, which is midway between the measured D and the EHTD-estimated D .

Because a relatively insignificant amount of tracer was added directly to the stream water, $D_V = V$ for both the measured and the EHTD-predicted results (Table 29). The exact match for both of the EHTD-predicted volumes with the measured V was surprising and is not expected to occur in other similar instances.

7.3.1.2. *Missouri River Tracer Test.* Flow in streams similar to the Missouri River is difficult to assess due to sheer size. The Missouri River tracer test used to evaluate EHTD probably represents the simplest case tested here because an impulse release of a large quantity of tracer was recovered sufficiently far from the injection point (243 km) as to not be adversely influenced by the actual injection. Figure 24 shows the results of the Missouri River tracer test. The nonreactive case adequately represents the results of the Missouri River tracer test, although the measured BTC was not ideally realized by the EHTD prediction because the nonreactive tracer test still suggested appropriate sampling times that would result in detection of the BTC. In addition, somewhat more tracer than was required was recommended by EHTD (Table 28) — a result of overestimating dispersion for such a simple flow system.

The reactive case allowed for a match of the measured BTC peak, but EHTD then recommended $1.5\times$ more tracer than was actually needed. EHTD-estimated $\bar{t} = 36.6$ hours and $v = 6623 \text{ m h}^{-1}$ reasonably matched the measured values, but required $R_d = 1.13$

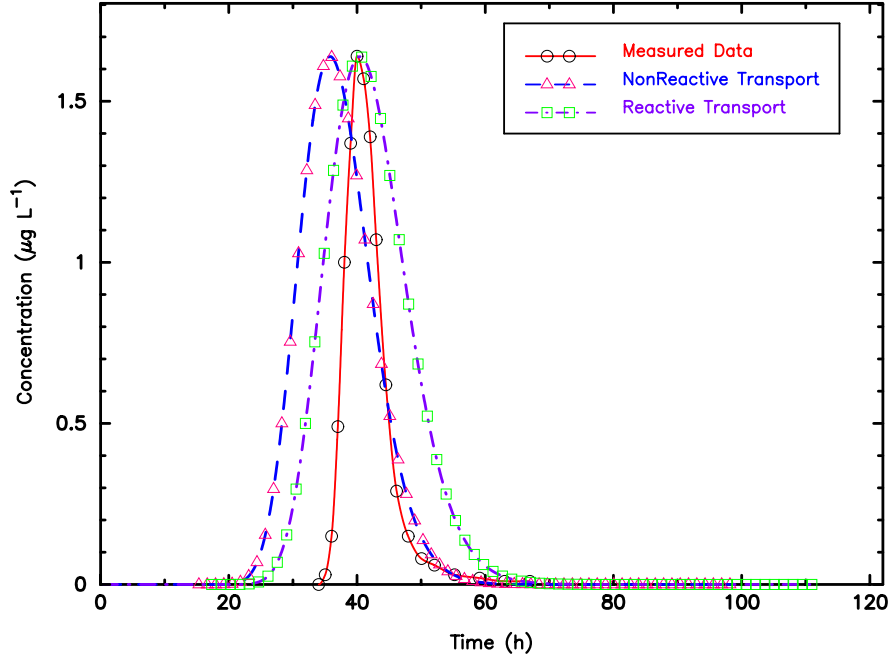


Figure 24. Comparison of measured data for the Missouri River tracer test with EHTD-predicted results for nonreactive and reactive transport. For reactive transport, $R_d = 1.13$ and $\mu = 0.0 \text{ h}^{-1}$.

to obtain a better match to the measured BTC and tracer mass injected. The EHTD-estimated $D = 1.90 \times 10^7 \text{ m}^2 \text{ h}^{-1}$ is clearly overestimated (Table 28), but this inaccuracy would not appear to adversely affect the tracer test because the measured BTC would have been defined if the EHTD-recommended sampling schedules were implemented.

As with the Uvas Creek tracer test, a relatively insignificant amount of tracer was added directly to the stream water, resulting in $D_V = V$ for both of the EHTD-predicted results (Table 29). Interestingly, although the EHTD-predicted V and D_V reasonably approximated the measured V , the EHTD-predicted V and D_V for the reactive case very nearly matches the measured V .

7.3.1.3. Dyers Spring Tracer Test. Ground-water flow and solute transport through solution conduits are commonly assessed by conducting quantitative tracer tests because conventional methods, such as pumping tests, are generally insufficient for adequately defining hydraulic parameters. Designing quantitative tracer tests in previously untraced karstic terranes can be very difficult. Typically, a trial-and-error approach that relies on

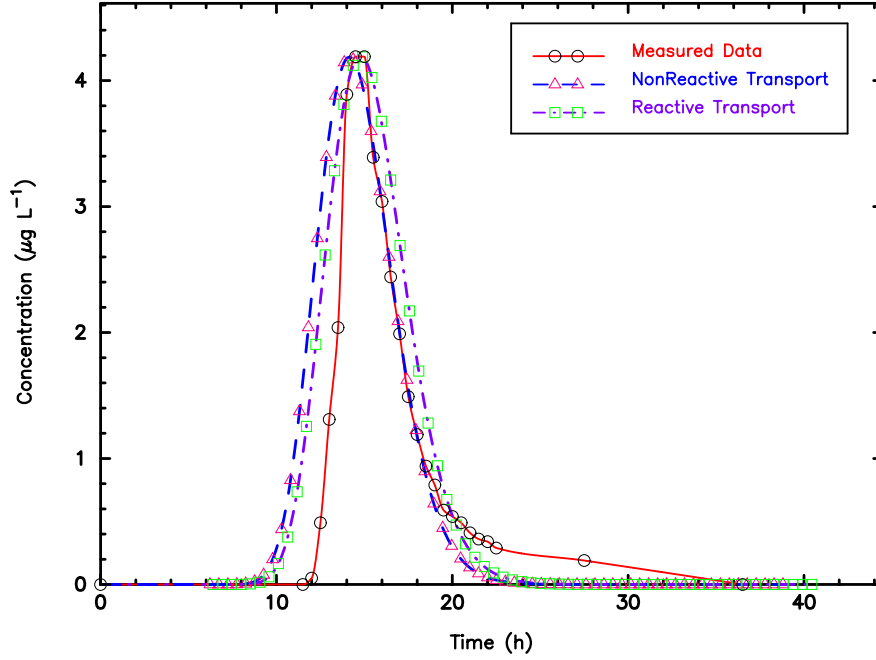


Figure 25. Comparison of measured data for the Dyers Spring tracer test with EHTD-predicted results for nonreactive and reactive transport. For reactive transport, $R_d = 1.05$ and $\mu = 0.018 \text{ h}^{-1}$.

more common qualitative tracer tests and past professional experience are used as a means for designing a quantitative tracer test (Mull et al., 1988a, pp. 26, 28).

Measured C_p at Dyers Spring occurred later than the nonreactive EHTD-predicted results when A is estimated from peak velocity v_p (Figure 25). No prior estimates for the Dyers Spring A coupled with the measured Q were available. Typically, conduit A is estimated using v calculated from the BTC, but the long BTC tails associated with Dyers Spring (Mull et al., 1988a, p. 69) as a result of immobile flow regions tends to skew v (Field and Pinsky, 2000). The long tails for the measured BTCs adversely affect the v calculation by inferring slower transport, which results in a smaller calculated cross-sectional area and consequently causes a later tracer breakthrough (Field, 2002c). Substituting v_p for v results in an earlier tracer breakthrough than that of the measured recovery, which suggests that v_p and v bracket the true velocity, as was shown to be the case by Field and Pinsky (2000).

Allowing for tracer retardation $R_d = 1.05$ and tracer decay $\mu = 0.018 \text{ h}^{-1}$ results in a BTC that adequately matches the measured BTC and a tracer-mass estimate that matches the actual tracer mass released (Table 29). Although the measured C_p was missed by the

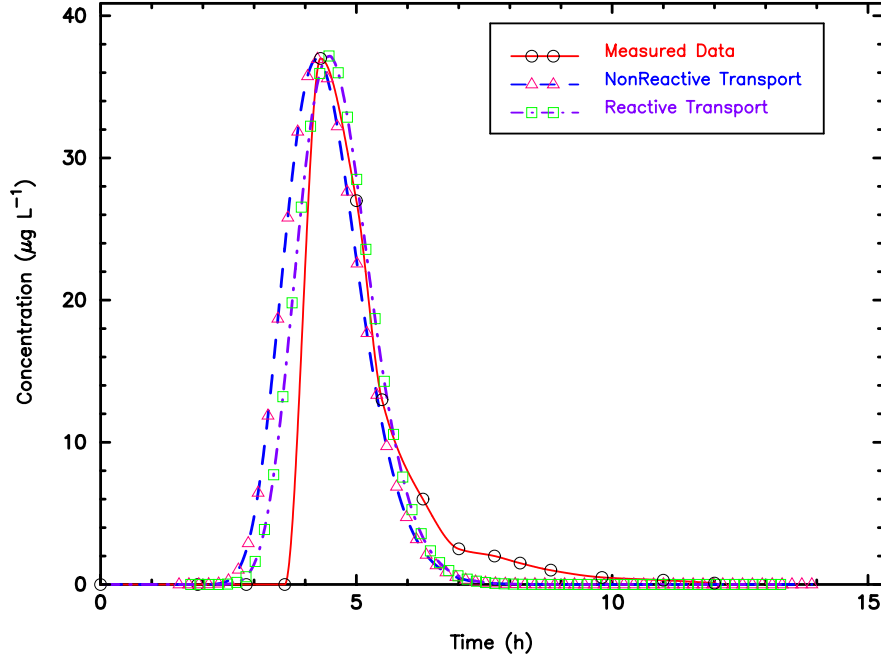


Figure 26. Comparison of measured data for the Variegated Glacier tracer test with EHTD-predicted results for nonreactive and reactive transport. For reactive transport, $R_d = 1.25$ and $\mu = 1.595 \text{ h}^{-1}$.

EHTD-predicted nonreactive results, EHTD was successful in that both nonreactive and reactive estimates for tracer mass were adequate and the suggested sampling times would approximate the measured BTC. Using the larger estimate for cross-sectional area obtained from v would also have been successful in that the suggested sampling times would have produced the measured BTC when the tracer test was implemented.

Again, a relatively insignificant amount of tracer was added directly to the stream water at the bottom of the karst window, causing $D_V = V$ for both the EHTD-predicted results (Table 29). Neither of the predictions for V by EHTD matched the measured V , but the approximations may be regarded as sufficiently close to the measured value for V to adequately represent the tracer test.

7.3.1.4. Variegated Glacier Tracer Test. Tracer testing is commonly used to define the hydraulic parameters associated with glacial outflows. The Variegated Glacier post-surge tracer test BTC was very reasonably approximated by EHTD for both nonreactive and reactive considerations (Figure 26). The EHTD-predicted hydraulic parameters $\bar{t} = 4.27$

hours, $t_p = 4.23$ hours, $v = 2342 \text{ m h}^{-1}$, $D = 3.58 \times 10^5 \text{ m}^2 \text{ h}^{-1}$, and $P_e = 65.5$ are close to the approximations obtained from the measured BTC. However, the EHTD prediction for the nonreactive case resulted in an earlier tracer breakthrough than that of the measured result (Table 28) and underestimated tracer mass by nearly three orders of magnitude (Table 29). Increasing tracer mass using EHTD required considerable tracer loss ($\mu = 1.595 \text{ h}^{-1}$) and some retardation ($R_d = 1.25$).

Accounting for retardation causes a slight shift in the EHTD-predicted BTC, allowing for a reasonable match with the measured BTC. Other than the inadequate estimate for tracer mass for the nonreactive case, the EHTD-predicted results for the Variegated Glacier tracer test were sufficient for defining the BTC. Prior knowledge of the nature of glacial outflows and the tracer used (Rhodamine WT for this tracer test) should allow for an approximation of the appropriate estimates to use for tracer decay and retardation.

For the Variegated Glacier tracer test, a relatively insignificant amount of tracer was added directly to the stream water as a small, short-duration pulse with the effect resulting in $D_V = V$ for both of the EHTD-predicted results (Table 29). The EHTD-predicted volumes bracket the measured value for V , suggesting that the EHTD-predicted volumes are reasonable, especially for the reactive case.

7.3.2. Porous Media Results

The second set of the four tracer tests listed in Table 26 represents a typical range of tests conducted in porous media aquifers. The tests included a natural-gradient tracer test, a forced-gradient tracer test, an injection/withdrawal tracer test, and a recirculation tracer test. EHTD prediction of tracer test results in porous media requires more measured and/or estimated parameters than is required for flowing streams. The parameters necessary for EHTD simulation of porous media systems are listed in Table 30. For porous media aquifers, EHTD requires measurements or estimates for Q , L , effective porosity n_e , thickness b , transverse spread T , t_2 , and \overline{C} . For all but natural-gradient tracer tests, EHTD estimates T (Field, 2002a). As with the flowing stream tracer tests, two listings for \overline{C} appear in Table 30. Tracer decay tends to cause predicted C_p to fall below the predicted C_p that occurs with no tracer decay and the measured C_p unless specific adjustments (e.g., increased \overline{C}) are incorporated. Decreases in C_p was a problem in each of the four porous media tracer tests listed in Table 30.

Hydraulic results of the EHTD-predicted BTCs for the four porous media tracer tests are compared with the actual BTC results in Table 31. Tracer injection specifics are listed

Table 30. Required porous media tracer test design specifics.

Parameter	Test Site Wilerwald	Kirchdorf Site ^a	Mobile Site ^a	Chalk River ^a
Q , $\text{m}^3 \text{h}^{-1}$	2.59×10^1	1.37×10^3	5.69×10^1	1.62×10^0
L , m	2.00×10^2	5.85×10^2	3.83×10^1	8.00×10^0
n	1.50×10^{-1}	1.40×10^{-1}	3.50×10^{-1}	3.80×10^{-1}
b , m	1.00×10^1	8.80×10^0	2.16×10^1	8.20×10^0
T , m	7.50×10^1
t_2 , h	1.00×10^0	...	7.66×10^1	7.73×10^1
t_V , m^3	9.00×10^{-2}	...	5.69×10^1	1.62×10^0
\overline{C}^b , $\mu\text{g L}^{-1}$	3.10×10^0	2.71×10^0	9.80×10^3	3.06×10^{-4}
\overline{C}^c , $\mu\text{g L}^{-1}$	1.84×10^0	2.66×10^0	1.09×10^4	3.64×10^{-4}

^a Transverse tracer spread not estimated for forced-gradient tracer tests.

^b Average tracer concentration for nonreactive tracer transport.

^c Average tracer concentration for reactive tracer transport.

Table 31. EHTD-Predicted BTCs versus measured BTCs for the porous media tracer tests.

Data Set ^{a,b}	\bar{t} , hours	t_p , hours	v , m h ⁻¹	D , m ² h ⁻¹	P_e , dimen.	t_1 , hours	t_f , hours
<i>Wilerwald Tracer Test</i>							
Measured	5.38×10^2	1.50×10^2	3.47×10^{-1}	5.76×10^0	1.21×10^1	3.00×10^1	3.00×10^1
EHTD-N	8.68×10^2	8.20×10^2	2.30×10^{-1}	1.46×10^0	3.16×10^1	1.22×10^2	6.10×10^1
EHTD-R	8.68×10^2	6.90×10^2	2.30×10^{-1}	1.46×10^0	3.16×10^1	1.23×10^2	4.41×10^1
<i>Kirchdorf-Unterropfingen Tracer Test</i>							
Measured	5.62×10^2	4.06×10^2	5.22×10^{-1}	3.82×10^1	8.00×10^0	6.00×10^1	2.00×10^1
EHTD-N	9.68×10^2	9.00×10^2	6.04×10^{-1}	1.23×10^1	2.86×10^1	1.89×10^2	4.24×10^1
EHTD-R	9.68×10^2	8.91×10^2	6.04×10^{-1}	1.23×10^1	2.86×10^1	1.89×10^2	4.24×10^1
<i>Mobile Site Tracer Test</i>							
Measured	3.60×10^2	2.10×10^2	1.24×10^{-1}	3.77×10^{-1}	1.80×10^1	6.30×10^1	5.00×10^0
EHTD-N	2.04×10^2	2.30×10^2	1.88×10^{-1}	2.97×10^{-1}	2.42×10^1	3.82×10^1	1.91×10^1
EHTD-R	2.04×10^2	2.08×10^2	1.88×10^{-1}	2.97×10^{-1}	2.42×10^1	4.18×10^1	2.09×10^1
<i>Chalk River Site Tracer Test</i>							
Measured	1.26×10^2	1.80×10^2	6.36×10^{-2}	1.04×10^{-2}	4.90×10^1	8.40×10^1	1.80×10^1
EHTD-N	1.29×10^2	7.74×10^2	6.21×10^{-2}	2.46×10^{-2}	2.02×10^1	2.42×10^1	1.21×10^1
EHTD-R	1.29×10^2	1.68×10^2	6.21×10^{-2}	2.46×10^{-2}	2.02×10^1	2.67×10^1	1.34×10^1

^a EHTD-N = nonreactive tracer test results. EHTD-R = reactive tracer test results.^b Reactive results are listed as though no tracer reactions have occurred.

Table 32. EHTD-predicted results versus measured results for the porous media tracer tests.

Data Set ^a	M , g	I_C , $\mu\text{g L}^{-1}$	C_p , $\mu\text{g L}^{-1}$	V_I , m^3	q , $\text{m}^3 \text{h}^{-1}$	V , m^3	D_V , m^3
<i>Test Site Wilerwald Tracer Test</i>							
Measured	1.00×10^3	1.11×10^4	3.20×10^0	9.00×10^{-2}	9.00×10^{-2}	9.43×10^4	...
EHTD-N	4.36×10^1	4.83×10^5	3.20×10^0	9.00×10^{-2}	9.00×10^{-2}	2.25×10^4	2.26×10^4
EHTD-R	1.00×10^3	1.12×10^7	3.20×10^0	9.00×10^{-2}	9.00×10^{-2}	2.25×10^4	2.26×10^4
<i>Kirchdorf-Unterropfingen Tracer Test</i>							
Measured	3.00×10^3	...	2.80×10^0	7.70×10^5	...
EHTD-N	2.34×10^3	...	2.80×10^0	1.32×10^6	1.32×10^6
EHTD-R	3.01×10^3	...	2.81×10^0	1.33×10^6	1.33×10^6
<i>Mobile Site Tracer Test</i>							
Measured	7.42×10^5	1.69×10^5	2.20×10^4	4.36×10^3	5.69×10^1	2.05×10^4	...
EHTD-N	1.89×10^5	4.34×10^4	2.20×10^4	4.36×10^3	5.69×10^1	1.16×10^4	2.32×10^4
EHTD-R	7.45×10^5	1.71×10^5	2.19×10^4	4.36×10^3	5.69×10^1	1.28×10^4	2.56×10^4
<i>Chalk River Site Tracer Test</i>							
Measured	5.21×10^{-4}	4.10×10^{-3}	8.32×10^{-4}	1.25×10^2	1.62×10^0	2.04×10^2	...
EHTD-N	1.54×10^{-4}	1.23×10^{-3}	8.33×10^{-4}	1.25×10^2	1.62×10^0	2.09×10^2	4.18×10^2
EHTD-R	5.21×10^{-4}	4.17×10^{-3}	8.34×10^{-4}	1.25×10^2	1.62×10^0	2.30×10^2	4.59×10^2

^a EHTD-N = nonreactive tracer test results. EHTD-R = reactive tracer test results.

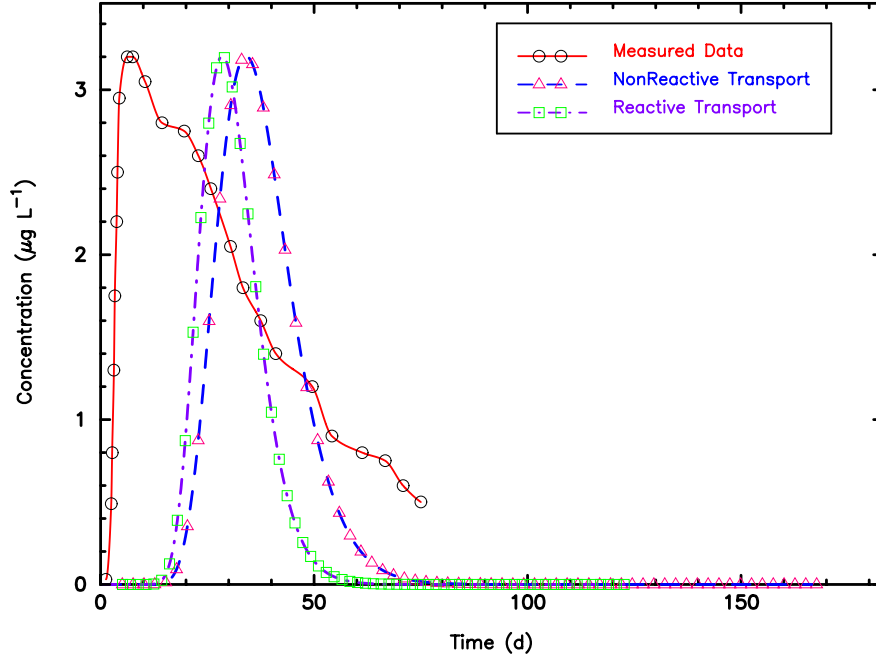


Figure 27. Comparison of measured data for the Test Site Wilerwald tracer test with EHTD predicted results for nonreactive and reactive transport. For reactive transport, $R_d = 1.80$ and $\mu = 0.0044 \text{ h}^{-1}$.

in Table 32.

7.3.2.1. Test Site Wilerwald Tracer Test. Natural-gradient tracer tests in porous media can be frustrating because of the time involved, the number and type of field measurements necessary, and the construction of injection and recovery sites. Unlike with karstic terranes, some basic transport parameters can be approximated prior to initiating the tracer test, which minimizes some of the design difficulties. However, errors in estimates for parameters that are difficult to estimate prior to conducting a tracer test (e.g., effective porosity) can result in substantial errors in the tracer test design.

The tracer test design parameters for Test Site Wilerwald were carefully measured and/or estimated by geophysics, which helped facilitate a good tracer test design (De Carvalho Dill and Müller, 1992, pp. 234–239). Using these same parameters in EHTD resulted in satisfactory fits to the measured BTC (Figure 27) with $\bar{t} = 868$ hours, $t_p = 794$ hours, $v = 0.23 \text{ m h}^{-1}$, and $D = 1.46 \text{ m}^2 \text{ h}^{-1}$, which do not approximate the measured results as well as desired (Table 31). Using the data provided and an estimate for discharge according

to Darcy’s law, estimated tracer travel times (Table 31) could not be improved, but an improvement in calculated tracer mass to release (Table 32) could be improved by providing an estimate for tracer decay. Evident from Figure 27 and Table 31 is that the estimated times of travel \bar{t} and t_p were underestimated by EHTD, which is a direct result of the application of Darcy’s law.

The actual tracer mass released was $24\times$ more than the EHTD-nonreactive recommended estimate. Setting μ to 0.0044 h^{-1} raised the tracer mass estimate to the actual amount released, but a consequent and significant decrease in estimated C_p was required (Table 30). The tracer used for the Test Site Wilerwald tracer test was fluorescein, which is generally regarded as being slightly retarded in granular aquifers and not very sensitive to degradation in the subsurface. For this test, fluorescein appears not to have been significantly retarded, but it may have been severely degraded according to EHTD. This contention is supported by the actual tracer test, which indicates that only about 77 g of fluorescein were recovered [85 g when evaluated using QTRACER2 and a straight-line projection for data extrapolation (Field, 2002b, pp. 57–58)].

Figure 27 shows that EHTD inadequately predicted the measured BTC for both the nonreactive and the reactive cases but that most of the BTC, including the long, relatively gently sloping BTC tail, would be identified during the sampling process even though EHTD failed to accurately predict the BTC when Darcy’s law is applied. For the Test Site Wilerwald tracer test, tracer was added as a small, short-duration pulse, the effect of which was a relatively insignificant amount so $D_V = V$ for both of the EHTD-predicted results (Table 32). The EHTD-predicted volumes only slightly exceeded the measured value for V , suggesting that the EHTD-predicted volumes are reasonable.

7.3.2.2. Kirchdorf-Unteropfingen Tracer Test. In porous media systems, forced-gradient tracer tests are preferred because the length of time for the test is greatly reduced and the transport parameters necessary for designing the tracer test are more easily estimated. However, errors in estimated parameters may still result in a poor tracer test design. The Kirchdorf-Unteropfingen tracer test was designed using parameters that were determined from a pumping test.

The EHTD-predicted BTCs poorly match the measured BTC, and initial tracer breakthrough was not adequately predicted (Figure 28). Peak concentration for the measured BTC was missed by both EHTD-predicted cases by more than 17 days (Table 31). The poor EHTD predictions for the Kirchdorf-Unteropfingen tracer test are directly related to

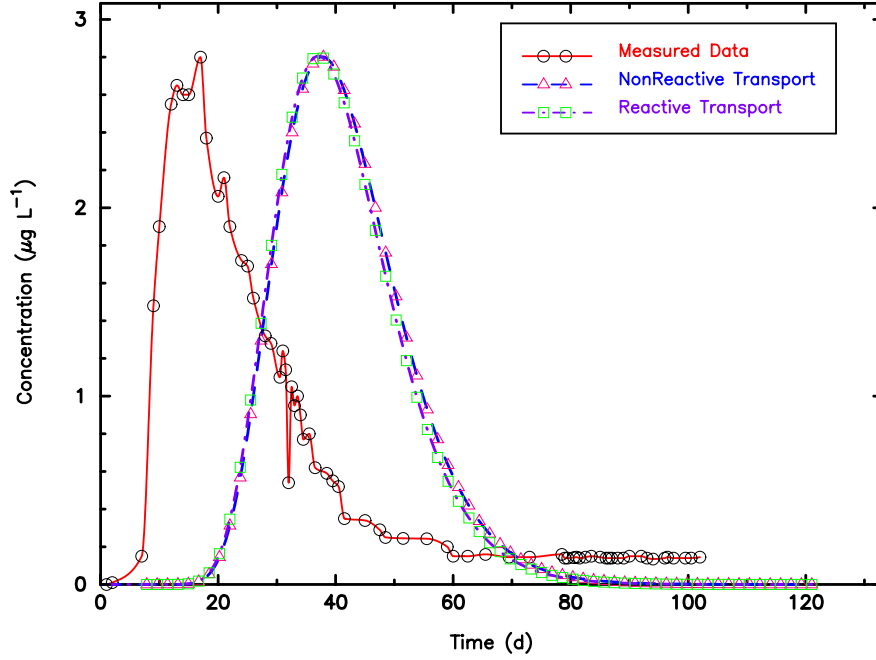


Figure 28. Comparison of measured data for the Kirchdorf-Unterropfingen site tracer test with EHTD-predicted results for nonreactive and reactive transport. For reactive transport, $R_d = 1.0$ and $\mu = 0.0003 \text{ h}^{-1}$.

the incorrectly estimated n_e obtained from the pumping test.

The tracer test design used an $n_e = 0.14$, which is the value of the specific yield obtained from the pumping test. This n_e was later found to be significantly in error. Tracer test analysis resulted in an $n_e = 0.08$ (Käb, 1998, pp. 515–516), which when applied to EHTD produces much better BTC fits to the measured BTC.

Estimated tracer mass for the nonreactive case closely matched the actual tracer mass released. Setting $\mu = 0.0003 \text{ h}^{-1}$ produced a slightly greater estimate for tracer mass than was released. However, this slight increase in tracer mass also resulted in a slight shift in the decreasing limb of the BTC.

Although the EHTD-predicted BTCs failed to adequately match the measured BTC, EHTD did reasonably predict the appropriate tracer mass to release. EHTD-recommended sample collection times for the Kirchdorf-Unterropfingen tracer test were generally adequate for defining the BTC, although initial tracer breakthrough was not predicted by EHTD.

For the Kirchdorf-Unterropfingen tracer test, tracer occurred as an impulse release, the effect of which was an insignificant amount, so $D_V = V$ for both of the EHTD-predicted

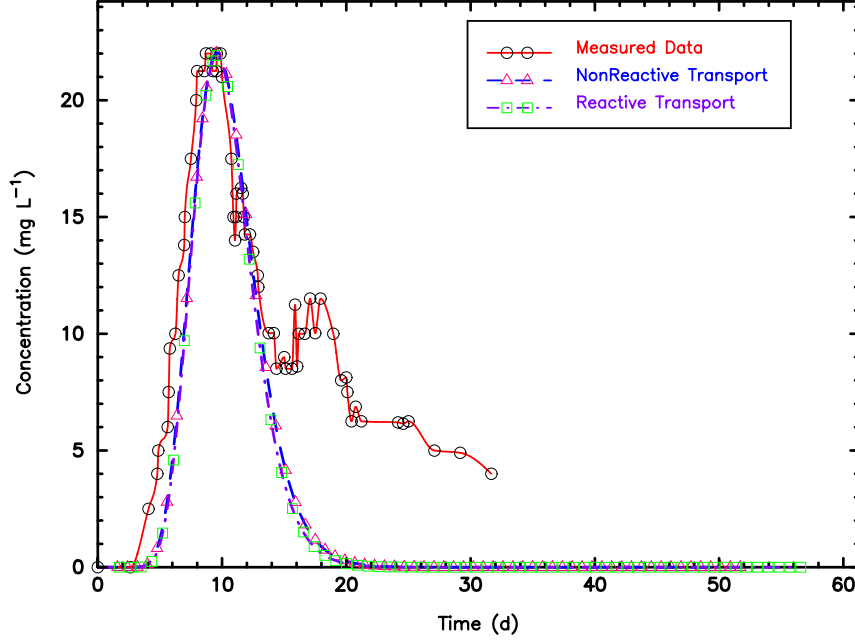


Figure 29. Comparison of measured data for the Mobile site tracer test with EHTD predicted-results for nonreactive and reactive transport. For reactive transport, $R_d = 1.1$ and $\mu = 0.0075 \text{ h}^{-1}$.

results (Table 32). Both of the EHTD-predicted volumes exceeded the measured value for V , reflecting the effect of the incorrect effective porosity.

7.3.2.3. Mobile Site Tracer Test. Injection/withdrawal tracer tests provide an opportunity to establish equilibrium conditions during ground-water extraction prior to initiating a tracer test. The Mobile Site tracer test was designed using transport parameters that were carefully determined from pumping tests and single-well tracer tests, which led to better estimates for the parameters necessary for designing the injection/withdrawal tracer test.

The EHTD-predicted BTCs closely matched the measured BTC (Figure 29). Only the long, somewhat multimodal erratic tail of the measured BTC was not adequately predicted by EHTD. The long tail is suspected to have occurred as a result of longer flow lines causing longer transport times, which occurs during well injection (Molz et al., 1986a, pp. 22, 58). Because EHTD does not predict long BTC tails the estimates for \bar{t} and v were incorrectly estimated by approximately 3 days, but t_p , D , and P_e were very well approximated (Table 31). Setting $\mu = 0.0075 \text{ h}^{-1}$ and $R_d = 1.1$ increased the estimate

for tracer mass enough to match the actual mass released and for predicted injection concentration to match the actual injection concentration. However, the increase in tracer mass also caused a slight negative shift of the descending limb of the predicted BTC because of the required steepening of the BTC to maintain the desired \bar{C} . Setting $\mu = 0.0075 \text{ h}^{-1}$ and $R_d = 1.1$ allowed for a good estimate for tracer mass and a slight positive shift in the BTC, but with a slight decrease in predicted t_p , a 2-hour increase for t_1 and t_f (Table 31), and a 1-hour increase for C_p (Table 32).

EHTD-suggested sampling times may be regarded as adequate for defining the measured BTC. The multimodal measured BTC for the Mobile Site clearly illustrates the need for frequent sampling if the BTC is to be properly defined (Figure 29). Although not as frequent as the average sample collection frequency t_f of 5 hours for the measured BTC, a $t_f = 19$ hours is probably reasonable for defining the BTC while not being excessive. Tracer sampling ceased prior to complete tracer recovery, so it is difficult to determine whether EHTD adequately predicted final tracer recovery.

Predicted dilution volumes for the Mobile Site tracer test exceeded the predicted system volumes, but the dilution volumes reasonably matched the measured system volumes (Table 32). The good estimation for D_V would have enhanced the predictions for M , but the poor match of the predicted V to the measured V was unexpected, although it appears not to have adversely influenced the tracer mass prediction for the reactive case.

7.3.2.4. Chalk River Site Tracer Test. Recirculation tracer tests are rarely employed to evaluate transport parameters in porous media systems. A recirculation tracer test conducted at the Chalk River Site was very well predicted by EHTD for both the non-reactive and reactive cases (Figure 30). The EHTD-predicted results for the nonreactive case produced a good fit to the measured BTC and a nearly exact match of the predicted \bar{t} to the measured \bar{t} but a very poor match for predicted t_p to the measured t_p (Table 31). The incorrectly estimated t_p was caused by recirculating the recovered tracer back into the injection well while tracer recovery from the start of the tracer test was still occurring. Average velocity, D , and P_e were also very well matched.

EHTD-estimated tracer mass for the nonreactive case was four times less than the actual tracer mass released. Setting $\mu = 0.011 \text{ h}^{-1}$ resulted in a close match to the actual tracer mass released and injection concentration, but it also produced a slight negative shift in the BTC. Setting $R_d = 1.1$ caused a positive shift of the BTC that matched the measured BTC and the mass released. Allowing for tracer decay caused the EHTD-predicted BTC to

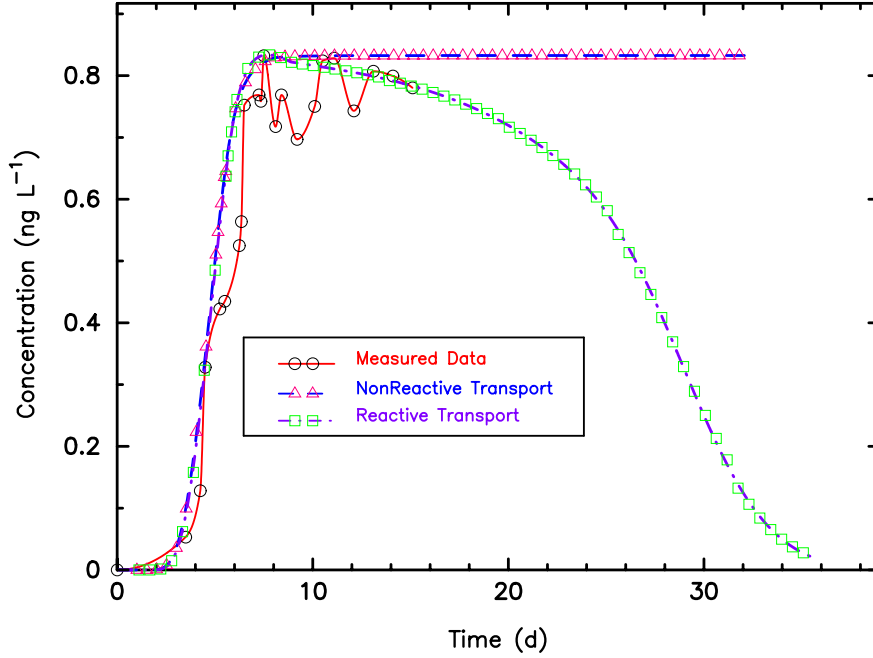


Figure 30. Comparison of measured data for the Chalk River site tracer test with EHTD-predicted results for nonreactive and reactive transport. For reactive transport, $R_d = 1.1$ and $\mu = 0.011 \text{ h}^{-1}$.

develop a slight peak at ≈ 8 days and a consequent decreasing limb. The EHTD-predicted BTC for the reactive case produced a visually better fit than have previous modeling efforts (Huyakorn et al., 1986), because \bar{C} was adjusted as necessary to obtain a C_p that matched the measured C_p (Table 30).

As with the Mobile Site tracer test, the EHTD-suggested sampling times may be regarded as ideal for defining the measured BTC. The multimodal measured BTC for the Chalk River Site also illustrates the need for frequent sampling if the BTC is to be properly defined (Figure 30). A $t_f = 12$ hours is sufficient for defining the BTC. However, tracer sampling ceased prior to complete tracer recovery, so it is not possible to determine whether EHTD-recommended sampling ended too soon.

Unlike the Mobile Site tracer test, the predicted system volumes for the Chalk River tracer test match the measured V quite well, especially for the nonreactive case. (Table 32). Predicted D_V was twice the predicted V , reflecting the recirculation aspect of this tracer test. The effect of $D_V = 2V$ was to increase the suggested tracer mass necessary for achieving a positive tracer test.

Part IV

ADDITIONAL APPLICATION OF EHTD



Release of slightly diluted uranine (Acid Yellow 73) into flow of water for tracer test. Note the contrast between the uranine color (fluorescent green) and the algae build-up on the sides of the stream flow. This tracer test was conducted in order to verify the integrity of the local production well from infiltration by toxic substances that may be accidentally or deliberately released in the future.

8. APPLICATION OF EHTD TO SUPPORT RISK ASSESSMENTS

A critical aspect of any contamination investigation (potential or existing) of a given hydrological system involves the development of a risk assessment to assess the threat to human health and the environment posed by the contamination. Risk assessments consist of three components: hazard identification, exposure assessment, and dose response. In this section, exposure assessments as related to solute transport will be the focus. Hazard identification (toxicity estimation) and dose-response assessment (estimation of the extent of increasing hazard as a function of increasing exposure) are not addressed here. In addition, that aspect of exposure assessment that deals with uptake (e.g., ingestion of contaminated water) is not addressed here. Rather, solute transport from a source area to a point of exposure in a hydrological system is the focus of this section. For more complete details on exposure and risk assessments, the interested reader is referred to Reichard et al. (1990) for a general overview of risk assessment methodology in ground water, USEPA (1992) for general exposure methodology, USEPA (1998a) for detailed ecological risk assessment methods and USEPA (1989) for detailed human health risk assessment methods. USEPA (1986a,b, 1991, 1996, 1998b) provide detailed risk assessment guidance for the development of various toxicological methods.

8.1. EXPOSURE ASSESSMENT OVERVIEW

A typical exposure assessment for real and potential contamination usually includes solute-transport modeling as a means of reducing uncertainties and/or forecasting the effects of any suggested changes. The exposure pathway (source to exposure point) requires field investigations which are often enhanced through modeling of the environmental systems which helps to lessen the impact of uncertainties. Uncertainties in exposure assessments are always an issue that must be addressed. Typical uncertainties associated with exposure assessments in hydrological systems are listed in Figure 31.

The value and importance of using a well calibrated model for risk assessment purposes is widely recognized. For example, McAvoy et al. (2003) used the well-known water quality model, QUAL2E (after calibration) to conduct a basic risk assessment regarding wastewater loading to Balatuin River in the Philippines. Rhodamine WT (Acid Red 388) dye tracing results were used to develop the necessary parameters for model calibration. Interestingly, the initial dye release included too little dye (9.52 g) and the two subsequent releases required

Source-Related Uncertainties

- Will release(s) of contaminants occur?
[Probability of release(s).]
- When will the release(s) occur and for how long?
[Timing and duration of release(s).]
- What contaminants will or are being released?
[Chemical, biological, or radiological contaminant releases.]
- How much will be or is being released?
[Mass loading.]

Pathway-Related Uncertainties

- Will contaminants reach exposure point?
[Flow trajectory and proximity of source to point of contact.]
- When will contaminants reach point of exposure?
[Time of travel and duration of exposure.]
- What contaminants will reach the point of exposure?
[Environmental fate of contaminants.]
- How much contamination will reach the point of exposure?
[Contaminant concentration at the point of exposure.]

Use-Related Uncertainties

- Water used for drinking and/or bathing and by whom?
[Exposure route, number, and sensitivity of exposed population.]
- How long will user be affected by the contamination?
[Duration and continuity of exposure.]
- What monitoring program is in place?
[Potential to avert exposure.]
- What dilution and/or treatment prior to exposure?
[Reduced exposure levels due to reduced contaminant concentrations.]

Figure 31. Uncertainties associated with exposure assessments in hydrological systems [adapted from Reichard et al. (1990, p. 6)].

slightly greater amounts of dye (14.28 g each) for a total release of (38.08 g). Analysis using EHTD suggested that even greater quantities of dye (100.11 g) would have been appropriate.

8.2. FORECASTING POLLUTION FOR RISK ASSESSMENTS

The appropriateness of EHTD for determining acceptable tracer mass and sampling times for proposed tracer tests has already been documented. However, after tracer tests have been conducted EHTD may be used for screening-level pollution forecasting. The EHTD-results may then be applied in a risk assessment at a rough screening level. Such an endeavor, the value of which not being immediately apparent, is useful because of the difficulty and expense of conducting multiple tracer tests several times during any given year and over several years. A single tracer test provides only a temporal “snapshot” of the hydrological system the results of which may not be relevant other periods.

8.2.1. Dimensionless Dye-Recovery Curve

The tracer testing conducted by McAvoy et al. (2003) was conducted during the dry season only. In their work, the authors assumed that greater dilution would occur during the wet months which may be true but is undocumented. For this reason, the U.S. Geological Survey (USGS) conducted several tracer tests in the same system over at least a year’s time to address temporal differences in flow (Mull et al., 1988b). A plot of the seven tracer tests conducted by the USGS indicates considerable real-time differences and real-concentration differences in the BTC’s (Mull et al., 1988a, p. 55). Figure 32 on the next page depicts the seven BTC’s. The differences in the BTC’s were muted by converting the BTC’s to dimensionless form, plotting the dimensionless BTC’s at the same scales and then developing a single standardized dimensionless dye-recovery curve or “type curve” (Mull et al., 1988a, pp. 68–75). Development of the standardized curve is a very slow tedious process where a BTC is drawn by eye and appropriate statistics calculated. This process is repeated several times until the calculated statistics meet some arbitrary level of acceptance.

After development of the standardized curve the effects of a given release into the hydrologic system could be forecast with some degree of confidence provided discharge was available (Mull et al., 1988a, pp. 75–79). Although useful and relevant, the method devised is a trial-and-error procedure requiring considerable subjective analysis. A simpler less expensive method is desirable.

8.2.2. EHTD for Forecasting pollution Effects

To be able to forecast the effects of any contaminant releases in any given hydrological system, a chosen model must either be properly calibrated for the given time period or be

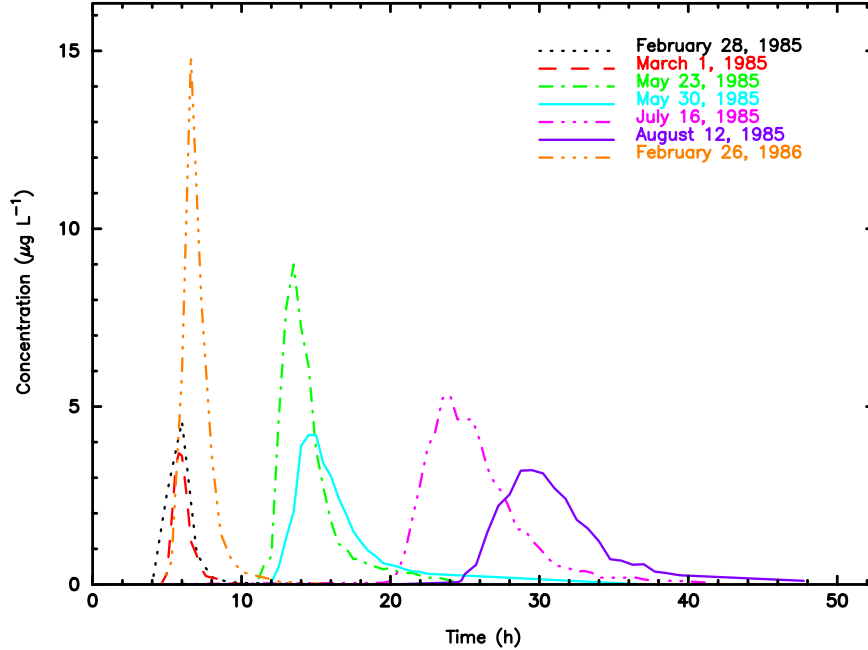


Figure 32. Seven BTC's developed by the U.S. Geological Survey between Dyers Spring and a nearby karst window over one year (1985) (Mull et al., 1988a, p. 73). Note that the May 30, 1985 curve is the Dyers Spring BTC that is examined in detail in Section 7. on page 128 and graphically as Figure 25 on page 139.

capable of approximating the environmental conditions for the given time period. This may be accomplished using EHTD provided it is recognized that EHTD may only be considered a screening-level model when used in this manner.

8.2.2.1. Using EHTD Directly to Forecast Pollution. Given some degree of confidence regarding the ability of EHTD to suggest the appropriate mass of tracer to release and sampling times, EHTD can be used as a quick screening model for addressing pollutant releases. Consider the Dyers Spring example developed in Section 7.3.1.3. on page 138 where EHTD was used to produce an acceptable estimate for time of travel and tracer mass released.

The USGS standardized curve for this site was applied to a hypothetical release of 0.19 m^3 (50 gallons) of a 5% solution of copper sulfate (1.13 kg copper) into the karst window from which the original tracer tests were conducted. Assuming a spring discharge $= 91.74 \text{ m}^3 \text{ h}^{-1}$ ($3.24 \times 10^3 \text{ ft}^3 \text{ h}^{-1}$) the standardized curve method suggested (Mull et al., 1988a, pp. 77–78):

1. $C_p = 2.61 \text{ mg L}^{-1}$
2. $t_1 = 14.0 \text{ h}$
3. $t_p = 18.0 \text{ h}$
4. $t_f \sim 40.0 \text{ h}$

Applying EHTD with assuming no pollutant reactivity to this hypothetical example and using a reasonable estimate for cross-section area to be 1.65 m^2 (17.73 ft^2) resulted in:

1. $C_p = 2.04 \text{ mg L}^{-1}$
2. $t_1 = 7.39 \text{ h}$ (measurable)
3. $t_p = 16.09 \text{ h}$
4. $t_f \sim 40.0 \text{ h}$

Including a pollutant decay factor would have caused a reduction in the EHTD-predicted peak concentration while including a pollutant retardation factor would have caused both a reduction in the peak concentration and later travel times. A comparison of the standardized-predicted BTC and EHTD-predicted BTC is shown in Figure 33 on the next page. Although there is no definitive way in which one BTC shown in Figure 33 can be selected over the other it will be noted that the standardized curve method tends to overestimate peak concentration (Mull et al., 1988a, p. 76) while it is likely that EHTD will underestimate peak concentration if a good measure or estimate for discharge, cross-sectional area (or transverse spread for porous media), and transport distance are not sufficiently accurate.

8.2.2.2. Using the LHS-Routine in EHTD to Forecast Pollution. As explained in Section 4.3. on page 70 a LHS-input file of mean values (see page 72) can be developed from any input file of measured values. Using the Dyers Spring data a LHS-developed file was created from 10,000 randomly-generated parameter values (Figure 34 on page 158). Note that Figure 34 on page 158 also includes the univariate statistics that describe the input parameters (see Table 20 on page 72 for identification of the variables). Using the EHTD-generated file (Figure 34) will not produce correct results because it in no way was intended to match the conditions identified (e.g., $Q \neq 91.74 \text{ m}^3 \text{ h}^{-1}$). For example, it

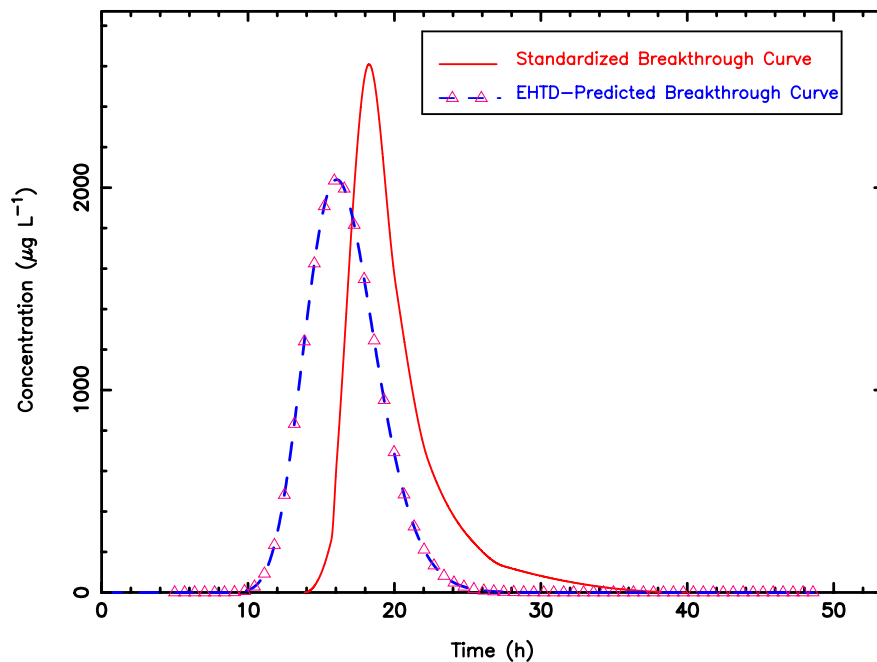


Figure 33. Standardized curve- and EHTD-predicted BTC for a hypothetical copper sulfate release to the karst window shown by dye tracing to be connected to Dyers Spring.

includes a slight overestimate for transport distance, a large overestimate for discharge and retardation, and other incorrect values. However, adjustments to this file are easily made. The file can then be run as often as necessary to gain a sense of those factors that are most influential to the transport of a solute.

One significant point to make about the LHS routine used in EHTD is that it will always create an input file with optimization “turned on” (Figure 34). Because optimization is requested, EHTD will ignore any user-entered tracer or solute mass and will optimize for the best mass for the listed conditions. If the user prefers to use a desired mass, then optimization must be reset to zero.

```

NAME OF DATA FILE
LATIN HYPERCUBE FILE NUMBER    1
FLOW      RELEAS      RTIM (h)      INFLOW (m^3/h)      UNITS
1          1          0.0          0.0          1
*****
STATION NAME
DYERS SPRING
DISCHARGE (m^3/h)      DISTANCE (m)      AREA (m^2)      SINUOSITY FACTOR
2.499E+02              9.195E+02      1.991E+00      1.0
INIT. CONC. (ug/L)      GAMMA1          GAMMA2
5.000E-01              5.000E-01      5.000E-01
RETARDATION            DECAP (1/h)      OPTIM          AVE. CONC. (ug/L)
1.483E+00              9.000E-02      1              4.120E+00
1                      1
1.0                    0.0
10.0                   5.0
*****
END OF RUNS
STOP PROCESSING
LHS SUGGESTED USER INPUT SOLUTE MASS = 7.662E+00 g

```

Univariate Statistics from UVSTA					
Variable	Mean	Variance	Std. Dev.	Skewness	Kurtosis
1	7.66154	79.211682	8.90009	1.4285	1.0497
2	249.88990	0.8427E+05	290.28670	1.4285	1.0497
3	1.99133	0.615789	0.78472	0.4743	-0.9535
4	919.47539	9349.850234	96.69462	0.1262	-1.1826
5	0.50000	0.083358	0.28872	-0.7563E-16	-1.2000
6	0.50000	0.083358	0.28872	-0.5487E-16	-1.2000
7	0.50000	0.083358	0.28872	0.3864E-16	-1.2000
8	1.48261	0.099951	0.31615	0.2561	-1.1282
9	0.09000	0.002701	0.05197	0.6316E-16	-1.2000
Variable	Minimum	Maximum	Range	Coef. Var.	Count
1	0.3563	35.6343	35.2779	1.1617	10000.0000
2	11.6225	1162.2528	1150.6303	1.1617	10000.0000
3	0.9202	3.6807	2.7605	0.3941	10000.0000
4	762.0000	1097.2800	335.2800	0.1052	10000.0000
5	0.0000	1.0000	1.0000	0.5774	10000.0000
6	0.0000	1.0000	1.0000	0.5774	10000.0000
7	0.0000	1.0000	1.0000	0.5774	10000.0000
8	1.0000	2.1000	1.1000	0.2132	10000.0000
9	0.0000	0.1800	0.1800	0.5774	10000.0000
Variable	Lower CLM	Upper CLM	Lower CLV	Upper CLV	
1	7.48708	7.83600	77.061028	81.454079	
2	244.19970	255.58010	0.8198E+05	86651.8540	
3	1.97595	2.00671	0.599069	0.633221	
4	917.57999	921.37080	9095.994980	9614.534266	
5	0.49434	0.50566	0.081095	0.085718	
6	0.49434	0.50566	0.081095	0.085718	
7	0.49434	0.50566	0.081095	0.085718	
8	1.47641	1.48881	0.097237	0.102780	
9	0.08898	0.09102	0.002627	0.002777	

Figure 34. LHS-generated input file of means using the Dyers Spring parameters. Note CLM and CLV represent the confidence levels for the mean and the variance, respectively. All other table headings should be readily apparent.

9. SUMMARY AND CONCLUSIONS

Hydrologic tracer testing is an essential method of study for evaluating solute transport processes. However, the initial design of most tracer tests can be problematic due to a lack of prior knowledge concerning the hydrologic transport properties for which the tracer test is intended. A simple, reliable method for designing tracer tests has been developed by solving the one-dimensional advection-dispersion equation (ADE) for a preset average tracer concentration. This tracer design method provides a sound theoretical basis for estimating tracer mass and sample collection frequency by combining basic field measurements for hydraulic and geometric parameters in functional relationships that describe solute transport processes to estimate flow velocity and times of travel.

These relationships are then applied to a hypothetical continuous stirred tank reactor (CSTR) as an analog for the hydrologic flow system to develop estimates for tracer concentration and axial dispersion based on the preset average tracer concentration. Solution of the one-dimensional ADE using the preset average tracer concentration then allows for an estimate of necessary tracer mass. Application of the predicted tracer mass with the hydraulic and geometric parameters in the ADE further allows for an approximation of initial sample-collection time and subsequent sample collection frequency.

Tracer retardation and decay cause an increase in tracer mass estimates because the set average tracer concentration is maintained by the method. Retardation has the added effect of delaying tracer breakthrough and causing more spread in the tracer-breakthrough curve (BTC), which can have significant consequences for determining when to initiate sample collection and at what frequency all subsequent samples should be collected. However, experience with common tracers in various environments serves to trivialize this problem. Prior evaluations of distribution coefficients and simulations using selected values for retardation and decay can further limit the errors that may occur from tracer reactions with solids.

The method does not attempt to physically predict the conditions that may cause multimodal or long-tailed BTCs because it is not possible or necessary to add such complexity. It also does not address the possible occurrence of density-induced sinking. Not only would estimates for unknown parameters be required (e.g., mass transfer coefficient), but the effect of adding such complexity would not greatly improve the estimates for required tracer mass or recommended sampling frequency.

Thirty-three tracer mass estimation equations and the computer program efficient hydrologic tracer-test design (EHTD) methodology were reviewed and tested using published test criteria. Testing 32 of the 33 equations and EHTD produced extreme ranges in the results. EHTD is the only method that was developed using established solute transport theory. The other 33 equations were all developed empirically. Although the review and testing described does not provide a means for determining the best tracer mass estimation method and sampling frequency method to employ, recent tracer testing successes using EHTD suggests that EHTD may be more reliable than the other methods (Field, 2000).

Sample collection schemes were also reviewed and shown to be difficult to implement and unreliable because of their haphazard nature. Darcy's law for porous media cases was not applied because of insufficient test data, but Darcy's law is believed to be a reasonable model for designing a sampling schedule, provided that difficult-to-obtain parameters (e.g., effective porosity) can be adequately estimated. For karstic media, application of an assumed average velocity equal to 0.02 m s^{-1} for designing a sampling schedule can be effective, provided tracer release and transport occur via solution conduits.

Given the complexities and difficulties associated with the published 33 tracer mass estimation equations and conventional sampling schemes, their continued use must remain suspect at best. As shown by EHTD, these previously developed equations/methods fail to yield consistent results. Application of the more scientifically sound method developed in EHTD is more likely to ensure successful tracer test results (Field, 2002a) and is suggested as a more reliable alternative.

A total of eight tracer tests representing a wide range of conditions and a minimum of pre-tracer test design parameters were used to evaluate EHTD. In all but the Test Site Wilerwald and Kirchdorf-Unteropfingen tracer tests, the measured BTC curves were approximated by EHTD for both nonreactive and reactive instances. Recommended sampling times were found to be adequate for defining the measured BTCs for all eight tracer tests. Only the initial tracer breakthrough times for the Test Site Wilerwald and Kirchdorf-Unteropfingen were inadequately predicted, which was directly related to the unreliability of Darcy's law in the first case and the use of an incorrectly determined effective porosity in the latter.

Most of the EHTD-predicted tracer mass estimates for nonreactive conditions were mostly fairly to the actual tracer masses released. For the flowing stream tracer tests, tracer mass estimates were inadequate only for the Uvas Creek and Variegated Glacier tracer tests. The tracer mass estimates for the Missouri River tracer test were slightly greater than the actual tracer mass released. For the porous media tracer tests, only the tracer mass

estimate for the Test Site Wilerwald tracer test was seriously problematic, although tracer mass estimates for all the porous media tracer tests were underestimated. Prior knowledge of the behavior of the type of system being traced and the type of tracer to be used can provide some indication of necessary estimates for retardation and decay.

EHTD simulations for the eight tracer tests evaluated resulted in very reasonable approximations for seven of the tracer tests. In some instances, (e.g., Test Site Wilerwald and Kirchrtdorf Unteropfingen) expected time to peak arrival (t_p) was inaccurately reproduced. In other instances (e.g., Uvas Creek, Missouri River, Test Site Wilerwald, and Kirchrtdorf Unteropfingen) axial dispersion (D_z) was inaccurately reproduced. However, in all these instances the results of EHTD for both the reactive and the nonreactive simulations resulted in adequate approximations for the hydraulic parameters of interest.

Future work should focus on refining EHTD to better approximate tracer mass estimates and transport parameters. Improvements may include consideration of the longer transport times associated with the longer transport crescents created by injection and the effects of stagnant regions. Although these improvements are not necessary for EHTD to develop a sampling schedule that will define a BTC, they will result in improved tracer mass estimates and some transport parameter estimates. Application of EHTD in its current form prior to initiating a tracer test leads to a more efficient design, fewer trial-and-error efforts, less expense related to excess tracer use and excess sample collection and analysis, and greater likelihood of tracer test success.

NOTATION

a	long dimension of rod-shaped particle (L)
α	slope parameter for median infection estimate
α^*	slope parameter for median morbidity estimate
A	cross-sectional area of flow system (L ²)
\mathbf{A}	matrix of time values used in the Chatwin analysis (T)
a_i	interval of data points that bracket the function $f(x^*)$; ($i = 1, 2$)
A_e	adsorption efficiency (dimen.)
b	short dimension of rod-shaped particle (L)
b_f	one half fracture width (L)
b_k	maximum allowable Chatwin parameter corresponding to t_k (T ^{1/2})
\mathbf{b}	vector of concentration parameters for the Chatwin analysis (T ^{1/2})
C	tracer concentration (M L ⁻³)
\overline{C}	average tracer concentration (M L ⁻³)
C^E	equilibrium tracer concentration (M L ⁻³)
\overline{C}^E	mean volume-averaged equilibrium tracer concentration (M L ⁻³)
C_r	dimensionless resident tracer concentration = $\frac{C}{c_0}$
C^B	dimensionless concentration for BVP
C^I	dimensionless concentration for IVP
C^P	dimensionless concentration for PVP
c_0	characteristic tracer concentration (M L ⁻³)
C_0	volume-averaged input concentration (M L ⁻³)
C_p	peak tracer concentration (M L ⁻³)
d_i	data value derivatives
D_z	axial dispersion (L ² T ⁻¹)
$f(x^*)$	function representing the real root of the ADE
g_i	input concentrations for pulse injection; ($i = 1, 2$; $g_0 = g_2 = 0$)
$g(t)$	function of values such that $g(t_i) = C_i$
γ	zero-order production coefficient (M L ⁻³ T ⁻¹)
γ^E	dimensionless production = $\frac{L(n_e\gamma_l + \rho_b K_d \gamma_s)}{n_e v c_0}$; $\frac{L(b_f \gamma_l + 2K_a \gamma_s)}{b_f v c_0}$; $\frac{L(r\gamma_l + 2K_a \gamma_s)}{r v c_0}$
γ_i	dimensionless exponential production (growth) constants for the PVP [$i = 1, 2$]
$\overline{\gamma}_i$	upper bounds on \mathbf{y}
$\underline{\gamma}_i$	lower bounds on \mathbf{y}

γ_l	zero-order production coefficient for the liquid phase ($\text{M L}^{-3} \text{T}^{-1}$)
γ_s	zero-order production coefficient for the adsorbed (solid) phase ($\text{M M}^{-1} \text{T}^{-1}$)
Γ_i^E	auxiliary functions for equilibrium transport [see Section 3.2.1.4.]
\hbar	Hermite cubic basis function
$\hat{\hbar}$	Hermite cubic basis function
H	solute-migration zone thickness (L)
H_I	hazard index for all pathways (dimen.)
H_{Q_1}	hazard quotient for ingestion (dimen.)
H_{Q_2}	hazard quotient for inhalation (dimen.)
H_{Q_3}	hazard quotient for dermal contact (dimen.)
I	integrand of a function
I'	approximate integrand of a function
I_g	amount of water ingested per day ($\text{L}^3 \text{T}^{-1}$)
I_h	inhalation rate ($\text{L}^3 \text{T}^{-1}$)
k	CSTR reaction rate constant (T^{-1})
k_L	number of uncertain variables to be developed by Latin Hypercube Sampling routine
K_a	fracture and/or solution conduit distribution coefficient (L)
K_d	solute distribution coefficient ($\text{L}^3 \text{M}^{-1}$)
K_f	volumetric conversion for water ($\text{L}^3 \text{L}^{-3}$)
L	characteristic distance from point of injection to point of recovery (L)
λ^P	dimensionless constant for exponential production (growth) profile
M	tracer mass (M)
M_B	dimensionless mass of applied tracer for a Dirac input = $\frac{M/A}{c_0 L}$
M_p	particle mass (M)
M_p^T	mass of total number of particles (M)
n	number of evaluation points (dimen.)
n_b	number of additional sample to be collected prior to expected tracer breakthrough
n_e	effective porosity (dimen.)
n_κ	number of evaluation points for Chatwin analysis (dimen.)
n_m	multiplier for estimating tracer test duration (dimen.)
n_s	number of samples to be collected
N_{50}	median infectious dose ($\# \text{T}^{-1}$)
N_{50}^*	median morbidity dose ($\# \text{T}^{-1}$)
N_p	concentration of particles ($\# \text{L}^{-3}$)

p	components M , R_d , and μ of vector \mathbf{y} to be optimized
P_e	Péclet number $= \frac{vL}{D_z}$ (dimen.)
P_c	skin permeability constant ($L \ T^{-1}$)
P_I	probability of infection (dimen.)
$P_{D:I}$	probability of morbidity (dimen.)
$P_{M:D}$	probability of mortality (dimen.)
θ	porosity (dimen.)
ρ_b	bulk density ($M \ L^{-3}$)
ρ_p	particle density ($M \ L^{-3}$)
q	inflow into injection point at time of injection ($L^3 \ T^{-1}$)
Q	flow system discharge ($L^3 \ T^{-1}$)
r	solute conduit radius (L)
$\hat{r}_i(y)$	twice continuously differentiable functions of y
R_d	solute retardation (dimen.)
RfC	reference concentration ($M \ M^{-1}$)
RfD	reference dose ($M \ M^{-1} \ T^{-1}$)
S_a	skin surface area (L^2)
S_d	shower duration (T)
S_f	sinuosity factor (dimen.)
σ_t^2	travel time variance (T^2)
t	time (T)
\bar{t}	average time of travel (T)
t_b	base time value for Δt time spacing (T)
t_d	tracer-test duration corresponding to last detectable tracer breakthrough (T)
t_i	individual tracer sampling times (T)
t_κ	maximum allowable time for Chatwin analysis $t_\kappa \leq \frac{z}{v}$ (T)
t_m	base time value for $n_m \Delta t$ time spacing (T)
t_0	time for pulse release (T)
t_p	expected time to peak arrival (T)
t_R	tracer release control (dimen.)
t_s	sample-collection times (T)
t_{sf}	sampling frequency (T)
t_{sm}	time corresponding to minimum concentration for sample collection (T)
Δt	time spacing for CSTR-generated BTC (T)

T	dimensionless time = $\frac{vt}{L}$
\bar{T}	dimensionless mean residence time = $\frac{v\bar{t}}{L}$
\hat{T}_i	dimensionless pulse time = $\frac{vt_0}{L}$; ($i = 1, 2$; $\hat{T}_1 = 0$)
μ	solute decay (T^{-1})
μ^E	dimensionless equilibrium decay = $\frac{L(n_e\mu_l + \rho_b K_d \mu_s)}{n_e v}$, $\frac{L(b\mu_l + 2K_a \mu_s)}{bv}$, $\frac{L(r\mu_l + 2K_a \mu_s)}{rv}$
μ_l	liquid phase solute decay (T^{-1})
μ_s	sorbed phase solute decay (T^{-1})
v	mean tracer velocity ($L T^{-1}$)
\bar{v}	mean tracer velocity for the CSTR-generated BTC ($L T^{-1}$)
v_i	measured tracer velocities for each sampling time ($L T^{-1}$)
v_p	peak tracer velocity ($L T^{-1}$)
V	flow system volume (L^3)
V_a	shower stall volume (L^3)
ω	concentration of particulate matter for a concentrated volume (%)
W	width of solute-migration zone (L)
W_u	water usage (L^3)
\mathbf{x}	vector of straight-line parameters used in the Chatwin analysis ($T^{1/2}$)
\mathbf{y}	vector of p components (M , R_d , and μ) to be optimized
z	distance (L)
Z	dimensionless distance = $\frac{z}{L}$

References

- Alexander, Jr., E. C., Quinlan, J. F., 1992. Practical Tracing of Groundwater with Emphasis on Karst Terranes. Tech. Rep. Short Course Manual, 2nd ed., Geological Society of America, Boulder, Colorado.
- Aley, T. J., 1999. The Ozark Underground Laboratory's Groundwater Tracing Handbook. Tech. rep., Ozark Underground Laboratory, Protem, Mo.
- Aley, T. J., Fletcher, M. W., 1976. The water tracer's cookbook. *Missouri Speleology* 16(3), 1–32.
- Barth, G. R., Illangasekare, T. H., Hill, M. C., Rajaram, H., 2001. A new tracer-density criterion for heterogeneous porous media. *Water Resources Research* 37(1), 21–31.
- Behrens, H., Beims, U., Dieter, H., Dietze, G., Eikmann, T., Grummt, T., Hanisch, H., Henseling, H., Käß, W., Kerndorff, H., Leibundgut, C., Müller-Wegener, U., Rönnefahrt, I., Scharenberg, B., Schleyer, R., Schloz, W., Tilkes, F., 2001. Toxicological and ecotoxicological assessment of water tracers. *Hydrogeology Journal* 9, 321–325.
- Bencala, K. E., Walters, R. A., 1983. Simulation of solute transport in a mountain pool-and-riffle stream: A transient storage model. *Water Resources Research* 19(3), 718–724.
- Bendel, L., 1948. *Ingenieurgeologie*, 832 p. Springer, Vienna.
- Blower, S. M., Dowlatabadi, H., 1994. Sensitivity and uncertainty analysis of complex models of disease transmission: An HIV model, as an example. *International Statistical Review* 62(2), 229–243.
- Bögli, A., 1980. *Karst Hydrology and Physical Speleology*, 284 p. Springer, Berlin.
- Brugman, M. M., 1987. Water Flow at the Base of a Surging Glacier. Ph.D. Dissertation, 267 p., California Institute of Technology, Pasadena, Cal.
- Chatwin, P. C., 1971. On the interpretation of some longitudinal dispersion experiments. *Journal of Fluid Mechanics* 48(4), 689–702.
- Davis, S. N., Campbell, D. J., Bentley, H. W., Flynn, T. J., 1985. *Ground water Tracers*, 200 p. National Ground water Association, Dublin, Ohio.

- De Carvalho Dill, A., Müller, I., 1992. Geophysical Prospecting. In: Leibundgut, C., De Carvalho Dill, A., Małoszewski, P., Müller, I., Schneider, J. (Eds.), Investigation of Solute Transport in the Porous Aquifer of the Test Site Wilerwald (Switzerland), Steirische Beiträge zur Hydrogeologie, 6th International Symposium on Water Tracing, Transport Phenomena in Different Aquifers (Investigations 1987–1992). Vol. 43. Joanneum Research, Graz, Germany, pp. 229–250.
- Dennis, J. E., Gay, D. M., Welsch, R. E., 1981. An adaptive nonlinear least-squares algorithm. *Math. Comp.* 7(3), 348–383.
- Dienert, F., 1913. Remarques au sujet des expériences avec la fluorescéine. *C. R. Académie Sciences* 157, 660–661.
- Drew, D. P., Smith, D. I., 1969. Techniques for the Tracing of Subterranean Drainage. Tech. Rep. 2, British Geomorphological Research Group Technical Bulletin, Great Britain.
- Dunn, B., 1968. Nomographs for determining amount of Rhodamine B dye for time-of-travel studies. In: In Selected Techniques in water Resources Investigations, 1966-67. U.S. Geological Survey Water Supply Paper 1892, pp. 9–14.
- Field, M. S., 1997. Risk assessment methodology for karst aquifers: (2) Solute-transport modeling. *Environ. Monit. Assess.* 47, 23–37.
- Field, M. S., 2000. Ground-water tracing and drainage basin delineation for risk assessment mapping for spring protection in Clarke County, Virginia. Tech. Rep. NCEA-W-0936, 36 p., U.S. Environmental Protection Agency, Washington, D.C.
- Field, M. S., 2002a. Efficient hydrologic tracer-test design for tracer-mass estimation and sample-collection frequency, 1, method development. *Environmental Geology* in press.
- Field, M. S., 2002b. The QTRACER2 Program for Tracer-Breakthrough Curve Analysis for Hydrological Tracer Tests in Karstic Aquifers and Other Hydrologic Systems. Tech. Rep. EPA/600/R-02/001, 179 p., U.S. Environ. Prot. Agency, Washington, D.C.
- Field, M. S., 2002c. A review of some tracer-design equations for tracer-mass estimation and sample collection frequency. *Environmental Geology* in press.
- Field, M. S., Nash, S. G., 1997. Risk assessment methodology for karst aquifers, 1, Estimating karst conduit-flow parameters. *Environ. Monit. Assess.* 47, 1–21.

- Field, M. S., Pinsky, P. F., 2000. A two-region nonequilibrium model for solute transport in solution conduits in karstic aquifers. *Journal of Contaminant Hydrology* 44, 329–351.
- Field, M. S., Wilhelm, R. G., Quinlan, J. F., Aley, T. J., 1995. An assessment of the potential adverse properties of fluorescent tracer dyes for groundwater tracing. *Environmental Monitoring and Assessment* 38, 75–96.
- Freeze, R. A., Cherry, J. A., 1979. *Groundwater*, 604 p. Prentice-Hall, Engelwood Cliffs, N.J.
- Gaspar, E., 1987. *Modern Trends in Tracer Hydrology*, 145 p. CRC Press, Inc., Boca Raton, Fla.
- Gunn, J., Lowe, D., 2000. Editorial. *Journal of Cave and Karst Science* (Transactions of the British Cave Research Association) 26, 99–100.
- Haas, J. L., 1959. Evaluation of ground water tracing methods used in speleology. *National Speleological Society Bulletin* 21(2), 67–76.
- Heys, B., 1968. Closing address. *Transaction of Cave Research Group, Great Britain* 10(2), 121.
- Huyakorn, P. S., Andersen, P. F., Molz, F. J., Güven, O., Melville, J. G., 1986. Simulations of two-well tracer tests in stratified aquifers at the Chalk River and the Mobile sites. *Water Resources Research* 22(7), 1016–1030.
- Iman, R. L., Helton, J. C., 1988. An investigation of uncertainty and sensitivity analysis techniques for computer models. *Risk Analysis* 8, 71–90.
- Kahaner, D. K., Moler, C., Nash, S. G., 1989. *Numerical Methods and Software*, 581 p. Prentice-Hall, Engelwood Cliffs, N.J.
- Käb, W., 1998. *Tracing Technique in Geohydrology*, 581 p. A.A. Balkema, Rotterdam, The Netherlands.
- Kilpatrick, F. A., 1993. *Simulation of Soluble Waste Transport and Buildup in Surface Wwaters Using Tracers*. Tech. Rep. Techniques of Water-Resources Investigations, Book 3, Chapter A20, 37 p., U.S. Geological Survey.

- Kilpatrick, F. A., Cobb, E. D., 1985. Measurement of Discharge Using Tracers. Tech. Rep. Techniques of Water-Resources Investigations, Book 3, Chapter A16, 52 p., U.S. Geological Survey.
- Kilpatrick, F. A., Taylor, K. R., 1986. Generalization and Application of Tracer Dispersion Data. Water Resources Bulletin 22(4), 537–548.
- Kilpatrick, F. A., Wilson, Jr., J. F., 1989. Measurement of Time of Travel in Streams by Dye Tracing. Tech. Rep. 27 Techniques of Water-Resources Investigations of the U.S. Geological Survey, Book 3, Chapter A9, 27 p., U.S. Geological Survey.
- Kinnunen, K., 1978. Tracing Water Movement by Means of *eschericia coli* bacteriophages. Tech. Rep. Publication of Water Research Institute, 25, 50 p., National Board of Waters, Finland.
- Leibundgut, C., 1981. Zum Anwendung Künstlicher Tracer in Gletscher, 85 p. Publikation Gewässerkde, No. 85, University of Bern.
- Leibundgut, C., 1992. Test Site. In: Leibundgut, C., De Carvalho Dill, A., Małoszewski, P., Müller, I., Schneider, J. (Eds.), Investigation of Solute Transport in the Porous Aquifer of the Test Site Wilerwald (Switzerland), Steirische Beiträge zur Hydrogeologie, 6th International Symposium on Water Tracing, Transport Phenomena in Different Aquifers (Investigations 1987–1992). Vol. 43. Joanneum Research, Graz, Germany, pp. 229–250.
- Leibundgut, C., De Carvalho Dill, A., 1992. Tracer Tests. In: Leibundgut, C., De Carvalho Dill, A., Małoszewski, P., Müller, I., Schneider, J. (Eds.), Investigation of Solute Transport in the Porous Aquifer of the Test Site Wilerwald (Switzerland), Steirische Beiträge zur Hydrogeologie, 6th International Symposium on Water Tracing, Transport Phenomena in Different Aquifers (Investigations 1987–1992). Vol. 43. Joanneum Research, Graz, Germany, pp. 229–250.
- Leibundgut, C., Wernli, H. R., 1982. Zur Frage der Einspeisemengenberechnung für Fluoreszenztracer. In: Leibundgut, C., Weingartner, R. (Eds.), Tracermethoden in der Hydrologie, Beiträge Geologie Schweiz – Hydrologie. Vol. 28(I). Geographischer Vrlag, Bern, Switzerland, pp. 119–130.
- Leibundgut, C., 1974. Fluoreszierende markierfarbstoffe in der hydrologie. In: Mitt. Naturforsch. Ges. Bern, N.F. Vol. 31. Bern, Switzerland, pp. 63–84.

- Levenspiel, O., 1999. Chemical Reaction Engineering, 668 p. John Wiley & Sons, New York.
- Lutz, T., Parriaux, A., 1988. The Identification of Uranine in Natural Water by High Pressure Liquid Chromatography (HPLC). In: Goldbrunner, J. (Ed.), Steirische Beiträge zur Hydrogeologie. Vol. 39. Joanneum Research, Graz, Germany, pp. 141–148.
- Mackay, D. M., Freyberg, D. L., Roberts, P. V., Cherry, J. A., 1986. A natural gradient experiment on solute transport in a sand aquifer: 1. Approach and overview of plume management. *Water Resour. Res.* 22(13), 2017–2029.
- Małoszewski, P., Harum, T., Benischke, R., 1992a. Mathematical modelling of tracer experiments in the karst of Lurbach system. In: Behrens, H., Benischke, R., Bricelj, M., Harum, T., Käß, W., Kosi, G., Leditzky, H. P., Leibundgut, C., Małoszewski, P., Maurin, V., Rajner, V., Rank, D., Reichert, B., Stadler, H., Stichler, W., Trimborn, P., Zojer, H., Zupan, M. (Eds.), Investigations with natural and artificial tracers in the karst aquifer of the Lurbach system (Peggau–Tanneben–Semriach, Austria), Steirische Beiträge zur Hydrogeologie, 6th International Symposium on Water Tracing, Transport Phenomena in Different Aquifers (Investigations 1987–1992). Vol. 43. Joanneum Research, Graz, Germany, pp. 116–136.
- Małoszewski, P., Leibundgut, C., Schneider, J., 1992b. Mathematical Modelling of the Tracer Experiment Performed in the Test Site Wilerwald. In: Leibundgut, C., De Carvalho Dill, A., Małoszewski, P., Müller, I., Schneider, J. (Eds.), Investigation of Solute Transport in the Porous Aquifer of the Test Site Wilerwald (Switzerland), Steirische Beiträge zur Hydrogeologie, 6th International Symposium on Water Tracing, Transport Phenomena in Different Aquifers (Investigations 1987–1992). Vol. 43. Joanneum Research, Graz, Germany, pp. 229–250.
- Martel, 1913. Sur les expériences de fluorescéine à grandes distances. *C. R. Academy Sciences* 157, 1102–1104.
- McAvoy, D. C., Masscheleyn, P., Peng, C., Morrall, S. W., Casilla, A. B., Lim, J. M. U., Gregorio, E. G., 2003. Risk assessment approach for untreated wastewater using the QUAL2E water quality model. *Chemosphere*, *in press*.
- McCann, M. R., Krothe, N. C., 1992. Development of a monitoring program at a superfund site in a karst terrane near Bloomington, Indiana. In: Quinlan, J. (Ed.), Proceedings of

- the Third Conference on Hydrogeology, Ecology, Monitoring, and Management of Ground Water in Karst Terranes. National Ground Water Association, Dublin, Ohio, pp. 349–370.
- McKay, M. D., Conover, W. J., Beckman, R. J., 1979. A comparison of three methods for selecting values of input variables in the analysis of output from a computer code. *Technometrics* 21, 239–245.
- Meigs, L. C., Beauheim, R. L., 2001. Tracer tests in a fractured dolomite, 1, Experimental design and observed tracer recoveries. *Water Resources Research* 37(5), 1113–1128.
- Milanović, P., 1981. *Karst Hydrogeology*, 434 p. Water Resources Publications, Littleton, Col.
- Molz, F. J., Güven, O., Melville, J. G., Crocker, R. D., Matteson, K. T., 1986a. Performance, analysis, and simulation of a two-well tracer test at the Mobile site. *Water Resources Research* 22(7), 1031–1037.
- Molz, F. J., Güven, O., Melville, J. G., Keely, J. F., 1986b. Performance and Analysis of Aquifer Tracer Tests with Implications for Contaminant Transport Modeling. Tech. Rep. EPA/600/2-86/062, 88 p., U.S. Envir. Prot. Agency, Washington, D.C.
- Mull, D. S., Liebermann, T. D., Smoot, J. L., Woosley, Jr., L. H., 1988a. Application of Dye-Tracing Techniques for Determining Solute-Transport Characteristics of Ground Water in Karst Terranes. Tech. Rep. EPA/904/9-88-001, 103 p., U.S. Envir. Prot. Agency, Region IV, Atlanta, Ga.
- Mull, D. S., Lyverse, M. A., 1984. Ground Water Hydrology of the Elizabethtown Area, Kentucky. Tech. Rep. WRI 84-4057, 59 p., U.S. Geol. Surv. Geol. Surv. Water-Resour. Invest., Washington, D.C.
- Mull, D. S., Smoot, J. L., Liebermann, T. D., 1988b. Dye Tracing Techniques Used to Determine Ground-Water Flow in a Carbonate Aquifer System Near Elizabethtown, Kentucky. Tech. Rep. WRI 87-4174, 95 p., U.S. Geol. Surv. Water-Resour. Invest., Washington, D.C.
- Novakowski, K. S., 1992. The analysis of tracer experiments conducted in divergent radial flow fields. *Water Resources Research* 28(12), 3215–3225.

- Oostrom, M., Hayworth, J. S., Dane, J. H., Güven, O., 1992. Behavior of dense aqueous phase leachate plumes in homogenous porous media. *Water Resources Research* 28(8), 2123–2134.
- Parriaux, A., Liskay, M., Müller, I., della Valle, G., 1988. Guide pratique pour l’usage des traceurs artificiels en hydrogéologues [Bilingual; also published in the same manual as: Leitfaden für den gebrauch kunstlicher tracer in der hydrogeologie]. Tech. Rep. GEOLEP EPFL 51 p. [49 p.], Société Géologique Suisse, Groupe des Hydrogéologie [Schweizerische Gruppe der Hydrogeologen, Arbeitsgruppe ‘Tracer’], Lausanne, Switzerland.
- Pearson, T. J., 1997. Pgplot graphics subroutine library. Tech. rep., California Institute of Technology, Pasadena.
- Pickens, J. F., Grisak, G. E., 1981. Scale-dependent dispersion in a stratified granular aquifer. *Water Resources Research* 17(4), 1191–1211.
- Rantz, S. E., 1982. Measurement and Computation of Streamflow: Volume 1. Measurement of Stage and Discharge. Tech. Rep. U.S. Geological Survey Water-Supply Paper 2175, 284 p., U.S. Geological Survey.
- Rathbun, R. E., 1979. Estimating and Gas and Dye Quantity for Modified Tracer Technique Measurements of Stream Reaeration Coefficients. Tech. Rep. U.S. Geological Survey Water-Resources Investigations 79-27, 42 p., U.S. Geological Survey.
- Reichard, E., Cranor, C., Raucher, R., Zapponi, G., 1990. Groundwater Contamination Risk Assessment: A Guide to Understanding and Managing the Uncertainties, 204 p. Vol. IAHS Publ. No. 196. International Association of Hydrological Sciences, Wallingford, Oxfordshire, U.K.
- Sardin, M., Schweich, D., Leij, F. J., van Genuchten, M. T., 1991. Modeling the nonequilibrium transport of linearly interacting solutes in porous media: A review. *Water Resources Research* 27, 2287–2307.
- Schudel, B., Biaggi, D., Dervev, T., Kozel, R., Müller, I., Ross, J. H., Schindler, U., 2002. Utilisation des Traceurs Artificiels an Hydrogéologie: Guide Pratique, Rapports de l’OFEG, Série Géologie. Tech. Rep. No. 3, 77 p., Groupe de Travail Traçage de la Société Suisse d’Hydrogéologie; SSH, Berne, Switzerland.

- Silebi, C. A., Schiesser, W. E., 1992. *Dynamic Modeling of Transport Process Systems*, 518 p. Academic Press, San Diego, Calif.
- Siline-Bektchourine, A. I., 1951. *Hydrogéologie Spéciale*, 394 p. Gossendarctvennoe Izdatelctvo Geologitcheshoi Litertouri, Moscow.
- Smart, C., Zabo, L., 1997. Experimental design, technique and protocol in fluorometric tracing of ground water. In: *Proceedings of the 12th International Congress of Speleology; 6th Conference on Limestone Hydrology and Fissured Media*. Vol. 2. International Union of Speleology and Swiss Speleological Society, La Chaux de Fonds, Switzerland, pp. 51–54.
- Smart, C. C., 1988. Artificial tracer techniques for the determination of the structure of conduit aquifers. *Ground Water* 26(4), 445–453.
- Smart, C. C., Karunaratne, K. C., 2001. Statistical characterization of natural background fluorescence as an aid to dye tracer test design. In: Beck, B. F., Herring, J. G. (Eds.), *Proceedings of the Eighth Multidisciplinary Conference on Sinkholes and the Engineering and Environmental Applications of Karst Geology and Hydrology*. Lamoreau and Assoc., Oak Ridge, Tenn., pp. 271–276.
- Smart, C. C., Simpson, B., 2001. An evaluation of the performance of activated charcoal in detection of fluorescent compounds in the environment. In: Beck, B. F., Herring, J. G. (Eds.), *Proceedings of the Eighth Multidisciplinary Conference on Sinkholes and the Engineering and Environmental Applications of Karst Geology and Hydrology*. Lamoreau and Assoc., Oak Ridge, Tenn., pp. 265–270.
- Smart, P. L., Atkinson, T. C., Laidlaw, I. M. S., Newson, M. D., Trudgill, S. T., 1986. Comparison of the results of quantitative and nonquantitative tracer tests for determination of karst conduit networks: An example from the Traligill Basin, Scotland. *Earth Surface Processes* 11, 249–261.
- Smart, P. L., Friederich, H., 1982. An assessment of the methods and results of water-tracing experiments in the Gunung Mulu National Park, Sarawak. *British Cave Research Association, Transactions* 9, 100–112.
- Sutton, D. J., Kabala, Z. J., Francisco, A., Vasudevan, D., 2001. Limitations and potential of commercially available rhodamine WT as a groundwater tracer. *Water Resources Research* 37(6), 1641–1656.

- Sweeting, M. M., 1973. Karst Landforms, 362 p. Columbia University Press, New York.
- Taylor, K. R., James, R. W., Helinsky, B. M., 1986. Traveltime and Dispersion in the Shenandoah River and its Tributaries, Waynesboro, Virginia, to Harpers Ferry, West, Virginia. Tech. Rep. WRI 86-4065, 60 p., U.S. Geol. Surv. Water-Resour. Invest., Washington, D.C.
- Timeus, G., 1926. Le indagini sull'origini delle acque sotterrane. In: Bertarelli, I. V., Timeus, E. (Eds.), In, Duemila Grotte. pp. 153–166.
- Toride, N., Leij, F. J., van Genuchten, M. T., 1993. A comprehensive set of analytical solutions for nonequilibrium solute transport with first-order decay and zero-order production. Water Resources Research 29(7), 2167–2182.
- Toride, N., Leij, F. J., van Genuchten, M. T., 1995. The CXTFIT Code for Estimating Transport Parameters from the Laboratory or Field Tracer Experiments; Version 2.0. Tech. Rep. 137, 121 p., U.S. Salinity Lab., Riverside, Calif.
- UNESCO, 1973-1983. Groundwater Studies; An International Guide for Research and Practice (with Supplements 1975, 1977, and 1983). United Nations.
- USEPA, 1986a. Guidelines for Health Risk Assessment of Chemical Mixtures. Tech. Rep. EPA/630/R-98/002, 28 p., U.S. Environ. Protect. Agency, Washington, D.C.
- USEPA, 1986b. Guidelines for Mutagenicity Risk Assessment. Tech. Rep. EPA/630/R-98/003, 17 p., U.S. Environ. Protect. Agency, Washington, D.C.
- USEPA, 1989. Risk Assessment Guidance for Superfund, Volume I, Human Health Evaluation Manual, (Part A). Tech. Rep. EPA/540/1-89/002, <http://www.epa.gov/superfund/programs/risk/ragsa/index.htm>, U.S. Environ. Protect. Agency, Washington, D.C.
- USEPA, 1991. Guidelines for Developmental Toxicity Risk Assessment. Tech. Rep. EPA/600/FR-91/001, 67 p., U.S. Environ. Protect. Agency, Washington, D.C.
- USEPA, 1992. Guidelines for Exposure Assessment. Tech. Rep. EPA/600/Z-92/001, 127 p., U.S. Environ. Protect. Agency, Washington, D.C.
- USEPA, 1996. Guidelines for Reproductive Toxicity Risk Assessment. Tech. Rep. EPA/630/R-96/009, 118 p., U.S. Environ. Protect. Agency, Washington, D.C.

- USEPA, 1998a. Guidelines for Ecological Risk Assessment. Tech. Rep. EPA/630/R-95/002F, 114 p., U.S. Environ. Protect. Agency, Washington, D.C.
- USEPA, 1998b. Guidelines for Neurotoxicity Risk Assessment. Tech. Rep. EPA/630/R-95/001F, 77 p., U.S. Environ. Protect. Agency, Washington, D.C.
- Webster, D. S., Proctor, J. F., Marine, I. W., 1970. Two-Well Tracer Test in Fractured Crystalline Rock. Tech. Rep. U.S. Geological Survey Water-Supply Paper 1544-I, 22 p., U.S. Geological Survey.
- Wolff, H. J., Radeke, K. H., Gelbin, D., 1979. Heat and mass transfer in packed beds—iv: Use of weighted moments to determine axial dispersion coefficients. *Chemical Engineering Science* 34, 101–107.
- Worthington, S. R. H., Davies, G. J., Ford, D. C., 2000. Matrix, fracture and channel components of storage and flow in a Paleozoic limestone aquifer. In: Wicks, C., Sasowski, I. (Eds.), *Groundwater flow and contaminant transport in carbonate aquifers*. A.A. Balkema, Rotterdam, The Netherlands, pp. 113–128.
- Worthington, S. R. H., Smart, C. C., 2001. Evaluation of equations estimating mass needed for sink to spring tracer testing in karst. *Journal of Cave and Karst Studies* 63, 115.
- Yevjevich, V., 1972. *Stochastic Processes in Hydrology*, 276 p. Water Resources Publications, Fort Collins, Col.
- Yotsukura, N., Fischer, H. B., Sayer, W. W., 1970. Measurement of Mixing Characteristics of the Missouri River Between Sioux City, Iowa, and Plattsmouth, Nebraska. Tech. Rep. 1899-G, 29 p., U.S. Geol. Surv. Water-Supply Paper, Washington, D.C.
- Yu, C., Warrick, A. W., Conklin, M. H., 1999. A moment method for analyzing breakthrough curves of step inputs. *Water Resources Research* 35(11), 3567–3572.
- Zand, S. M., Kennedy, V. C., Zellweger, G. W., Avanzino, R. J., 1976. Solute Transport and Modeling of Water Quality in a Small Stream. *J. Res. U.S. Geol. Surv.* 4(2), 233–240.
- Zötl, A., 1974. *Karsthydrogeologie*, 291 p. Springer, Vienna.